

EVALUATION AND OPTIMIZATION OF THE CONTROL SYSTEM OF THE SYMPHONY WAVE POWER DEVICE



ILIAS SFIKAS



Evaluation and optimization of the control system of the Symphony Wave Power Device

Ilias Sfikas

4513916

In partial fulfilment of the requirements for the degree of

Master of Science

In Sustainable Energy Technology

At the Delft University of Technology, Faculty of Electrical
Engineering, Mathematics and Computer Science

January 2018

Supervisor: Dr. Ir. Henk Polinder

Thesis Committee: Dr. Jianning Dong

Dr. Ir. Arno Smets

Company: Teamwork Technology

Front picture source: <http://www.susansinkblog.com/2016/09/25/waves/>



Preface

Humans have a vital connection to planet Earth. This is something that I started understanding more and more by growing up, as I gained a lot of respect for the natural environment. Unfortunately, today it is more obvious than ever that human intervention on it has gone much too far. To realize this, it is in many cases not even necessary to read a scientific article. A look at the amount of rubbish on the streets or the smell of polluted air already give an idea about the extent to which the ecosystem is being destroyed. In modern society, everything is interpreted in terms of economic loss or profit, but we tend to forget that money is not edible. In my opinion, the basic human characteristic behind all this is arrogance. Nevertheless, significant efforts can be made in order to reduce the impact.

These observations led me to study renewable energy, as it is one of the ways to combat the problems that arise from human activity on nature. As I have always been interested in water, I followed the track of ocean energy. This field has a huge potential. Luckily, I found an interesting thesis topic on a wave energy device and got a lot of help, both from my supervisor and from the company. Although the whole experience of studying for this MSc degree was not really pleasant, due to the excessive work load, I do not regret for making this choice. Apart from the valuable scientific knowledge that I obtained, I also learned some important life lessons, which will help me make the correct choices later on.

However, I strongly believe that renewable energy should not be used as an 'excuse' to keep the system running the way it does. We should also put a lot of effort in reducing the energy consumption and waste. By this, I do not only mean to manufacture and use more energy efficient devices, but also to take some steps back from the modern, seemingly infinite, freedom of behaviour in a finite world. Moreover, technological innovations should not always be blindly admired and focused on, especially in cases when health concerns or environmental impacts are involved. It is high time to start reviewing and prioritizing our needs. To achieve these goals, proper education will play the most important role. We, as future engineers, carry a high degree of responsibility in teaching the younger generations how to act sustainably and respectfully, because, after all, there is no plan(et) B.

In any case, I am glad to have contributed, even on a small scale, towards a cleaner future, by working on this topic. I hope you enjoy reading this thesis and be able to use the contained information in even more areas.

Delft, January 2018

Ilias Sfikas

Acknowledgements

For the completion of this thesis, I want to thank most of all the staff of Teamwork Technology and especially Fred Gardner and Bauke Vriesema, for all their invaluable help, sharing of incredible knowledge, problem solving, brilliant ideas, team spirit and relaxed work environment. Without them, this thesis would not have been a success. I also want to thank Hans van Noorloos, Djurre Wikkerink, Joost Kolken and Wouter de Winter, for providing me some necessary tools and calculations.

From TU Delft, I want to thank my supervisor Henk Polinder for providing me this subject, for his continuous assistance and for his positive attitude towards the choices I made in this thesis. I also want to thank Jianning Dong and Udai Shipurkar for their help in the courses related to the thesis topic. Moreover, I want to thank Arno Smets for being in my exam committee.

Additionally, I would like to thank Pavlos Georgilakis and Yiannis Katsigiannis, as it were they who introduced me to the GAMS software and helped me with it, during my BSc thesis in Greece. This software has played a key role in this MSc thesis.

Finally, special thanks need to be given to my family and friends, who stood by my side and supported me on all levels during this extremely difficult, more than I could ever imagine, procedure of obtaining this MSc degree.

Abstract

Raising environmental concerns have stimulated the development of renewable energy, including energy from the oceans, which contain a huge potential. In this thesis, particular emphasis is given to wave energy, which can deliver up to $2\ TW$ on a global scale. The aim of this thesis is to optimize the control system of the Symphony Wave Power Device, which is a point absorber, so that the energy that is being delivered to the electrical grid is maximal and the device functions in a stable way.

The device is analytically described in terms of structural parts, operating principle and presentation of all the forces that act on the moving part, which is called the floater. The device is in fact a mass-spring-damper system, for which the spring constant needs to be tuned according to the period of the incoming waves, so as to maximize the energy extraction. For this tuning, not only the actual mass of the floater, but also the added equivalent mass due to the inertia of the inner turbine need to be taken into account.

The whole device is modelled with the help of a Matlab/Simulink programme, in which simulations can be performed, to observe the motion and make certain calculations. The already existing PI controller, which makes use of an energy error, is briefly described and the relevant calculations for the energy extraction are presented. The energy losses in the electrical parts also need to be taken into account.

To evaluate the current controller, it is necessary to calculate the upper boundary of the energy that the Symphony can obtain from a certain wave. This is done with the help of the GAMS software. The code, as well as the necessary assumptions and approximations, are presented in a mathematical way. The results, both in numerical and graphical form, provide a good insight as to how the ideal theoretical control system looks like.

Next, simulations are performed in the Matlab programme and comparisons with the GAMS results are made. The essential parts of the controller are tuned to their optimal values. Only a proportional part for the PI controller is needed and the energy should not flow in two directions.

The results show that, with correct tuning of the proportional part, as well as of the spring constant, the Symphony operates very well in all realistic sea states at the location where it will be placed. A high percentage of the theoretical energy boundary is being extracted from the waves and the motion of the floater is close to the optimal pattern. It is thus concluded that the existing controller has a remarkable performance, if regulated correctly. Finally, recommendations for future research on many levels are given.

Table of Contents

1	Introduction.....	1
1.1	Introduction.....	1
1.2	Renewable energy.....	1
1.3	Wave energy.....	2
1.4	Scope of thesis.....	3
1.4.1	The device.....	3
1.4.2	Main goal.....	4
1.4.3	Modelling.....	4
1.4.4	Research questions.....	4
1.5	Structure of this report.....	5
2	Symphony Wave Power Device.....	6
2.1	Introduction.....	6
2.2	Basic parts.....	6
2.3	Principle of operation.....	7
2.4	Mathematical modelling.....	8
2.5	The mass-spring-damper system.....	12
2.5.1	Initial design.....	12
2.5.2	Influence of the turbine's inertia.....	13
3	Time Domain Model.....	18
3.1	Introduction.....	18
3.2	Matlab script.....	18
3.3	Simulink model.....	18
3.4	The existing controller.....	19
3.5	Converter.....	21
3.6	Energy calculations.....	22
3.6.1	Initial energy.....	22
3.6.2	Copper losses.....	22
3.6.3	Cable losses.....	23
3.6.4	Final energy.....	24
4	Maximum Energy Yield.....	25
4.1	Introduction.....	25
4.2	Literature overview.....	25
4.3	The GAMS software.....	27
4.3.1	General information.....	27
4.3.2	Structure of the GAMS code.....	28
4.4	The developed code.....	29
4.4.1	Wave modelling/fixd inputs.....	29
4.4.2	Variables.....	29
4.4.3	Spring force modelling.....	30
4.4.4	Drag force modelling.....	32
4.4.5	Iron loss torque modelling.....	33
4.4.6	Equations.....	34
4.4.7	Solving.....	35

4.5	Optimization results.....	36
4.5.1	Monochromatic waves.....	36
4.5.2	Irregular waves.....	39
4.5.3	Special case.....	43
4.6	Sensitivity analysis.....	43
4.6.1	Sensitivity to parameters.....	43
4.6.2	Sensitivity to spring modelling.....	44
4.6.3	Sensitivity to sampling rate.....	45
5	Simulation Results.....	47
5.1	Introduction.....	47
5.2	Controller components investigation.....	47
5.2.1	Integrating part.....	48
5.2.2	Energy flow direction.....	49
5.2.3	Conclusion.....	54
5.3	Evaluation/optimization results for monochromatic waves.....	54
5.4	Evaluation/optimization results for irregular waves.....	58
5.5	Sensitivity analysis.....	66
5.5.1	Sensitivity to the linear spring constant.....	66
5.5.2	Sensitivity to K_p	67
5.5.3	Sensitivity to the electromagnetic torque.....	68
6	Conclusions & Recommendations.....	70
6.1	Introduction.....	70
6.2	Conclusions.....	70
6.2.1	Spring tuning.....	70
6.2.2	GAMS modelling.....	70
6.2.3	GAMS results.....	71
6.2.4	Controller parts.....	71
6.2.5	Matlab results.....	71
6.2.6	Sensitivity.....	71
6.3	Recommendations.....	71
6.3.1	Hardware.....	72
6.3.2	Other control systems.....	72
6.3.3	GAMS improvements.....	72
6.3.4	Radiation force.....	72
	References.....	74
	Appendix.....	77
A	The GAMS code.....	77
B	Scatter diagram.....	79

Symbols

Symbol	Description	Unit
a	Factor that determines the energy flow direction	J
A_b	Area related to the bottom of the floater	m^2
A_{iron}	Iron loss factor	J
a_{iron}	Iron loss factor	J
A_{mb}	Area related to the bottom of the membrane	m^2
A_{mu}	Area related to the top of the membrane	m^2
A_{pp}	Area related to the pressure point	m^2
α_{20}	Temperature coefficient of resistance of copper at $20^\circ C$	$^\circ C^{-1}$
B_{iron}	Iron loss factor	$J \cdot s$
b_{iron}	Iron loss factor	$J \cdot s$
C_{Ddw}	Drag coefficient in the downwards movement	–
C_{Dup}	Drag coefficient in the upwards movement	–
c_{hyd}	Hydrodynamic damping coefficient	$\frac{kg}{s}$
d_{out}	Outer diameter of the membrane	m
$E_{cableloss}$	Cable loss energy	J
$E_{copperloss}$	Copper loss energy	J
E_f	Machine excitation voltage	V
E_{final}	Final extracted energy from the waves	J
$E_{initial}$	Initial energy	J
E_{kin}	Kinetic energy of the floater	J

E_{max}	Maximum mechanical energy	J
E_{mech}	Mechanical energy	J
<i>energy</i>	GAMS extracted energy/objective function	J
<i>error</i>	Energy error	J
E_{spring}	Energy contained in spring	J
f	Frequency	Hz
F_{drag}	Drag force	N
f_{el}	Electrical frequency of stator voltages	Hz
F_g	Gravitational force	N
F_{gas}	Chamber air force	N
F_{hs}	Hydrostatic force	N
F_{iron}	Iron loss force	N
F_{PTO}	PTO force	N
F_{rad}	Radiation force	N
F_{spring}	Spring force	N
F_t	Force that the turbine blades exert on the liquid	N
F_{top}	Floater air force	N
F_{wave}	Wave force	N
f_0	Peak frequency	Hz
g	Gravitational acceleration	$\frac{m}{s^2}$
G_{turb}	Factor related to the volume of the turbine	m^{-3}
H	Wave height for monochromatic waves	m
H_b	Distance related to the bottom of the floater	m
H_{mb}	Distance related to the bottom of the membrane	m

H_{pp}	Distance related to the pressure point	m
H_s	Significant wave height for random waves	m
I_a	Machine phase current	A
i_{DC}	Cable DC current	A
I_t	Inertia of the turbine	$kg \cdot m^2$
k	Spring constant	$\frac{N}{m}$
K	Machine constant	$V \cdot s$
k_{fin}	Final spring constant	$\frac{N}{m}$
K_i	Integrating constant of controller	–
k_{ini}	Initial spring constant	$\frac{N}{m}$
k_{lin}	Linear region spring constant	$\frac{N}{m}$
K_p	Proportional constant of controller	–
k_{stiff}	Stiff region spring constant	$\frac{N}{m}$
l	Cable length	m
m	Mass of the floater plus the mass of the moving liquid	kg
m_{added}	Added mass at infinity	kg
m_{eq}	Equivalent mass due to turbine inertia	kg
m_{fl}	Mass of the floater	kg
m_{inn}	Moving mass of the inner liquid	kg
m_{tot}	Total mass of the floater and the moving liquid plus added mass at infinity	kg
P_{amb}	Ambient air pressure at sea level	Pa
$P_{cableloss}$	Cable loss power	W
$P_{copperloss}$	Copper loss power	W
P_{eq}	Pressure of chamber air at equilibrium	Pa

$P_{initial}$	Initial power	W
$P_{ironloss}$	Iron loss power	W
P_{mean}	Average output power of the Symphony	W
Pr	Probability of occurrence of a certain sea state	—
P_{out}	Power output of the converter	W
R_{cable}	Cable resistance	Ω
R_{phase}	Resistance per phase	Ω
$R_{phase,initial}$	Initial resistance per phase	Ω
$R_{phase,final}$	Final resistance per phase	Ω
S	Cable cross-section area	m^2
$S(f)$	Wave spectrum	$\frac{m^2}{Hz}$
t	Time	s
T	Total duration of wave	s
T_e	Electromagnetic torque of the electrical machine	$N \cdot m$
$ T_{e,max} $	Maximum electromagnetic torque	$N \cdot m$
T_{en}	Wave energy period for random waves	s
$T_{initial}$	Initial temperature of resistance	$^{\circ}C$
T_{iron}	Iron loss torque	$N \cdot m$
T_m	Wave period for monochromatic wave	s
T_t	Inner liquid torque	$N \cdot m$
T_{final}	Final temperature of resistance	$^{\circ}C$
T_0	Natural period	s
V_{ac}	Factor related to the initial pressure	—
V_{air}	Volume of air in the chamber	m^3

V_{DC}	Cable DC voltage	V
V_{eq}	Volume of chamber air at equilibrium	m^3
V_{top}	Volume of the hull at equilibrium position	m^3
z	Position of the floater	m
$z_{control}$	Control amplitude of oscillation	m
z_d	Velocity of the floater	$\frac{m}{s}$
z_{dd}	Acceleration of the floater	$\frac{m}{s^2}$
$ z_{max} $	Maximum oscillation amplitude	m
z_{ovac}	Distance related to the initial pressure	m
γ	Adiabatic constant	–
ΔP	Pressure difference on the turbine	Pa
ΔV_{gas}	Volume of the membrane that is coming up	m^3
ρ	Density of sea water	$\frac{kg}{m^3}$
ρ_{Cu}	Resistivity of copper	$\Omega \cdot m$
ΣF	Sum of forces on the floater	N
φ	Angle between excitation voltage and phase current phasors	rad
ω_t	Rotor/turbine angular speed	$\frac{rad}{s}$
$\dot{\omega}_t$	Angular acceleration of the rotor/turbine	$\frac{rad}{s^2}$
ω_0	Natural angular frequency of the system	$\frac{rad}{s}$

1. Introduction

1.1 Introduction

In this chapter, the foundations of this thesis are set. Firstly, a discussion is made on renewable energy and, more specifically, on energy from the oceans. Particular emphasis is given to wave energy and the various relevant technologies are described. Next, the scope of this thesis is presented in terms of device to focus on, main objective and computer software. All this is expressed in the research questions. Finally, the content of the following chapters is summarized.

1.2 Renewable energy

Today, an effort is made on a global scale to reduce fossil fuel-based emissions and all their polluting consequences for the environment. One of the many solutions for a cleaner and more sustainable future is the use of renewable energy. This is defined as the energy obtained from natural, persistent flows of energy that occur in the immediate environment. This energy flow is present independent of whether it is intercepted by a device [1]. There are different forms of renewable energy, such as wind energy, solar energy, energy from biomass, ocean energy, geothermal energy and others.

Ocean energy is of particular interest for this thesis. The oceans cover 71% of the Earth's surface and contain a huge potential [2]. The main types of ocean energy are [3]:

-Wave energy: The wind creates waves on the water surface, which contain kinetic energy.

-Tidal energy: Due to the gravitational forces between the Earth, the sun and the moon, the water surface elevation varies constantly in time. If the water is captured, this results in potential energy due to height difference. At the same time, tidal currents contain kinetic energy.

-Ocean thermal energy (OTEC): The temperature difference between the warm ocean surface water and the cold water deep down can be used to drive a turbine. This technology is appropriate for areas near the equator.

-Aquatic biomass: Plants and animal materials that grow in the oceans, for example seaweed or algae, can be used as biomass for energy production [4].

-Salinity gradient: The mixture of fresh water, for example from rivers, with salty ocean water results in potential energy through electrochemical processes [5].

The main reasons why ocean energy technologies are not as developed as other renewable energy technologies are the high cost of energy, the lack of trained engineers and the hostile weather conditions [3];[6]. This thesis aims to contribute towards more 'blue' and less 'dirty' energy.

1.3 Wave energy

A lot of energy can be extracted from ocean waves. On a worldwide scale, there is a potential of approximately $1\ TW$ to $2\ TW$ [6];[2]. The amount of wave power on a map is shown in Figure 1.1 [7]. It can thus be seen that the northwest of Europe is an interesting location for developing the relevant technologies.

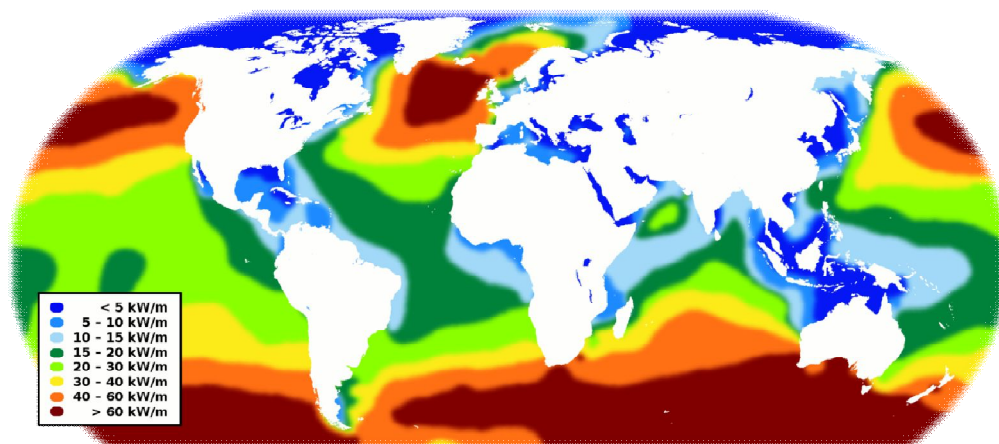


Figure 1.1: Annual mean wave power per meter of wave front

The basic categories of wave power systems are [3]:

i) Attenuators: These are floating devices that operate parallel to the direction of the incoming waves and consist of several pieces connected to each other. As these pieces move due to the waves, energy is extracted with the help of hydraulic cylinders, which are located in between the pieces and are connected to electrical generators [8].

ii) Point absorbers: These devices are very small in comparison to one wavelength [9]. They can be a floating buoy or a fully submerged device. They can follow different ways of movement, such as heaving or surging. Submerged devices that oscillate in heaving mode because of the hydrostatic pressure difference between the crest and trough of the wave, are also called submerged pressure differential, which can be seen as a separate category. There are various power take-off mechanisms that convert this oscillating movement into electricity, for example an inner fluid is pumped through a system [10].

iii) Oscillating wave surge: Flaps that are fixed to the seabed move back and forth due to the incoming waves. With this movement, an inner liquid can be pumped to an onshore station, where it drives a hydraulic turbine, which is connected to an electrical generator [11].

iv) Oscillating water column: In a volume that contains air, an oscillating water height occurs due to the incoming waves, so the air is pressurised and flows through a tube to the atmosphere or vice versa. An air turbine, connected to an electrical generator, intercepts this air flow, so energy can be extracted [11].

v) Overtopping device: The waves run over a barrier and fill a tank. The water in the tank is then driven back to sea through an opening at the bottom of the tank, which contains a turbine that drives a generator [11].

vi) *Bulge wave*: A snake-like device, in fact a rubber tube with openings on both ends, floats parallel to the direction of the waves. The sea water enters in the one end and the incoming wave causes differences in pressure along the length of the device, which result in a bulge that travels through the device and grows. The bulge exits the tube on the other end through a turbine, so energy can be extracted [10].

vii) *Rotating mass*: A floating device oscillates because of the waves. A mass contained in a chamber of this device rotates around an axis because of this oscillation. This axis is connected to an electrical generator [10].

Some examples of the above mentioned devices are shown in Figure 1.2 [12]. Wave energy converters can also be categorized according to their location, namely onshore, in shallow water or offshore [11].

Compared to other ocean energy technologies, the advantages of wave energy are the high potential and the fact that a long distance from the shore is not necessarily required. The disadvantages are the unpredictability of the waves and the unstable extreme conditions that can occur [13].

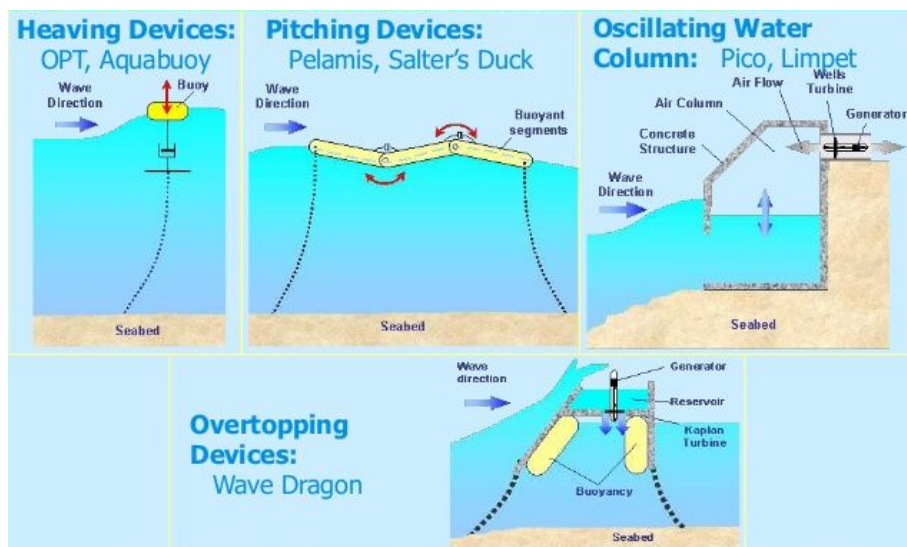


Figure 1.2: Different wave energy technologies (top left: point absorber, top middle: attenuator)

1.4 Scope of thesis

1.4.1 The device

The subject of this thesis is the Symphony Wave Power Device, which is a point absorber. This device is developed by the company Teamwork Technology, located in Alkmaar, Netherlands. It is fully submerged and it is based on an earlier similar concept by the same company, namely the Archimedes Wave Swing (AWS). This device was tested successfully in Portugal in 2004 [11]. The Symphony is a significantly improved version of the AWS, because the inner geometry of the device has been changed and new materials have been used [14]. The Symphony is currently being developed at the company with the help of university students. Stability tests are also performed in special basins with a small-scale model. The realistic device should have a rated power of

approximately 20 kW and will be placed off the coast of Leixões, Portugal [6]. Future scale-ups for power ratings in the order of MW are also planned. For the moment, subsidies, apart from the already existing ones such as WETFEET, are needed to finance the different parts of the project [11]. In general, the Symphony has innovative, breakthrough qualities, as will be clarified in this thesis.

1.4.2 Main goal

The main research objective of this thesis concerns the optimal control of the movement of the Symphony, in order to extract as much energy as possible from the incoming waves. This is a topic that has been addressed a lot in the literature, for various wave power systems. Different control strategies can be applied to make the movement of a device follow a desired pattern, in an environment that has the disadvantage of being mostly unpredictable, because of irregular waves. Here, with the help of computer programmes, significant observations and calculations can be made, in order to tune certain parameters of the Symphony to their optimal values.

1.4.3 Modelling

The realistic behaviour of the Symphony can be simulated with the help of a Matlab time domain model, which accurately represents the device in a mathematical way. Thus, different types of waves can be used as input and different control systems can be tested, to observe the response of the Symphony on many levels.

Also, the GAMS software can be used to calculate the theoretical potential of the Symphony, in other words the energy that the 'perfect' control system would extract from a certain wave. This can then be used for comparison with the Matlab result, in order to evaluate a certain control system.

1.4.4 Research questions

To sum up the previous information, the main research question can be formulated as follows:

“Which control method for the Symphony Wave Power Device results in optimal energy extraction from the incoming waves?”

This main question can be divided into certain sub-questions:

“Which calculations are relevant for the actual energy extraction from the waves?”

“What is the maximum energy that can theoretically be obtained from a certain wave?”

“Which assumptions and approximations need to be made in order to calculate this maximum energy?”

“How good is the performance of the already developed controller?”

“How sensitive is the Symphony to the various parameters?”

All these questions will be analyzed extensively and answered throughout the report, so that a final statement can be made.

1.5 Structure of this report

The structure of this report is as follows:

In Chapter 2, the Symphony Wave Power Device is analytically presented. The structural parts are shown and their operational role is explained. The way the Symphony functions is clarified with pictures and a mathematical modelling, which leads to categorizing the device in the area of mass-spring-damper systems. An analysis is made on the appropriate value of the spring constant.

In Chapter 3, the time domain model, which is a representation of the Symphony in a Matlab/Simulink programme, is described. Particular emphasis is given to the control system, the principle of which is analytically explained. A discussion is made on the AC/DC converter. Finally, the calculations for the energy output and losses are presented.

In Chapter 4, the subject of controlling a wave energy device is analyzed, with the help of an extensive literature overview. The relation of this subject to the Symphony is presented. The GAMS optimization software is described, as it is used as a tool to calculate the upper energy boundary. Next, the results of running the code are shown with graphs and a discussion is performed. Finally, a sensitivity analysis, concerning various parameters and factors, is made.

In Chapter 5, the results of experimenting with the Matlab time domain model are analytically presented. An investigation is made on the necessity of an integrating part in the control system and on the direction in which the energy can flow. The model is then run for monochromatic and irregular waves and the results are presented in tables and graphs. The controller is optimally tuned and a comparison with the GAMS results is made on many levels. Finally, a sensitivity analysis, concerning some important parameters of the Symphony, is performed.

In Chapter 6, the final conclusions of this thesis are drawn and recommendations for further research on the topic are presented.

2. Symphony Wave Power Device

2.1 Introduction

In this chapter, an extensive description is given about the Symphony Wave Power Device. First of all, the structural parts are shown and their functional role is explained. Then, the principle of operation is presented with pictures, to understand the way the Symphony responds to the sea waves, in terms of movement of the various parts. For a better understanding, the forces that govern the movement are presented one by one in a mathematical way. In this way, it is proven that the Symphony is a mass-spring-damper system, with a special form of the spring force. Finally, a more in-depth investigation shows that, due to the impact of the turbine on the movement of the device, the spring needs to be stiffened in an appropriate way.

2.2 Basic parts

The Symphony consists of several pieces, as can be seen in Figure 2.1 [6].

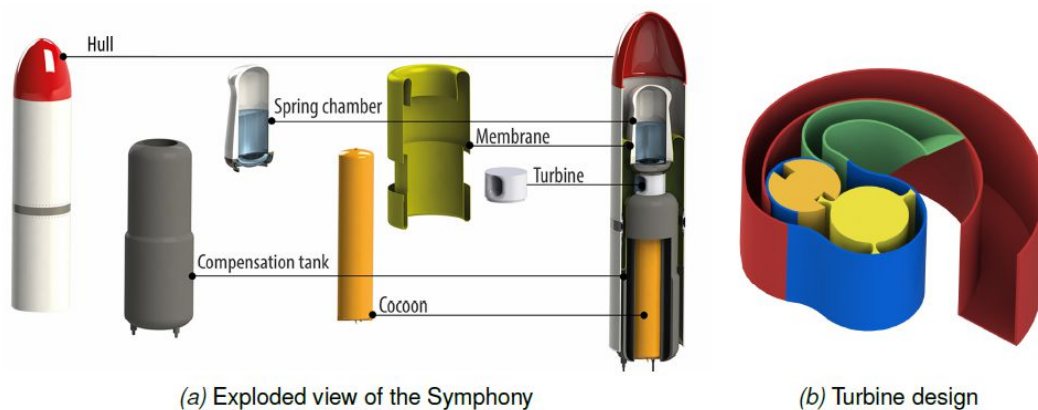


Figure 2.1: Pieces of the Symphony

There is a stationary part on the inside and a moving part on the outside, namely the floater, which can oscillate in the vertical direction. These two parts are connected through a rubber membrane. At the centre of the Symphony there is a chamber which contains a certain mass of air and a liquid below it. This liquid is also present in the membrane, thus, as the floater moves up and down, the liquid flows inside its variable given space. The flow of the liquid is intercepted by a specially designed positive displacement turbine [11], which adds resistance to the flow, so that energy can be extracted. The axis of the turbine is connected to the rotor of an electrical generator lower down the structure. An iron-cored permanent magnet synchronous generator has been chosen. Electronics are also present inside the stationary part. Everything, including the liquid, is watertight from the sea. The lower part of the Symphony is attached via a special structure to the sea bottom, so that it stays fixed. Finally, a mechanism to compensate for the tides has been designed, so that there is always the same vertical distance of approximately 6 m between the top of the floater and the sea

surface when both these things are in their equilibrium position [15]. This vertical distance is needed for safety reasons, as the Symphony must always be completely submerged.

2.3 Principle of operation

The sea waves cause an excess or lack of hydrostatic force on the Symphony with respect to when the sea surface is at its equilibrium position and it is this force that sets the device in motion. In the following paragraph, an ideal sinusoidal wave is assumed.

The incoming wave crest causes an extra hydrostatic force on the top of the Symphony, so the floater starts moving downwards. In this way, the volume inside the membrane decreases, so more liquid enters the chamber, while the liquid flow makes the turbine rotate in the one direction. This causes the volume of the air in the chamber to decrease, so pressure builds up. At some point, namely when the wave trough starts coming, this air pressure is high enough to push the liquid downwards and out of the chamber towards the membrane, so the turbine rotates now in the other direction due to the liquid flow. This means that the floater will start to move upwards, as the membrane expands in volume on its top side. These situations are depicted in Figure 2.2 [15], where the big arrows at the top show the direction of movement of the floater and the small arrows show the movement of the liquid.

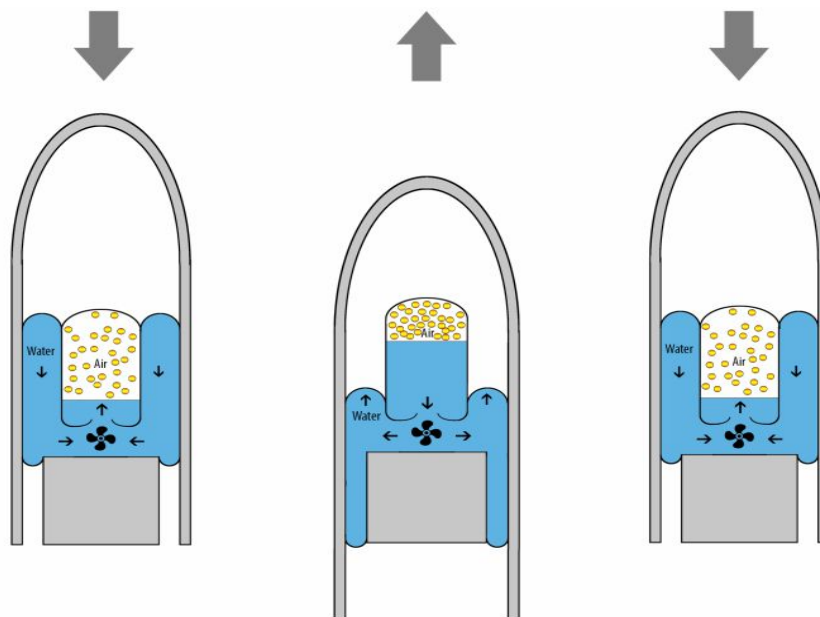


Figure 2.2: Directions of movement

The sequence of events for this ideal particular case of a sinusoidal wave can be seen more clearly in Figure 2.3 [11]. It can be seen that there is a phase shift of 90° between the position of the floater and the sea surface elevation, because, for example, the wave crest corresponds to the middle/equilibrium position of the floater with maximum downwards velocity. In other words, the velocity of the floater is in phase with the wave excitation force. In general, the higher half of the wave causes downwards motion of the floater and the lower half of the wave causes upwards motion [15]. The sequence repeats itself constantly, so the floater performs an oscillation. In reality, the waves are not perfectly sinusoidal, so the sequence deviates from that shown in Figure 2.3. The

purpose of the control system is to keep the motion of the floater as close as possible to this 90° phase shift, as will be shown later on. This is because, as seen in the literature and as proven with the optimization software, this phase shift results in the optimal energy extraction from the waves.

The acceleration of the floater, and consequently the velocity and position, are determined at every instant by the force balance. The dominating forces are the total hydrostatic force on top of the floater and the force that the air in the chamber exerts on the liquid, which are of course opposite in direction for the floater as a whole [6].

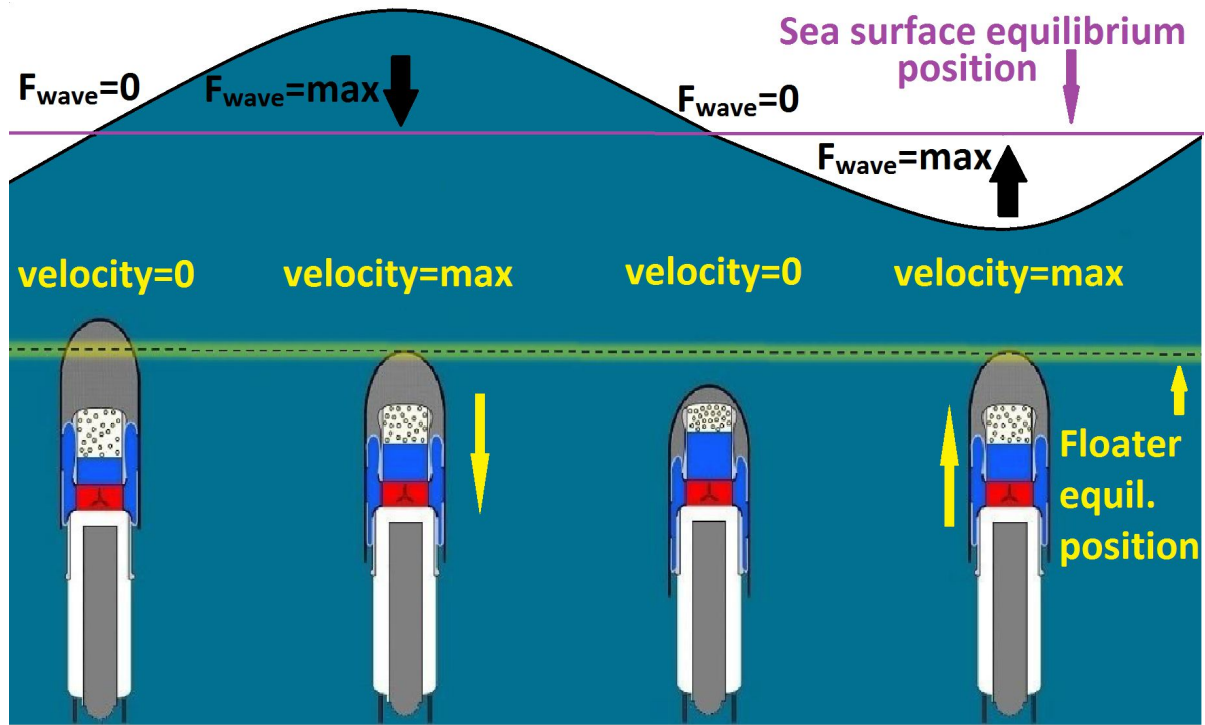


Figure 2.3: Operation of the Symphony

2.4 Mathematical modelling

To better understand the previously explained mechanism, the forces that act on the floater as a whole are presented. The upwards direction is defined as positive. The force balance is presented in Equations 2.1 and 2.2, where z , z_d and z_{dd} are the position, the velocity and the acceleration of the floater, respectively, m is the mass of the floater plus the mass of the moving inner liquid and ΣF is the sum of all the forces. The symbol t represents time.

$m \cdot z_{dd} = \Sigma F$	(2.1)
$m \cdot z_{dd} = F_g + F_{hs}(z) + F_{gas}(z) + F_{top}(z) + F_{drag}(z_d) + F_{rad}(z_d, z_{dd}) + F_{iron}(z, z_d) + F_{wave}(t) + F_{PTO}(z, z_{dd}, t)$	(2.2)

Now, a short description is given for each of the forces. A more analytical explanation of these forces and the relevant parameters is given in [6]. For a better understanding, some of the forces are depicted in Figure 2.4 [15], which shows a cross section of the Symphony.

(i) *Gravitational force, F_g* : This is the force that the Earth acts upon the floater and is always negative, with a fixed value, independent of the position of the floater. The mass of the floater as well as the moving mass of the liquid are taken into account. Thus, the equation is:

$$F_g = -m \cdot g = -(m_{fl} + m_{inn}) \cdot g \quad (2.3)$$

where g is the gravitational acceleration, m_{fl} is the mass of the floater and m_{inn} is the moving mass of the inner liquid.

(ii) *Hydrostatic force, F_{hs}* : This is the force due to the fact that the Symphony is submerged. As seen in Figure 2.4, this force acts on the top of the floater (black arrow), on the bottom of the membrane (orange arrows) and also on the bottom of the floater (purple arrows). The total result is always negative, with an absolute value increasing when going deeper, which means that the definition of a negative spring is fulfilled. For the calculation of this force, the related distances are measured with respect to the equilibrium sea surface height, thus independently of whether there are waves. The equation for this force is:

$$F_{hs}(z) = -A_{pp} \cdot \left(P_{amb} + \rho \cdot g \cdot (H_{pp} - z) \right) + A_{mb} \cdot \left(P_{amb} + \rho \cdot g \cdot \left(H_{mb} - \frac{z}{2} \right) \right) + A_b \cdot \left(P_{amb} + \rho \cdot g \cdot (H_b - z) \right) \quad (2.4)$$

where P_{amb} is the ambient air pressure at sea level, ρ is the density of sea water and H_{pp} , H_{mb} and H_b are the distances from the equilibrium sea surface to the pressure point, bottom of membrane and bottom of floater (all at equilibrium position of the floater), respectively. The factors A_{pp} , A_{mb} and A_b are related to these three distances and represent a corresponding area. See Figure 2.4 for the distances and locations of the corresponding areas. Note that in this figure, the floater is at its equilibrium position, $z = 0$. When the actual position of the floater changes, the factors H_{pp} , H_{mb} and H_b remain the same. This is why z or $\frac{z}{2}$ is being subtracted in the brackets in the previous equation. The result is that the hydrostatic force is linear with respect to the position of the floater.

(iii) *Chamber air force, F_{gas}* : The pressurised air in the chamber has a tendency to push the liquid down (brown arrow in Figure 2.4). The total volume of the liquid must remain the same, so the liquid pushes the walls of the membrane (the force is transferred to the membrane via the pressure in the liquid, see the pink arrows). The upper part of the membrane (which is attached to the floater) can roll, so the total volume of the membrane expands. This extra volume that is being created is of course taken by the liquid. In this way, the force caused by the air in the chamber has always a tendency to push the floater up, so it is always in the positive direction, as seen in the central part of Figure 2.2. The lower the floater, the smaller the volume of the air in the chamber, thus the higher the resulting force is. This means that the definition of a positive spring is fulfilled. The equation for this force is:

$$F_{gas}(z) = (A_{mu}(z) - A_{mb}) \cdot P_{eq} \cdot \left(\frac{V_{eq}}{V_{air}(z)} \right)^\gamma \quad (2.5)$$

where $A_{mu}(z)$ is related to the upper area of the membrane, $V_{air}(z)$ is the volume of the air in the chamber, V_{eq} and P_{eq} are the volume and pressure of this air, respectively, at equilibrium position of the floater and γ is the adiabatic constant. In other words, the ideal gas law is followed.

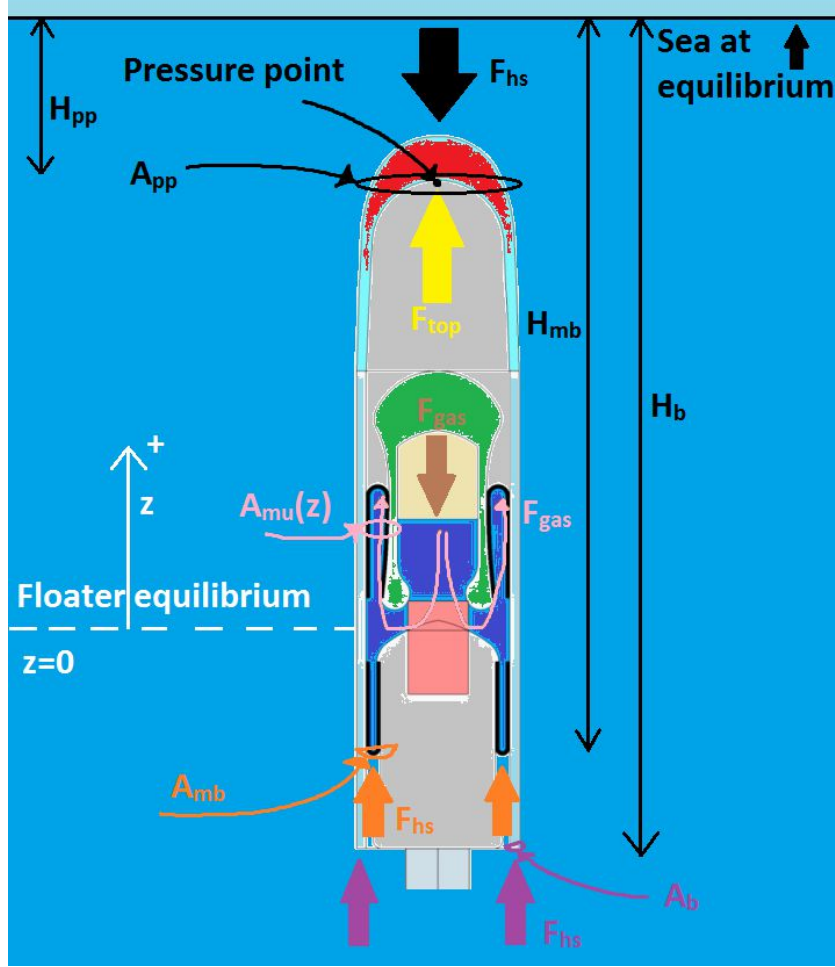


Figure 2.4: Some of the forces acting on the floater

(iv) *Floater air force, F_{top}* : The air inside the hull of the floater, above the membrane and chamber, has a certain pressure, which changes as the floater moves up and down. The resulting force on the floater as a whole is always in the positive direction, see the yellow arrow in Figure 2.4. The higher the position, the lower this force is, because the volume of the hull increases, so the pressure drops. Thus, again the definition of a positive spring is fulfilled. The equation for this force is:

$$F_{top}(z) = V_{ac} \cdot P_{amb} \cdot \left(\frac{V_{top}}{V_{top} + \frac{\pi}{4} \cdot d_{out}^2 \cdot (z - z_{0vac}) - \Delta V_{gas}(z)} \right)^\gamma \cdot \left(\frac{\pi}{4} \cdot d_{out}^2 - A_{mu}(z) \right) \quad (2.6)$$

where V_{ac} and z_{0vac} are factors related to the initial pressure in the hull [6], V_{top} is the volume of the hull at equilibrium position, d_{out} is the outer diameter of the membrane and $\Delta V_{gas}(z)$ is the volume of the membrane that is coming up.

(v) *Drag force, F_{drag}* : As the solid floater moves through the sea water, there is some resistance to this movement. The drag force is always opposite to the direction of the velocity and its absolute value depends on the square of the velocity, as well as on the drag coefficient, which is different in the upwards movement than in the downwards movement, because of the shape of the Symphony. Thus, this force is nonlinear. The expression is:

$$F_{drag}(z_d) = \begin{cases} -\frac{1}{2} \cdot \rho \cdot A_{pp} \cdot z_d \cdot |z_d| \cdot C_{Ddw} & \text{if } z_d < 0 \\ -\frac{1}{2} \cdot \rho \cdot A_{pp} \cdot z_d \cdot |z_d| \cdot C_{Dup} & \text{if } z_d > 0 \end{cases} \quad (2.7)$$

where C_{Ddw} and C_{Dup} are the drag coefficients in the downwards and upwards movement of the floater, respectively.

(vi) *Radiation force, F_{rad}* : The floater itself also radiates waves by oscillating in the sea. In this way, the sea water exerts a certain force on the floater, which has two components: one that depends linearly on the acceleration with a factor that is called added mass at infinity and one that is a convolution of the velocity with a so called retardation function, in other words there is some kind of ‘memory’ [16]. As the second component is very small compared to the other forces and also complicated to integrate in the model, it is neglected. However, a term that is kept in this model is the hydrodynamic damping, which is linear with respect to the speed. So, it can simply be stated that the floater has a fixed extra mass when it moves plus a linear damping. Thus, the expression used here for the radiation force is:

$$F_{rad}(z_d, z_{dd}) = -m_{added} \cdot z_{dd} - c_{hyd} \cdot z_d \quad (2.8)$$

where m_{added} is the added mass at infinity and c_{hyd} is the hydrodynamic damping coefficient.

(vii) *Iron loss force, F_{iron}* : The iron core of the electrical machine causes power losses when the rotor, thus also the turbine, rotates. These iron losses of the machine consist of hysteresis losses (proportional to the electrical frequency of the stator voltages, f_{el}) and eddy current losses (proportional to the square of the electrical frequency of the stator voltages) [2]. Thus, they are calculated as follows:

$$P_{ironloss} = -A_{iron} \cdot |f_{el}| - B_{iron} \cdot f_{el}^2 \quad (2.9)$$

As the electrical frequency f_{el} and the angular speed of the turbine ω_t are proportional, the previous equation can be rewritten as:

$$P_{ironloss} = -a_{iron} \cdot |\omega_t| - b_{iron} \cdot \omega_t^2 \quad (2.10)$$

The absolute value is put, because power is lost regardless of the direction of movement. This means that there must be a sort of ‘braking torque’ on the axis of the rotor/turbine, which extracts energy from the system, as represented by the negative signs. By choosing:

$$T_{iron} = -a_{iron} \cdot \text{sign}(\omega_t) - b_{iron} \cdot \omega_t \quad (2.11)$$

it is easily verified that:

$$P_{ironloss} = T_{iron} \cdot \omega_t \quad (2.12)$$

as expected. Note that this torque depends only on the speed of the turbine, thus it is independent of whether energy is being extracted or not from the system by a power take-off mechanism. This torque can be translated to a force on the floater as a whole with the following equation:

$$F_{iron}(z, z_d) = T_{iron} \cdot (A_{mu}(z) - A_{mb}) \cdot G_{turb} \quad (2.13)$$

The factors $(A_{mu}(z)-A_{mb})$ and G_{turb} , as well as the relation between ω_t and z_d , will be explained in Section 2.5.2.

It is not so easy to calculate the parameters a_{iron} and b_{iron} , so an estimation needs to be made. In the datasheet of the machine [17], the efficiency is given at rated power, so the total iron losses at rated power can be calculated. This gives one linear equation for a_{iron} and b_{iron} . The total iron losses for different types of iron core are given in [18]. By comparing the losses at different electrical frequencies, the ratio a_{iron}/b_{iron} can be calculated. This ratio is approximately stable around 33.5 s^{-1} for the different types. Thus, with the linear equation and the ratio, the parameters are calculated to be $a_{iron} = 6.44 \text{ J}$ and $b_{iron} = 0.19 \text{ J} \cdot \text{s}$. This means that at the rated turbine angular velocity of 350 rpm , thus 36.65 rad/s , the hysteresis losses and eddy current losses are approximately equal.

(viii) Wave force, F_{wave} : The waves create more or less hydrostatic force on the floater, with respect to when the sea surface is at equilibrium. This wave force depends only on the wave and not on the position of the floater (because only the 'extra' or 'missing' water column is taken into account), in contrast to the hydrostatic force mentioned in (ii), which depends only on the position of the floater and not on the wave (because everything is measured from the sea surface equilibrium point). In this report, the waves will be modelled as either monochromatic waves, which implies a perfectly sinusoidal sea surface elevation over time with fixed frequency and amplitude, or random irregular waves that follow the Bretschneider spectrum and are of course closer to reality. The Matlab time domain model can generate such waves in the form of a time-series of a force. This force is then used as an input on the floater. A closer look at the waves will be taken in Chapter 4.

(ix) Power take off (PTO) force, F_{PTO} : By applying torque on the generator, this torque is transferred to the turbine, thus resistance to the flow of the inner liquid is created. In this way, energy can be extracted from the system. This force will be analyzed more extensively in the next section.

It can be seen that forces (i) to (vii) are 'internal' in the Symphony, as they only depend on the position, velocity and acceleration of the floater and on intrinsic parameters of the Symphony that are already designed, such as the geometry and the mass. The wave force is 'external' to the Symphony and is the source of energy. The objective of this thesis is to make the PTO force follow a certain pattern, in order to optimally control the movement of the floater.

2.5 The mass-spring-damper system

2.5.1 Initial design

It is obvious that forces (ii), (iii) and (iv), namely the hydrostatic, chamber air and floater air forces, depend only on the position, which fulfils the definition of a mechanical spring. The geometry of the device has been designed in such a way that the total of these three forces plus the gravitational force is linear with respect to the position of the floater when it is close to the equilibrium point and becomes nonlinear further away. The spring becomes much stiffer in the nonlinear region, so the floater cannot easily oscillate more than it should, even in high waves. This is also a form of built-in protection for the case of control system or generator failure [6].

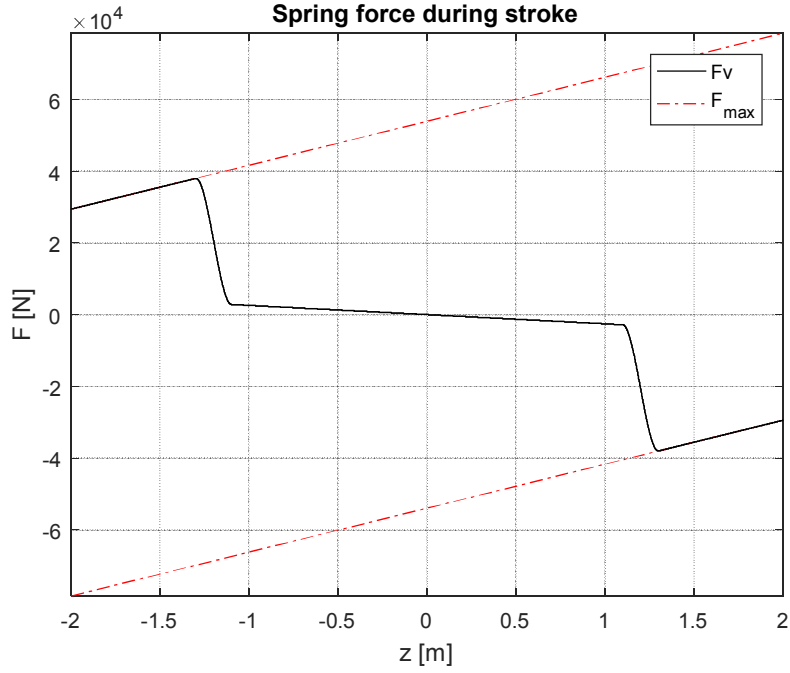


Figure 2.5: Spring force as a function of position, initial design

This can be seen more clearly in Figure 2.5, which is generated from the Matlab time domain model. For positions $|z| < 1.12 \text{ m}$, thus in the linear region, the spring is positive, with a constant of $k_{ini} = 2574 \text{ N/m}$ in the initial design, prior to this thesis. This can be seen from the small negative slope in the figure (a negative slope means a positive spring). For positions $1.12 \text{ m} < |z| < 1.3 \text{ m}$, the positive spring has a much higher constant of approximately $k_{stiff} = 200000 \text{ N/m}$. This can be seen from the fact that the slope suddenly increases very much. For positions $1.3 \text{ m} < |z| < 2 \text{ m}$, the slope changes in sign, but the spring force has an opposite sign than the position, which means that the spring ‘pulls’ the floater back to the equilibrium point, but the magnitude of this ‘pulling’ decreases as the floater moves further away. In any case, the spring is very stiff for positions $|z| > 1.12 \text{ m}$. This special total form of the spring force is due to the combination of positive springs with a negative spring in the Symphony. The total mass of the floater and the moving liquid plus the added mass at infinity add up to $m_{tot} = 6520 \text{ kg}$. Thus, the natural frequency of the system is [19]:

$\omega_0 = \sqrt{\frac{k_{ini}}{m_{tot}}} = 0.63 \text{ rad/s}$	(2.14)
--	--------

This corresponds to a period of $T_0 = 10 \text{ s}$. This is also the period of the sea waves in the arbitrary chosen reference case, so the Symphony has been tuned optimally.

2.5.2 Influence of the turbine’s inertia

A problem with this initial spring constant design in the linear region is that it did not take into account the inertia of the turbine. To understand this, a closer look at the PTO force is necessary. The torque balance on the turbine is:

$I_t \cdot \dot{\omega}_t = T_t + T_e$	(2.15)
--	--------

where I_t is the inertia of the turbine, $\dot{\omega}_t$ is the angular acceleration of the turbine, T_t is the torque that the inner liquid flow exerts on the turbine blades and T_e is the torque that the generator exerts on the turbine. Here, a lot of care needs to be taken with the signs. Throughout this thesis, the velocity of the floater and the angular velocity of the turbine have always the same sign. Thus, if, for example, the floater is moving upwards and the generator causes resistance to the rotational movement of the turbine, it is $z_d > 0$, $\omega_t > 0$ and $T_e < 0$.

The torque T_t is a result of the other forces that act on the floater and of the generator torque. In the next example, it will be assumed that there is no generator torque, thus $T_e = 0$. See Figure 2.6 for better understanding, where a simplified turbine model is shown. Now, let's imagine that the floater is moving upwards at constant speed ($z_d > 0$, $\omega_t > 0$) and at some point a force in the negative direction (downwards) is applied on the floater. This means that the volume flow of the inner liquid through the turbine will have a tendency to decrease, thus the angular speed of the turbine ω_t will also have a tendency to decrease ($\dot{\omega}_t < 0$). As the turbine has some inertia, it will resist and have a tendency to keep the angular speed constant, by 'pushing' the liquid through. This means that a force F_t is exerted on the liquid (green arrow in Figure 2.6). This force causes a pressure difference at the turbine. This pressure is transferred through the liquid towards the membrane, where it becomes a force, which has a tendency to push the floater upwards. It is this force on the membrane that is defined as the PTO force.

Of course, according to the 3rd law of Newton, a force equal in magnitude and opposite in direction to F_t will be exerted on the turbine (red arrow) and this is translated to a torque. This is the torque T_t , thus the torque that the liquid exerts on the turbine blades. Thus, in this case it is $F_{PTO} > 0$ and $T_t < 0$, because the PTO force in this case has a tendency to maintain the upwards (positive direction) movement of the floater.

For the same direction of movement, a similar result is obtained if there is no external force, but the generator exerts a torque that has a tendency to speed up the turbine ($T_e > 0$). This is because, in this case, the turbine 'pushes' the liquid in the direction that maintains the upwards movement of the floater ($F_{PTO} > 0$) and the liquid exerts a 'braking' torque on the turbine ($T_t < 0$), according to the 3rd law of Newton. The opposite result, thus $F_{PTO} < 0$ and $T_t > 0$, is obtained if, with no generator torque, an external force has a tendency to lift the floater up (force in the positive direction) or if, with no external force, the generator acts as a brake on the turbine ($T_e < 0$).

In reality, the final sign of the PTO force is determined by the directions and magnitude of all the forces acting on the floater and of the generator torque, because all these affect the liquid flow.

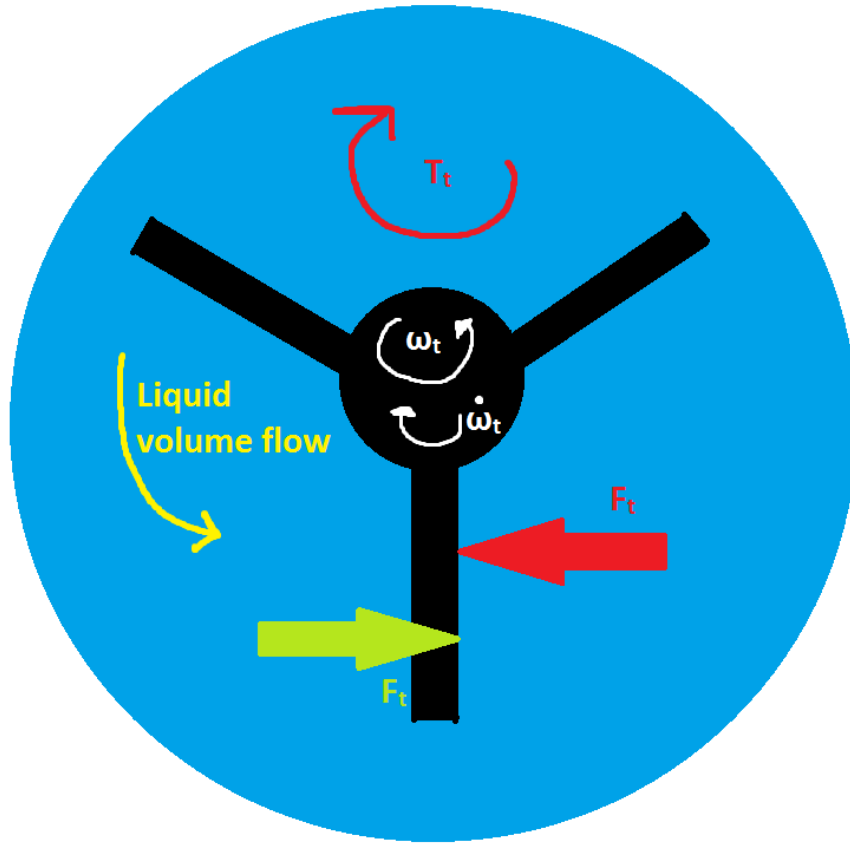


Figure 2.6: Example of torque on turbine and force on liquid

The torque on the turbine is translated to the PTO force on the floater as a whole with the following equations [6]:

$\Delta P = G_{turb} \cdot T_t$	(2.16)
$F_{PTO} = -(A_{mu}(z) - A_{mb}) \cdot \Delta P$	(2.17)

where ΔP is the pressure difference on the turbine and the difference $A_{mu}(z) - A_{mb}$ is related to the top and bottom areas of the membrane, as seen previously. This difference is slightly dependent on the floater position, but has always a positive value fluctuating around 0.11 m^2 . This can be seen more clearly in Figure 2.7, which is generated from the Matlab time domain model and shows this difference as a function of the floater position.

The factor G_{turb} , which is equal to 531.19 m^{-3} , is related to the volume of the turbine, which has been calculated by the fact that a liquid volume flow of approximately 69 l/s occurs at the nominal speed of 350 rpm [8]. The result is that T_t and F_{PTO} will always have opposite signs, as expected.

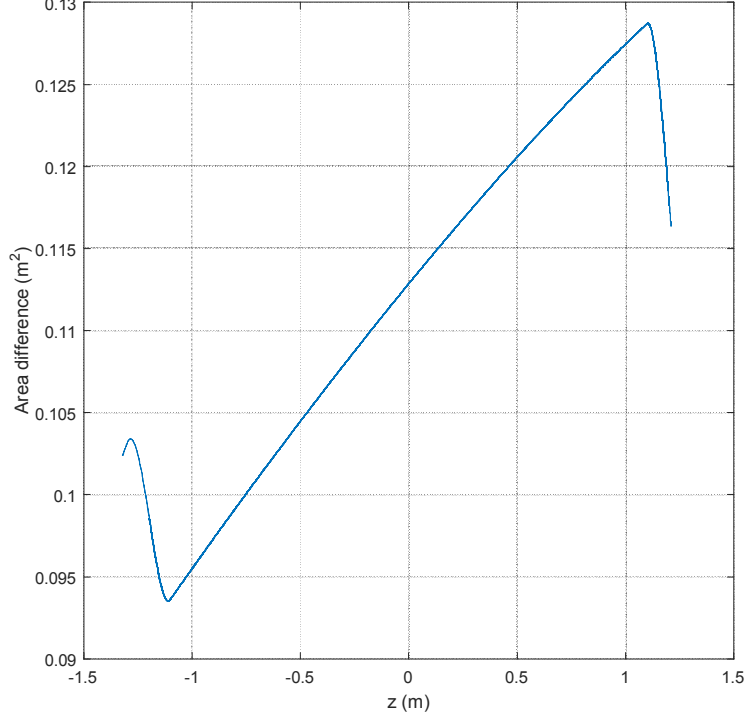


Figure 2.7: Area difference as a function of floater position

The ratio between the angular velocity of the turbine and the velocity of the floater, $\frac{\omega_t}{z_d}$, which is equal to the ratio between the angular acceleration of the turbine and the acceleration of the Symphony, $\frac{\dot{\omega}_t}{z_{dd}}$, is equal to $G_{turb} \cdot (A_{mu}(z) - A_{mb})$, as this reflects the design of the membranes and is related to the liquid flow.

Thus, the final expression for the PTO force is:

$$F_{PTO}(z, z_{dd}, t) = -(A_{mu}(z) - A_{mb}) \cdot G_{turb} \cdot (I_t \cdot (A_{mu}(z) - A_{mb}) \cdot G_{turb} \cdot z_{dd} - T_e(t)) \quad (2.18)$$

By taking the mean value of the difference $A_{mu}(z) - A_{mb}$ and by inserting the value of the inertia, which has been calculated to be $I_t = 4.87 \text{ kg} \cdot \text{m}^2$, the 'mean' PTO force can be written as follows:

$$\begin{aligned} \overline{F_{PTO}} &= -59.97 \text{ m}^{-1} \cdot (292.15 \text{ kg} \cdot \text{m} \cdot z_{dd} - T_e) \\ &= -17520.46 \text{ kg} \cdot z_{dd} + 59.97 \text{ m}^{-1} \cdot T_e \end{aligned} \quad (2.19)$$

The first term in this equation denotes that there is in fact a sort of equivalent mass, which fluctuates around $m_{eq} = 17520.46 \text{ kg}$. This is very high compared to the original mass of $m_{tot} = 6520 \text{ kg}$, so the turbine's inertia makes the whole system much 'heavier' than expected. It is this equivalent mass that needs to be taken into account for the design of the spring constant, because the 'total final mass', $m_{tot} + m_{eq}$, is more than 3 times higher than the original one, so the spring constant needs to adapt to this. As the natural frequency of the Symphony needs to remain at $\omega_0 = 0.63 \text{ rad/s}$ in the standard case, the final spring constant k_{fin} in the linear region can be calculated from the following equation:

$$\frac{k_{ini}}{m_{tot}} = \frac{k_{fin}}{m_{tot} + m_{eq}} \quad (2.20)$$

This leads to $k_{fin} = 9491 \text{ N/m}$, which makes a significant difference. This number can also be seen from the slope of the linear part in Figure 2.8. Note that it is only the linear region that changes, the stiff region remains as before. This means that the geometry of the membrane and the gas pressure in the chamber still need to be tuned in an appropriate way, so as to reach this final spring constant. The membrane can only be designed once, so it will be ‘tuned’ to this particular spring stiffness of 9491 N/m , which corresponds to the reference case of 10 s sea waves. For the gas pressure, a mechanism to alter it manually has been foreseen in the Symphony, so this can easily be adapted in an appropriate way to the period of the incoming waves (which changes over a long time), so as to keep the Symphony resonant. Of course, as the membrane geometry does not change, there will be an insignificant nonlinearity in the spring for wave periods (or, equally, natural periods of the Symphony) other than 10 s.

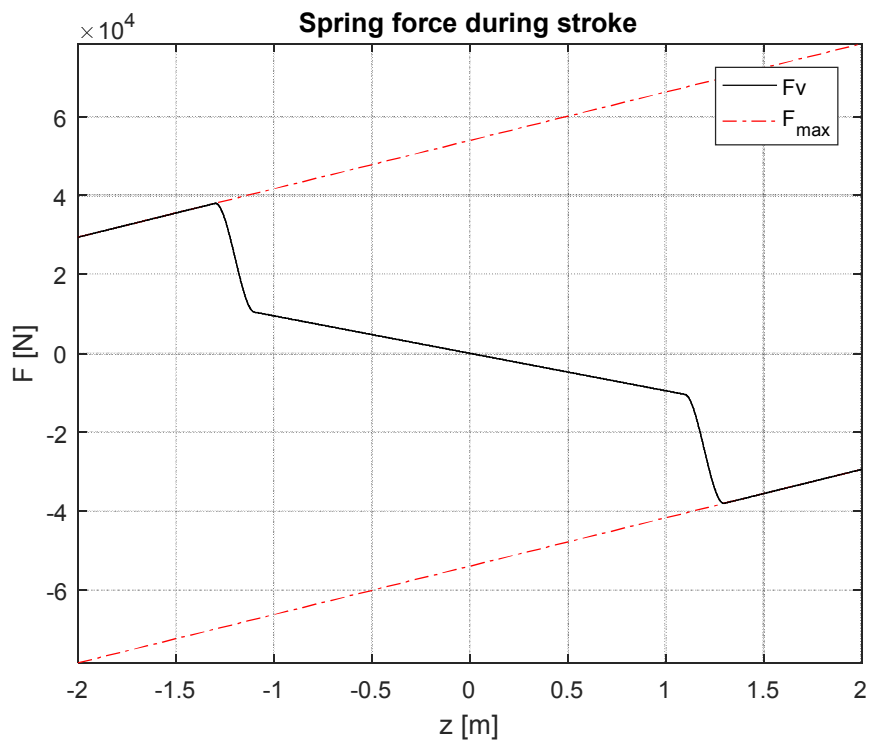


Figure 2.8: Spring force as a function of position, final design

To sum up, the drag force, radiation force, iron loss force and PTO force damp the oscillation, ‘internally’ and ‘externally’, but the former three are much smaller than the latter, as will be seen later on. Thus, the floater is in a fact a mass-spring-damper system that is forced to oscillate by the external, mostly unknown, wave force, and this oscillation needs to be controlled.

3. Time Domain Model

3.1 Introduction

A model is needed to simulate in real time how the Symphony responds to an incoming wave. For this reason, Teamwork Technology has developed a code in Matlab/Simulink. In this chapter, a brief description is given of both the Matlab script and the Simulink model, to understand its basic role in representing the Symphony. The most important part of the model concerns the control system, which applies the desired torque on the turbine, by real-time measurements of certain quantities and calculations. Next, the equations that govern the necessary AC/DC converter are presented. Finally, the way, in which the final energy output of the Symphony is calculated, is shown. For this, the energy losses of the generator as well as of the cable that goes to shore need to be taken into account.

3.2 Matlab script

The Matlab script is very big and consists of various files, in which all the properties of the Symphony and the surrounding media are described with a very high detail. For example, the geometry is fully specified, so that the 'internal' forces acting on the floater can be calculated precisely for every value of position, speed and acceleration of the device. Also, the code can generate various time series of waves, which are then used as an input force on the floater.

In this thesis, most of the code is left untouched, as it concerns fixed values and functions. Some parameters have been introduced or changed here and there, of course. The most important things that are varied by the user are:

-The type of waves that are used: The user chooses whether the waves are monochromatic or random, their duration, their height, their period etc. Also, when concerning random waves, a new wave can be put on the Symphony every time or a saved wave, in other words a fixed time-series of wave force, can be used. The latter is needed for comparison of the Matlab, thus realistic, response of the Symphony with the GAMS optimal output, because in such a case the same wave must be used of course.

-The output of Matlab: Some extra lines of code can be put to calculate the necessary results, such as the actual energy that the Symphony has obtained from the waves during the whole time period. Also, the results can be visualised with the help of figures, for example the position or a certain force can be plotted as a function of time.

3.3 Simulink model

The Matlab script is linked to a Simulink model, in order to implement the concept of time in the software. As seen in Figure 3.1, the model basically consists of several blocks, which represent subsystems. Most of the blocks contain calculations of the forces mentioned in Chapter 2. For these, some of the parameters mentioned in the script are used. By coupling either the block 'Savedwave'

or the block 'Waves' to the summation block, the choice between a certain saved wave or a newly generated wave, respectively, is made. In the block 'Floater dynamic', Equation 2.1 is in fact applied, so that the acceleration z_{dd} of the floater is calculated. By using integrator blocks, the velocity z_d and position z of the floater are calculated. These three calculated quantities are the output of this block and are fed back as inputs to the force calculation blocks. The iron loss 'torque' is not viewable in this figure, because it is used inside the 'Generator' block. Finally, a block is used to stop the simulation if the position of the floater exceeds 2 m in any direction from the equilibrium point.

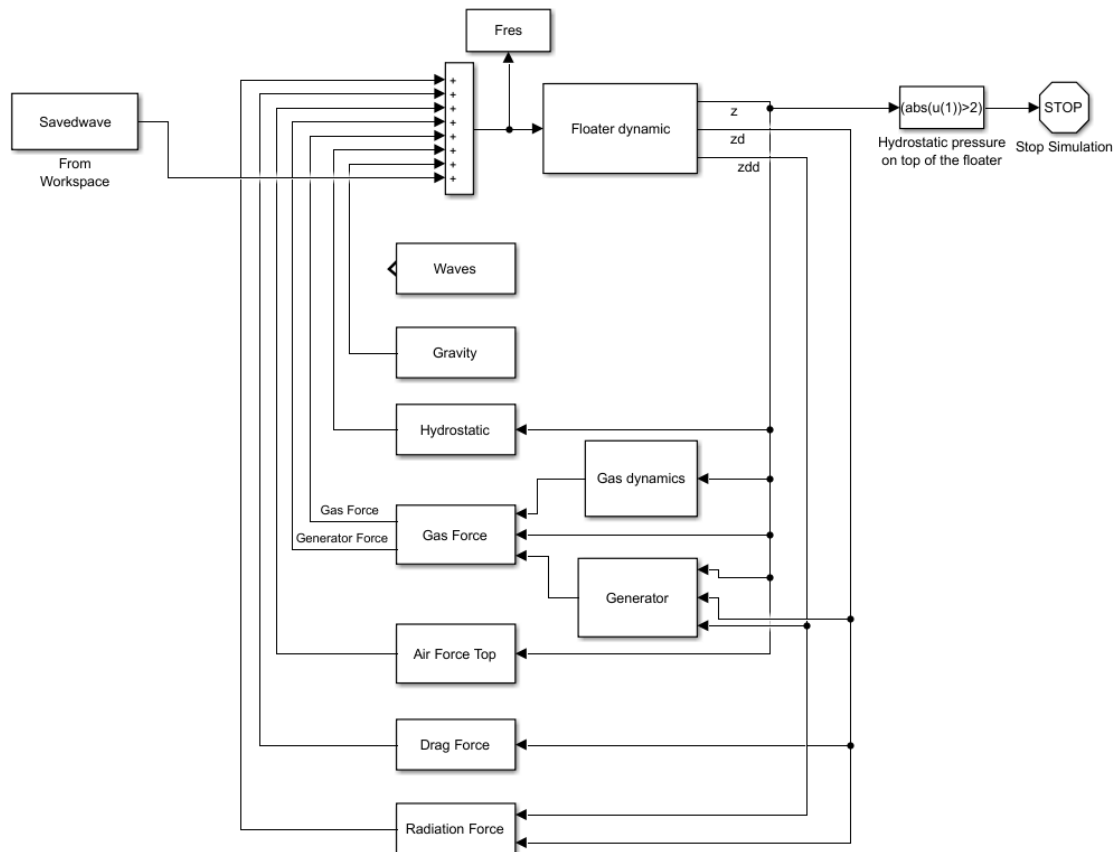


Figure 3.1: The Simulink model

3.4 The existing controller

The block 'Generator' is of particular interest for this thesis. There, the pressure difference on the turbine is calculated, which can then be used to calculate the PTO force further on. The most important part of this block for this thesis concerns the calculation of the electromagnetic torque that the generator has to apply on the rotor, and consequently on the turbine, with the help of the control system.

The ideal control system would be to apply an amount of electromagnetic torque that represents the 'internal' damping of the system: the damping caused by the drag force and the radiation force (hydrodynamic damping), translated into torque via the factor $\frac{1}{(A_{mu}(z) - A_{mb}) \cdot G_{turb}}$, as seen in Equation 2.18, plus the 'damping' caused by the iron losses. The reason why the electromagnetic torque is chosen to be equal to the 'internal' damping of the floater is that this is the condition for optimal energy absorption under no oscillation amplitude constraints [20]. This non-constrained

situation occurs in fact at really small waves, because then the ideal amplitude of oscillation (the amplitude for which the energy extraction is maximum) is in the linear spring region.

However, at higher waves, the ideal amplitude of oscillation is far above the limits of the linear spring region, it is even above the $\pm 2 m$ limit that is allowed for the floater. Thus, in this case, which occurs most of the time, the previous method with the internal damping can no longer be used. For this reason, an innovative control system has been designed by Teamwork Technology. A picture of this system is shown in Figure 3.2. The actual position of the floater, its speed and the angular velocity of the turbine are used to calculate the energy contained in the spring, E_{spring} , and the kinetic energy of the device, E_{kin} , respectively, as shown in Equations 3.1 and 3.2.

$E_{spring} = 0.5 \cdot k(z) \cdot z^2$	(3.1)
$E_{kin} = 0.5 \cdot m_{tot} \cdot z_d^2 + 0.5 \cdot I_t \cdot \omega_t^2$	(3.2)

where $k(z)$ is the spring constant at every position.

The sum of these two equals the mechanical energy, E_{mech} . Then, a subtraction is made between the actual mechanical energy and the ‘maximum mechanical energy’, which is the mechanical energy that the floater would have if it performed a desired sinusoidal oscillation with a period that is equal to the period of the incoming waves and an amplitude of $1.1 m$, with a linear spring, optimally tuned to the period of the incoming waves. For the standard case of $10 s$ waves, this maximum mechanical energy is equal to:

$E_{max} = 0.5 \cdot k_{lin} \cdot z_{control}^2 = 0.5 \cdot 9491 \frac{N}{m} \cdot 1.1^2 m^2 = 5742 J$	(3.3)
---	-------

The result of the subtraction is called the ‘energy error’ and is symbolized as *error*. When the energy error is positive, it means that the floater has an excess of energy with respect to the ideal sinusoidal operation described previously. This excess energy should be harvested from the floater. When the energy error is negative, it means that the floater has a lack of energy with respect to the ideal sinusoidal operation. This means that, in this case, the control method with the internal damping can be used. However, if this other control method is not used at all, then, for the case of a negative energy error, the lack of energy should be provided to the floater, only if this lack does not exceed a certain value. This implies that energy flows in both directions, which means that the electrical machine at the bottom of the Symphony will sometimes act as a generator and sometimes as a motor. It is desired that the generator action is dominant, as, in total, energy must be supplied to the grid. The amount of energy that may be provided to the floater, in the case of a negative energy error, is a subject that will be investigated in Chapter 5.

The energy error signal is then passed through a simple PI controller, the parameters of which need to be tuned in this work. The result is multiplied with the speed and then reversed in sign. This is because, when the energy error is positive, a kind of brake on the floater is needed and not an accelerator. Similarly, when the energy error is negative, a kind of accelerator on the floater is needed and not a brake. In other words, the output of the controller and z_d must always have opposite signs for positive errors and must always have the same sign for negative errors.

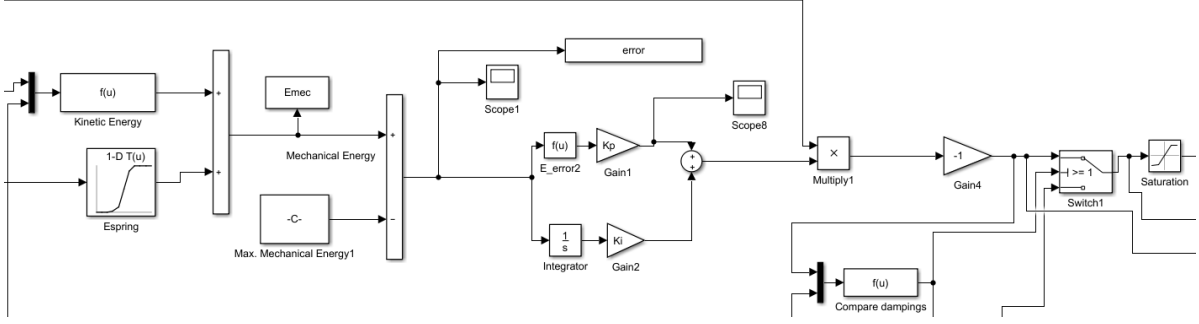


Figure 3.2: Close-up view of the controller

Afterwards, a ‘switch’ block is used to choose between this torque signal from the PI controller output (signal1) and the torque signal that represents the ‘internal’ damping of the system (signal2). Signal1 passes through when it is bigger in absolute value than signal2, otherwise signal2 passes. This method is used to ensure that there will be a sufficient amount of electromagnetic torque on the generator in really small waves, when the energy error is too negative to be taken into account or when the output of the PI controller is quite small due to a small energy error. Otherwise, no energy or not enough energy would be harvested in this case.

Finally, the signal is passed through a saturation block with limits $|T_{e,max}|$ and $-|T_{e,max}|$. To sum up, the final output of the controller is the electromagnetic torque, which is described by:

$$T_e = \begin{cases} -z_d \cdot \left(K_p \cdot error + K_i \cdot \int_0^t error(\tau) \cdot d\tau \right) = signal1, & \text{if } |signal1| > |signal2| \\ \frac{F_{drag}(z_d) - c_{hyd} \cdot z_d}{(A_{mu}(z) - A_{mb}) \cdot G_{turb}} + T_{iron} = signal2, & \text{if } |signal1| < |signal2| \end{cases} \quad (3.4)$$

where

$$error = E_{mech} - E_{max} \quad (3.5)$$

3.5 Converter

The controller calculates the electromagnetic torque that needs to be developed in the generator. For this to happen in reality, some current must flow through the stator windings. This is why the output of the controller is connected to an AC/DC converter, which makes sure the current is as desired. The precise function and choice of the converter is the subject of further research on the Symphony. The only thing needed here is the calculation of the current.

It can be assumed that the converter aligns the phasors of the stator current I_a and excitation voltage E_f of the synchronous machine. This is a commonly used practice, which results in the decoupling of the field flux and the flux caused by the stator currents [21]. The excitation voltage depends linearly on the angular velocity of the rotor/turbine [21]:

$$E_f = K \cdot \omega_t \quad (3.6)$$

where K is the machine constant. Note that RMS values are being used for I_a and E_f . The electromagnetic torque is equal to [21]:

$$T_e = 3 \cdot \frac{E_f \cdot I_a \cdot \cos\varphi}{\omega_t} \quad (3.7)$$

where φ is the angle between the phasors of E_f and I_a . If these phasors are aligned, it is $\cos\varphi = 1$, so, by using Equation 3.6, it is concluded that:

$$I_a = \frac{T_e}{3 \cdot K} \quad (3.8)$$

which is a linear relation. The constant K can be calculated from the datasheet of the machine used, so in this case it is equal to $4.12 \text{ V} \cdot \text{s}$ [17], which means that the (per phase) current I_a can also be calculated at every moment in Matlab.

3.6 Energy calculations

As stated previously, this thesis deals with the energy that the Symphony can extract from the waves and provide to the grid. Thus, the most important calculations concern energy absorption and losses.

3.6.1 Initial energy

The energy that is taken from the waves and flows to the stator windings is the integral of the power of the electromagnetic torque. This extracted energy is calculated as follows over a period of time T , where the minus sign is put so that the result is positive:

$$E_{initial} = \int_0^T P_{initial}(t) \cdot dt = \int_0^T -T_e(t) \cdot \omega_t(t) \cdot dt \quad (3.9)$$

3.6.2 Copper losses

Some energy is lost in the electrical machine, the converter and the electrical cable that goes to shore. The copper losses, because of the resistance of the stator windings, are calculated as follows over a period of time T [2]:

$$E_{copperloss} = \int_0^T P_{copperloss}(t) \cdot dt = \int_0^T 3 \cdot I_a^2(t) \cdot R_{phase} \cdot dt \quad (3.10)$$

where R_{phase} is the resistance per phase of the stator windings, which is equal to $R_{phase,initial} = 0.2 \Omega$ at a temperature of $T_{initial} = 20^\circ\text{C}$ [17]. It can be assumed that the windings have a temperature of $T_{final} = 60^\circ\text{C}$ during operation, thus the final value of the resistance is [22]:

$$R_{phase,final} = R_{phase,initial} \cdot (1 + \alpha_{20} \cdot (T_{final} - T_{initial})) \quad (3.11)$$

where α_{20} is the temperature coefficient of resistance of copper at 20°C . By using the value $\alpha_{20} = 3.86 \cdot 10^{-3} \text{ }^{\circ}\text{C}^{-1}$ [22], it is calculated that $R_{\text{phase,final}} = 0.23 \text{ } \Omega$, which does not make a big difference.

3.6.3 Cable losses

The cable that goes from the converter to shore will have a DC voltage of $V_{DC} = 400 \text{ V}$. A distance of 200 m is assumed, so the total length of the cable will be $l = 400 \text{ m}$ (back and forth). The DC current in this cable can be calculated with the help of the power output of the converter, P_{out} . The calculation is as follows:

$$i_{DC} = \frac{P_{\text{out}}}{V_{DC}} = \frac{P_{\text{initial}} - P_{\text{copperloss}}}{V_{DC}} \quad (3.12)$$

Thus, the energy loss on the cable is:

$$E_{\text{cableloss}} = \int_0^T P_{\text{cableloss}}(t) \cdot dt = \int_0^T i_{DC}^2(t) \cdot R_{\text{cable}} \cdot dt \quad (3.13)$$

where R_{cable} is the total resistance of the cable.

It is not possible to have no losses on this cable. A reference case is chosen, where the energy losses on the cable do not exceed 2% in most waves. By experimenting in Matlab, it is calculated that for this reference case, the resistance of the cable needs to be $R_{\text{cable}} = 0.35 \text{ } \Omega$. The equation for the resistance is:

$$R_{\text{cable}} = \rho_{Cu} \cdot \frac{l}{S} \quad (3.14)$$

where $\rho_{Cu} = 1.72 \cdot 10^{-8} \text{ } \Omega \cdot \text{m}$ is the resistivity of copper [23]. The result is that $S = 19.44 \text{ mm}^2$.

The type of cable that will be used has not been chosen yet, so it is not possible at the moment to determine its price. However, a method is presented here to facilitate this future decision. The Symphony has an approximate annual energy yield of 16000 kWh [6], which gives 240000 kWh for 15 years. This has been calculated for no cable losses. For this period, the feed-in tariff in Portugal is $0.26 \text{ } \text{€}/\text{kWh}$ [2]. This means that the total income, for no losses, can be estimated at $0.26 \frac{\text{€}}{\text{kWh}} \cdot 240000 \text{ kWh} = 62400 \text{ } \text{€}$. In this way, each number of cable losses, as a percentage of the energy that flows to the converter, corresponds to a certain economical cost. For example, 1% extra/less energy losses on the cable correspond to an economic loss/profit of $1\% \cdot 62400 \text{ } \text{€} = 624 \text{ } \text{€}$.

Experiments in Matlab are performed for cases of other percentages (than the reference case) that must not be exceeded in most waves. The results are shown in Table 3.1, where the corresponding necessary resistance and thickness of the cable are shown. Also, the economic loss or profit due to the more or less energy losses on the cable, as compared to the 2% reference case, is shown. Positive values indicate economic profit and negative values indicate economic loss. When the type of cable will be known, the economic loss or profit of buying a thicker or thinner cable, compared to

the thickness of the cable for 2% losses, can be calculated, thus a cost/benefit analysis can be made then, so as to choose the optimal cable thickness.

Table 3.1: Energy cost and resistance calculations

Cable losses as percentage of energy at converter	Economic profit/loss as compared to reference case (€)	Necessary resistance $R_{cable} (\Omega)$	Necessary cable thickness $S (mm^2)$
0.25%	1092	0.04	155.55
0.5%	936	0.09	77.78
1%	624	0.18	38.89
2% (reference)	0	0.35	19.44
3%	-624	0.53	12.96
4%	-1248	0.71	9.72

For the rest of this thesis, the reference scenario of not more than 2% losses most of the time will be used, thus R_{cable} is set in Matlab equal to 0.35 Ω .

3.6.4 Final energy

Thus, finally, the net energy that has been extracted from the waves is formulated as follows:

$$E_{final} = E_{initial} - E_{copperloss} - E_{cableloss} \quad (3.15)$$

All this can easily be calculated in Matlab, as long as the relevant parameters are known. The result can be used to evaluate the performance of the control system.

Note that, as stated in Chapter 2, the iron losses have already been taken into account here as 'internal' in the system. A separate calculation for them can be made of course, but they must not be subtracted from the initial or final energy.

4. Maximum Energy Yield

4.1 Introduction

In order to evaluate the previously described control system or, more generally, any control system for the Symphony, it is necessary to find out how the optimal control system looks like. This concerns various parameters, such as the type and amplitude of oscillation, dealing with the constraints and uncertainties, the extracted energy and the mathematical modelling. Such an investigation can be performed both on a theoretical level, with the help of the available literature, and on a practical level, by using specifically designed optimization software.

This chapter starts with an extensive literature overview about optimal control of wave energy devices and how some of this knowledge can be applied to the Symphony. Then, the GAMS software, which is all about optimization and is used for this thesis, is shortly described. This is followed by a brief presentation, piece by piece, of the GAMS code used for the optimization problem concerning the Symphony and of the necessary assumptions made. Next, the code is run and the results, concerning the extracted energy and the movement of the Symphony, are presented. This is done both for regular and irregular waves. Finally, an analysis is performed, to observe how sensitive the GAMS result is to changes in certain parameters.

4.2 Literature overview

Control of the movement of wave energy converters is a topic that has been addressed a lot in the literature. In [9];[24];[25], the principles of wave energy capturing are described and it is proven that a wave energy converter oscillating only in heave mode, such as the Symphony, can extract up to 50% of the incoming wave energy, if the phase and amplitude of oscillation are appropriate. Absorption of waves means generation of waves by the oscillation of the device and the interaction between the incoming and the radiated waves needs to be as destructive as possible. An efficiency of even 100% can be reached in some cases when there are multiple modes of oscillation. In [9], two upper limits are presented for the power that can be extracted from sinusoidal waves.

In [26], the general principles for optimal control of wave energy devices are stated. Among other things, it is important that the velocity of the device is in phase with the wave excitation force and that the amplitude of oscillation has a certain optimal value, which increases as the wave height increases. Thus, when there are amplitude constraints, this optimal value cannot be reached at high waves. For this case, an upper limit to the power extraction is given, which depends on the volume of the device. In any case, the paper states that short-term future prediction of the wave or movement of the device is needed. In [27], an analysis is made of a simple control method with a feedback loop, with which the velocity of the oscillating wave energy device and the wave force are always in phase and at a stable ratio for all frequencies, without the need of prediction. In this method, a transfer function on the feedback signal (of the velocity) is designed, which takes into account the open-loop transfer function between the wave force and the velocity of the device, in such a way that the closed-loop transfer function between the wave force and the velocity of the

device is a constant number. By applying this method to the Symphony and by assuming a completely linear spring and linear damping, the result is a PTO force that is proportional to the velocity of the floater with a fixed proportionality constant. In [24], an analysis is made of the method of latching control, which implies locking the position of the device at some moments, in order to keep the phase of oscillation as desired. In this way, the velocity is more 'concentrated' at the maximum values of the wave force, so the power increases. This method also requires future prediction of the waves. In [28], laboratory experiments are conducted with a floating wave energy converter, so as to examine, among other things, the influence of certain nonlinearities in the forces. In [29], control methods are presented for a point absorber that has a hydraulic power take off system, which can be connected to an electrical generator or to additional energy accumulators.

For the Symphony, it is important to examine the literature about its predecessor, the Archimedes Wave Swing (AWS). In [30], internal model control is applied to the AWS. This is a method that uses a block diagram containing the system to control, the inverse of the system, a model of the system and a filter. It is concluded that with internal model control the energy absorption from the waves can be more than five times higher compared to the situation without control (where a residual force of the electrical generator extracts energy), which is a better result than the originally developed PID controller for the AWS. In [20], an analysis is made of the motion of the AWS in the frequency domain, as a Laplace transform is applied on the position and the forces. The concept of impedance is used, which is defined as the external force acting on the device divided by its velocity. Two control strategies are proposed, namely reactive control, which implies cancellation of the imaginary part of the impedance and phase and amplitude control, which implies making the velocity in phase with the wave force. Both strategies lead to much more extracted energy, however they deal with non-causal functions. In [31], eight different control methods are tested on the AWS, each having its advantages and disadvantages, and a comparison is made about the power that can be extracted from the waves. Feedback linearization seemed the best option, concerning the average extracted power during the whole year.

Many control methods require prediction of future values. In [32], different methodologies are described for prediction some time into the future of the wave elevation, based only on past measurements. In [33], model predictive control (MPC), a method that includes estimation of future values of the wave elevation and uses a lot of matrices and vectors, is implemented on the point absorber named L10 and it is shown that this method works well under position, velocity and generator force constraints. The essence of MPC is to minimize a cost function, which includes the tracking error and the controller effort, by using the appropriate control action over a period of time that is called the prediction horizon. As the mooring system of the L10 is nonlinear, a comparison between the use of linear MPC and nonlinear MPC is performed in [34] and it is shown that the latter can maximize the energy absorption under the constraints. In [35], MPC is applied to a point absorber with linear behaviour. Vectors, matrices and an objective function to be minimized are used. The result is that the velocity of the device is in phase with the wave force and that the constraints are met, however in irregular waves the PTO force is too large and should be limited. A similar paper on MPC is [16], where a different, non-conventional objective function to be maximized is used: the absorbed energy from the waves.

Concerning the Symphony, a conclusion that can be drawn from the literature is that keeping the velocity of the device in phase with the wave excitation force is a condition for optimal energy

extraction. The perfect controller should achieve this in some way. As for the position, the floater of the Symphony is not allowed to oscillate with a too high amplitude. If it exceeds $\pm 2 m$, the movement is blocked for safety reasons. Thus, only in relatively small waves can the Symphony extract the theoretical maximum energy out of a certain wave. For higher waves, the amplitude of oscillation should be as high as possible under the constraint. Here, because of the particular shape of the several parts of the Symphony, the nonlinearities play a crucial role. As seen previously, the spring stiffness changes a lot over the whole position range and the drag force depends on the square of the speed, as well as on the direction of movement. Thus, the linear equations seen in the literature cannot be applied in the same way. Finally, it can be seen that for many of the above mentioned methods to be applied, the issue concerning the unpredictability of the waves needs to be tackled. A system to measure in advance the waves that will act on the Symphony is not foreseen. A very complex and costly system would be needed for knowing accurately the exact wave elevation at every instant for a satisfyingly long future period, as this depends on many parameters. Thus, the controller needs to be designed only on the basis of what can be measured at the moment itself or on past measurements or, alternatively, a quite complex estimation method, such as MPC, should be used.

In this chapter, a software-based innovative method to calculate, with a high precision, the maximum amount of energy that the Symphony can theoretically extract from a certain known wave will be presented. This method takes into account all the parameters and constraints of the Symphony and tackles the unpredictability issue, because the (fixed) wave is completely known in advance. The software can regulate the response of the Symphony, without taking the factor of time into account, while the equations that govern the movement are satisfied at all instants. The position, velocity, PTO force etc. at every moment can be adapted continuously, until the optimal movement as a whole is found. This is of course unrealistic, but gives an idea of how the perfect control system should be. This ideal response can then be used as a tool to evaluate the responses from other realistic control systems, such as the one with the energy error that is currently being used.

4.3 The GAMS software

4.3.1 General information

The General Algebraic Modeling System (GAMS) is a software used specifically for determining, analyzing and solving optimization problems. It is in fact a programming language, as the user writes a code, which is then compiled. There is a variety of solvers available which can tackle the problem. The software can be used for linear programming, nonlinear programming, mixed-integer nonlinear programming and others. It is especially useful in solving big, difficult and complex optimization problems. GAMS has a wide range of applications on an academic and commercial level.

As a mathematical tool, GAMS has many advantages. Firstly, a small and a big problem, in terms of number of variables and equations, can be solved with practically the same amount of code. This is because one parameterized equation in the code can represent many equations, one for each value of the parameter. Secondly, the modelling of the problem is independent of the solving technique, as the code is written first and then the user can choose a solver that is built-in in the software. In this way, the user does not need to write any piece of code that contains algorithmic solving

methods. Thirdly, the code is easy to write and user-friendly, as it gives a good visual interpretation of the problem and its form is very mathematical. Finally, sensitivity analysis can easily be performed [36];[37].

For these reasons, GAMS is really appropriate for solving the optimization problem concerning the response of the Symphony to a wave. Only a few lines of code are needed to represent the equations of Chapter 2, as well as the amplitude and generator torque restrictions. Everything is written in a parameterized way, because each equation is valid for all time moments. Also, it is not necessary to use difficult algorithms, as this is automatically done by the software. The objective is to determine the movement of the floater that results in maximum energy extraction from the input wave, which is viewed by GAMS as an array of values, without the concept of time. Thus, GAMS assigns values to the position, velocity, PTO force etc. (which are also arrays and each cell represents a time moment), until the movement during the whole time period is optimal in terms of total extracted energy. This procedure is done internally by the software, the user only needs to describe the model and determine the objective.

4.3.2 Structure of the GAMS code

In order to better understand the previously explained mechanism, a short description is given here of how a GAMS code looks like. It is important to obtain a rough overview of the basic elements in the code and their operational role, as the next parts of this chapter will be 'in line' with them.

A typical GAMS code has certain elements. In the beginning, the *Sets* and their size are determined. These are letters/indices that can take different values and represent the 'states' at which the problem takes place. For example, the letter t can be used as a *Set* with values t_1, t_2, t_3, t_4, t_5 and the letter j as a *Set* with values j_1, j_2, j_3 .

Next, the *Parameters* and *Tables* are given. These elements are closely linked with the *Sets*. For example, $a(j)$ can be a 3-dimensional *Parameter* and $v(j, t)$ can be a 3x5 *Table*. Some *Scalars* can also be given, which means fixed numerical values. Then, the *Variables* are determined, which can be 1-dimensional, vectors or tables. Examples are x , $y(t)$, $u(t)$ and $z(t, j)$. The content of the *Variables* is of course unknown and will be determined by GAMS after running the code. Here, extra code lines with upper/lower boundaries for some of the *Variables* or fixed values of one or more *Variables* at some 'states' can be put.

The following piece of the code consists of the *Equations*. One of them is the objective function, which means that there is one specific *Variable* that needs to be minimized or maximized. The objective function is in fact an equality that shows the dependence of this one *Variable* on others. The other *Equations* are called constraints and can be equalities or inequalities. It is important to note that an *Equation* can represent one or more 'states'. For example, the relation $y(t) = u(t) + 3$ takes only one line of code, but means that the equality is valid for all five values of the *Set* t .

Afterwards, the solver is determined and some extra *Options* can be stated. This leads to the 'solve' command, where the type of programming, as well as the choice between minimization and maximization are determined by the user. Finally, the *Variables*, which will be displayed in the file with the results, are given.

The elements described here are the basic ones. Extra commands can be put in more complex problems, for example interaction with other software. By running the code, GAMS presents in a separate file the resulting value of the objective function's *Variable*, the values of other things that were ordered to be displayed and also the type of solution.

4.4 The developed code

For this thesis, a code has been written in GAMS, so as to find the upper boundary of the energy that the Symphony can obtain from a certain, pre-determined wave. This code is presented in Appendix A, accompanied by comments, so that every command can be clearly understood. The benefits of GAMS are proven by the fact that only few lines of code are actually needed to describe the complex problem concerning the Symphony.

4.4.1 Wave modelling/fixed inputs

As mentioned previously, the Matlab time domain model generates time-series of waves. The type of waves (monochromatic or random) and their properties, such as the significant wave height and the energy period, can be chosen by the user. In this way, data is obtained that represents the wave force $F_{wave}(t)$ acting on the Symphony at every instant. This data is stored in a Microsoft Excel file. There are two conflicting parameters, for which a balance needs to be found. On the one hand, the duration of the wave must be long enough for realistic conclusions. On the other hand, the number of values of the *Set* that represents the time must not be too large, otherwise the optimization problem takes an extreme amount of time to be solved or cannot even be solved at all by GAMS. For these reasons, the time-series of waves that will be used in this chapter have a duration of 50 s and a sample of the wave force is taken every 0.02 s, thus there will be 2501 'states'/time segments. If the sampling rate were reduced, waves of longer duration could be used, however this would not give good numerical results. This will further be investigated at the end of the chapter. These 2501 time segments will be represented in GAMS by the *Set* t . In other words, t_1 represents the time segment $t = 0$ s, t_2 represents the time segment $t = 0.02$ s, t_3 represents the time segment $t = 0.04$ s etc., until t_{2501} represents the time segment $t = 50$ s. Then, the appropriate wave force data is read from the Excel file and stored in a GAMS *Parameter*. Also, the *Scalar* values of the total mass, the hydrodynamic damping coefficient and the inertia of the turbine are defined. This is what concerns the fixed numerical inputs in GAMS.

4.4.2 Variables

There are six *Variables* in the model: the total *energy* that is obtained from the wave during the 50 s, the position $z(t)$, velocity $z_d(t)$ and acceleration $z_{ad}(t)$ of the floater at every time segment, the PTO force $F_{PTO}(t)$ at every time segment and the electromagnetic torque of the generator $T_e(t)$ at every time segment. For a good initiation, the position, velocity and acceleration are fixed to 0 at the time segment $t = 0$. Also, a lower and an upper boundary are put to the position at all time segments.

The nominal power of the generator is 20 kW and the nominal rotational speed of the turbine, thus also of the rotor of the generator, is 350 rpm, which is equivalent to 36.65 rad/s. This means that the maximum electromagnetic torque $|T_{e,max}|$ that the generator can develop is:

$$|T_{e,max}| = \frac{20 \text{ kW}}{36.65 \text{ rad/s}} = 545.67 \text{ Nm} \quad (4.1)$$

Thus, in GAMS, a lower and upper boundary of -546 Nm and 546 Nm , respectively, are put to the electromagnetic torque at all time segments.

4.4.3 Spring force modelling

As seen in Figure 2.8, the total spring force is very nonlinear with respect to the position of the Symphony over the whole range. The force is fully linear for values of z between -1.12 m and 1.12 m and approximately linear in each of the other four parts, with a different slope each time. However, it is difficult to use a piecewise function in GAMS. A possible option is to approximate the spring force with a polynomial function. This can easily be done with the commands *polyfit* and *polyval* in a Matlab programme. An effort is made to keep the order of the polynomial not higher than 10, so that GAMS can function well.

In Figure 4.1, which is generated by a Matlab programme, various approximations are presented. The blue line is the real spring force, as taken from the time domain model. The orange line is the approximation with a 10th degree polynomial function of z , where equal importance is given to the whole range of z . It can be seen that although the orange line has a tendency to follow the blue line as much as possible, there are quite a lot of fluctuations.

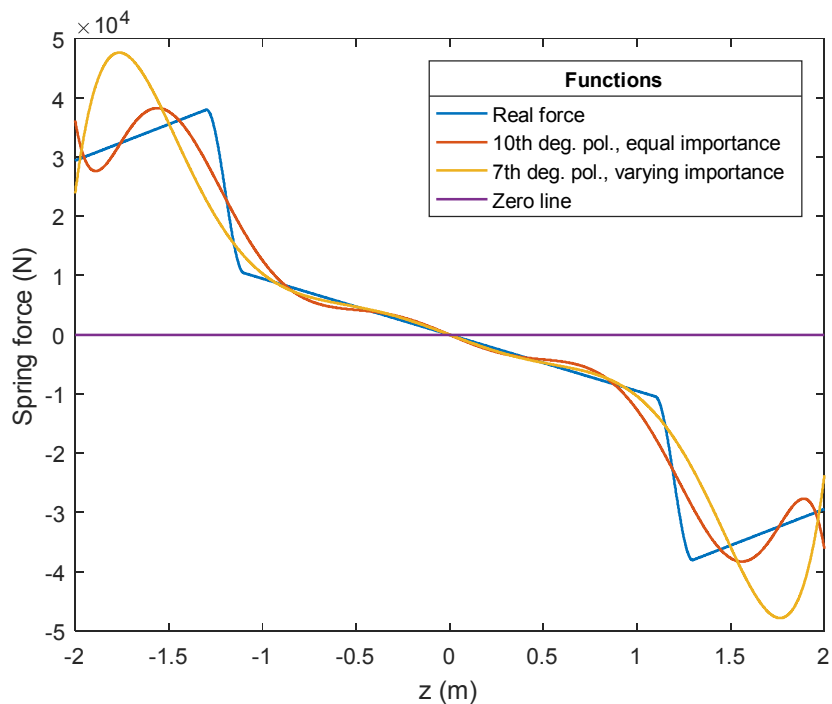


Figure 4.1: Spring force and unsatisfying approximations

Another method can be used, where more importance is given to the central linear region, less importance to the stiff spring regions and very little importance to the regions furthest from the equilibrium position. This is because in reality the Symphony oscillates mostly in the central linear region, especially at small waves, thus this area needs to be modelled more accurately than the others. The method consists of taking all the points of the real function in the linear region and only

few points in the other regions. If the polynomial approximation command is then applied, the result is the yellow line in Figure 4.1. A 7th degree polynomial function of z is now used. It can be seen that the yellow line deviates more from the blue line than the orange line does far from the equilibrium position, but is closer to the blue line than the orange line does in the linear region. However, the deviation from the blue line is too big, even in some parts of the linear region, because the order of magnitude of this deviation is similar to the order of magnitude of the wave force.

In other words, any approximation of the spring force results in too much deviation from the real values at some points. As the spring force is very important in the Symphony, it is not a good option to tolerate this. However, for the region from -1.3 m to 1.3 m , the spring force can be approximated by a polynomial function of the form $-a \cdot z^k - b \cdot z$, where a and b are positive numbers and k is a positive odd number. The results for different values of a, b, k are shown in Figure 4.2, which is made from a Matlab programme. A closer look shows that the deviations from the real spring force (blue line, as taken from the time domain model) can reach up to 10000 N in some areas, which is the order of magnitude of the wave force and PTO force, thus this approximation is not perfect. In any case, these lines, especially the green one, are close enough to the real spring force (blue line) to be used as satisfying approximations. However, if these functions with a high power on z are used in GAMS, the numerical result of the objective function is fine, but the electromagnetic torque has a peculiar unstable pattern. These approximations will be further investigated at the end of the chapter.

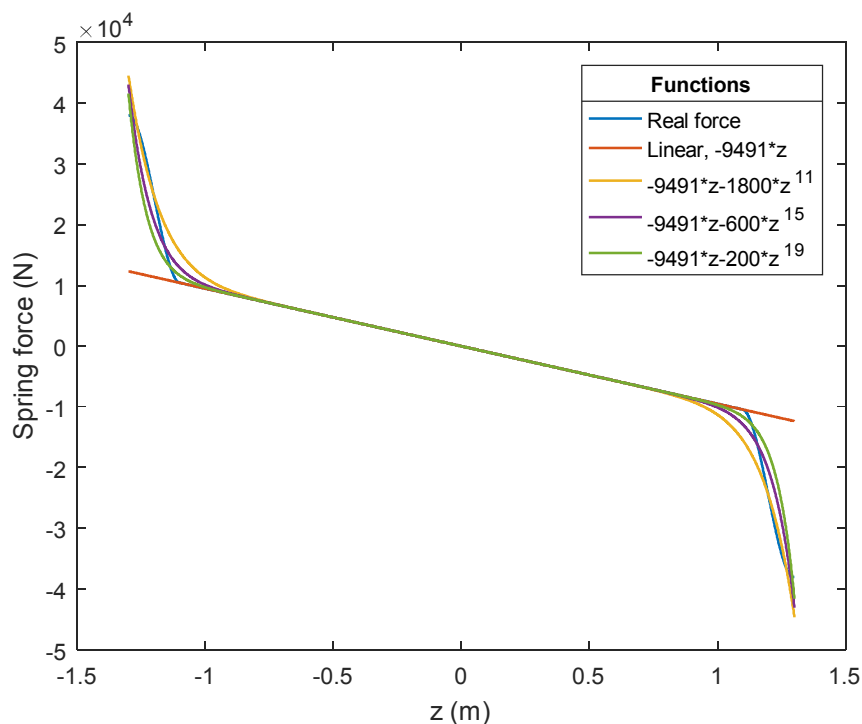


Figure 4.2: Spring force and approximations in a certain region

It is thus clear that it is not possible to calculate the exact maximum amount of energy that the Symphony can theoretically extract from a certain wave. However, clear upper boundaries to the possible energy extraction can be put.

First of all, the highest boundary is obtained by putting the maximum limits to the position, thus -2 m and 2 m , and by putting no limit on the generator torque. This boundary will be defined as the ‘Global Limit’. It cannot be reached with any control system, but one thing for sure is that it cannot be surpassed. For this case, the spring will be modelled as a linear one with the previously defined coefficient, so the GAMS equation becomes:

$F_{spring} = -k \cdot z, \quad z \leq 2$	(4.2)
---	-------

where k is equal to 9491 for the standard case of 10 s waves. For other wave periods, it needs to be adapted accordingly. In the GAMS code, everything is of course dimensionless, because all *Parameters*, *Scalars* and *Variables* take simply numerical values.

Next, a somehow lower and more realistic boundary is obtained by considering the fact that in most cases the uttermost position of the floater is not very far from the linear region. This is because the suddenly very stiff spring stops the floater from oscillating too much, thus it fulfils its safety role well. To have some margins, limits of -1.3 m and 1.3 m are put in GAMS and again a linear spring representation is used. Even if, in reality, the floater goes beyond this point, it will happen only very few times, so the impact is insignificant, which means that the GAMS result can well be considered an upper boundary. Another reason for this consideration is that, in order for the floater to frequently surpass these position limits in reality, either a generator of higher power would be needed, in order to provide enough accelerating torque to the turbine, or a very high wave would be needed, something which the Symphony cannot handle with the current generator torque constraint. Thus, by putting these position limits and also by keeping the limit on the generator torque, the GAMS output for this case will be called ‘Realistic Limit’. For this case, the GAMS equation becomes:

$F_{spring} = -k \cdot z, \quad z \leq 1.3$	(4.3)
---	-------

where k is also in this case equal to 9491 for the standard case of 10 s waves and for other wave periods, it needs to be adapted accordingly.

4.4.4 Drag force modelling

The drag force can be modelled much more easily and accurately. This is because a function for the real drag force exists. However, as seen in Chapter 2, this function includes absolute values and a varying coefficient, so an approximation is needed. A similar method as previously is used and it is concluded that a 7th order polynomial function is sufficient. Equal importance is given to all the points of the real function. A speed range from -3 m/s to 3 m/s is taken, which is more than enough.

In Figure 4.3, which is also generated by a Matlab programme, the real drag force (blue line, taken from the time domain model) and the polynomial approximation (orange line) are plotted together. It is obvious that the two lines almost collide, which is a very good result. In any case, the drag force is much smaller than the spring, wave and PTO forces, so the small deviations do not play any significant role.

The equation represented by the orange line is:

$F_{drag} = -1.00 \cdot z_d^7 + 20.93 \cdot z_d^5 - 217.38 \cdot z_d^3 + 257.01 \cdot z_d^2 - 177.92 \cdot z_d$	(4.4)
---	-------

A rounding has been done here with respect to the numbers actually used in GAMS, for readability.

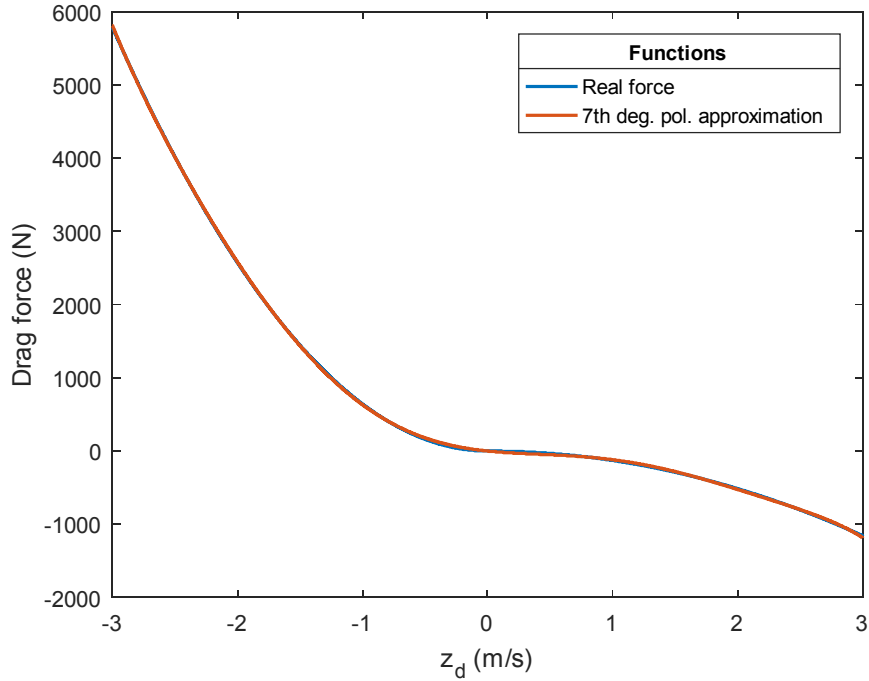


Figure 4.3: Drag force and approximation

4.4.5 Iron loss torque modelling

The ‘torque’ that causes the iron losses is also in fact a piecewise function, due to the $sign(\omega_t)$ term, thus an approximation needs to be made for GAMS. A similar method with *polyfit* is used, with a 3rd order polynomial function, so as not to make things too complex. Equal importance is given to all the points of the real function. An angular speed range of the turbine from -90 rad/s to 90 rad/s is taken, which is more than enough.

In Figure 4.4, which is also generated by a Matlab programme, the real iron loss torque (blue line, taken from Equation 2.11) and the polynomial approximation (orange line) are plotted together. It can be seen that there is some difference between the two lines, but this is not really important, because the iron loss torque is very small compared to the electromagnetic torque of the generator, so these fluctuations do not have a serious impact on the whole movement of the floater.

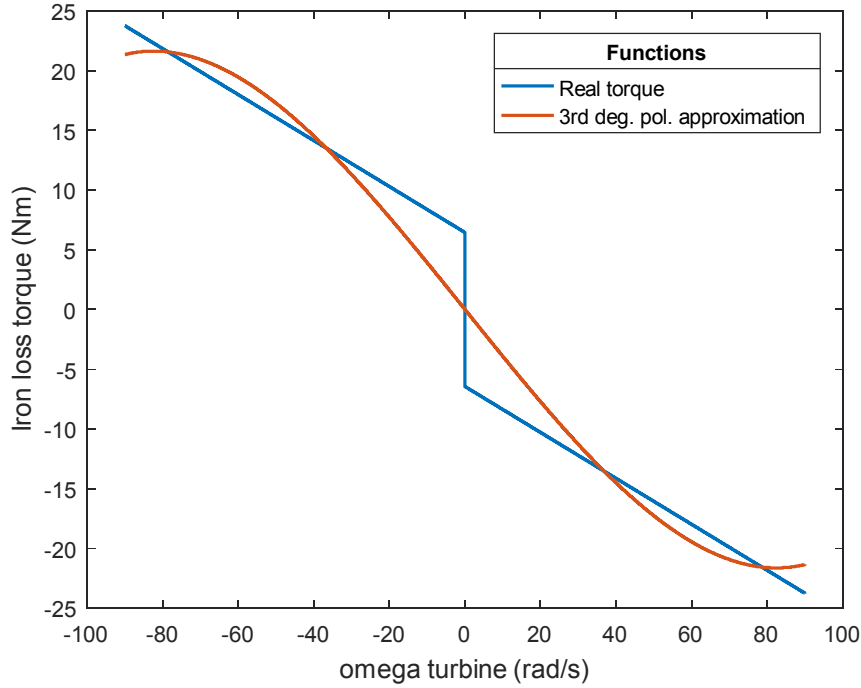


Figure 4.4: Iron loss torque and approximation

The equation represented by the orange line is:

$$T_{iron} = 1.93 \cdot 10^{-5} \cdot \omega_t^3 - 0.39 \cdot \omega_t \quad (4.5)$$

Again, a rounding has been done here with respect to the numbers actually used in GAMS, for readability. By using the mean numerical value of the ratio $\frac{\omega_t}{z_d}$, which is equal to 59.97, Equation 4.5 becomes:

$$T_{iron} = 4.17 \cdot z_d^3 - 23.61 \cdot z_d \quad (4.6)$$

In Chapter 2, this iron loss torque was translated to a force on the floater as a whole. However, here in GAMS, it will be kept as a torque and make part of the PTO force, to avoid unnecessary calculations. This is realistic, because it is indeed a torque on the turbine, but any of the two approaches give of course the same result.

4.4.6 Equations

Now, the *Equations* can be presented. The GAMS model consists of one objective function and four constraints. The purpose of the GAMS code is to maximize the *energy*, which is the final extracted energy from the waves that goes to the grid, in fact the same as E_{final} from Chapter 3. As a reminder, this is generally defined as:

$$energy = \int_0^T (-T_e(t) \cdot \omega_t(t)) \cdot dt - \int_0^T 3 \cdot I_a^2(t) \cdot R_{phase} \cdot dt - E_{cableloss} \quad (4.7)$$

The first term, the integral of the electromagnetic torque of the generator multiplied by the angular speed of the turbine, is the 'pure' energy that comes out of the Symphony. The second term

represents the copper losses of the generator and the third term represents the losses on the cable that goes to shore. In GAMS, the integral is approximated by a sum, because the electromagnetic torque and speed are only defined at discrete time segments (*Set t*). By using the mean numerical value of the ratio $\frac{\omega_t}{z_d}$, which is equal to 59.97, by using the relation between the phase current I_a and electromagnetic torque T_e , as presented in Section 3.5, and by taking the cable losses as always being 2% of the energy at the converter, otherwise it is too complex for GAMS, the previous equation (objective function) becomes:

$energy = 0.02 \cdot 0.98 \cdot \sum_{t_1}^{t_{2501}} (-T_e(t) \cdot 59.97 \cdot z_d(t) - 3 \cdot \left(\frac{T_e(t)}{3 \cdot K}\right)^2 \cdot R_{phase})$	(4.8)
---	-------

The first two constraints concern the relation between the position, the velocity and the acceleration. The real derivatives are approximated by differences as follows:

$z_d(t) = \frac{z(t) - z(t - 1)}{0.02}$	(4.9)
---	-------

$z_{dd}(t) = \frac{z_d(t) - z_d(t - 1)}{0.02}$	(4.10)
--	--------

The next constraint concerns the force balance:

$m_{tot} \cdot z_{dd}(t) = F_{spring}(t) + F_{drag}(t) - c_{hyd} \cdot z_d(t) + F_{wave}(t) + F_{PTO}(t)$	(4.11)
---	--------

where $F_{spring}(t)$ and $F_{drag}(t)$ are taken from Equations 4.2/4.3 and 4.4, as functions of $z(t)$ and $z_d(t)$, respectively, c_{hyd} is the hydrodynamic damping coefficient and $F_{wave}(t)$ is read from the Excel file.

The final constraint concerns the link between the PTO force, the acceleration, the generator torque and the speed. The mean value of the ratio $\frac{\omega_t}{z_{dd}}$, which is equal to 59.97 and the mean value of the factor $(A_{mu}(z) - A_{mb}) \cdot G_{turb}$, which is also equal to 59.97, are used. Thus, according to Equation 2.18, the GAMS constraint is:

$F_{PTO}(t) = -59.97 \cdot (59.97 \cdot I_t \cdot z_{dd}(t) - T_e(t) - T_{iron}(t))$	(4.12)
--	--------

Note that here the iron loss torque T_{iron} , which is a function of the speed, according to Equation 4.6, has been incorporated in the PTO force.

4.4.7 Solving

Finally, after some necessary options are put, the command is given to solve the optimization problem. Some of the results can be written on a different Excel file, in order to be able to make graphs.

4.5 Optimization results

By running the GAMS code, interesting results are obtained. These will be shown for the two main categories of waves. In any case, only the 'Realistic Limit' will be used in this section, because, for the moment, only the GAMS behaviour is examined. Thus, all the previously mentioned constraints and equations will be used.

4.5.1 Monochromatic waves

The ideal regular waves are perfectly sinusoidal. The wave height, which is defined as the vertical distance between a crest and its successive trough and is, of course, two times the amplitude, as well as the wave period, which can either be defined as the time between two consecutive moments that a particle at a fixed location has zero elevation with upwards velocity (zero up-crossing period) or between two consecutive moments that it has zero elevation with downwards velocity (zero down-crossing period) [38], are fixed. This means that the wave force also has a sinusoidal form. An example of a monochromatic wave is shown in Figure 4.5 [39].

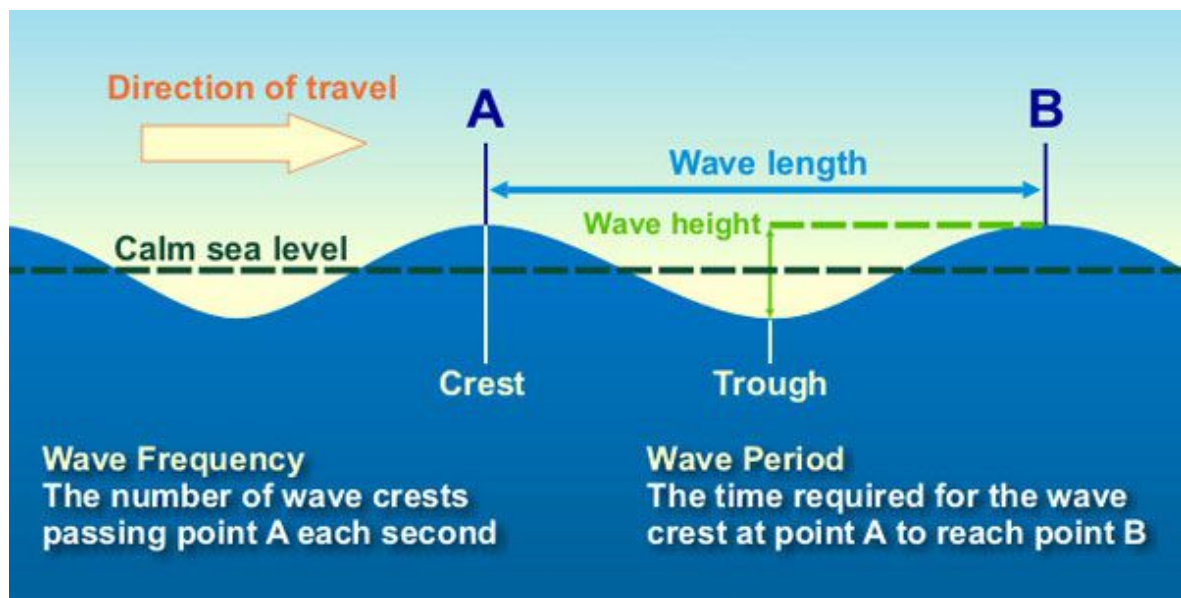


Figure 4.5: Basic properties of a regular wave

The wave height and period are very easily tuned in the Matlab model, so that time-series of the wave force for a monochromatic wave are obtained. A sampling is made and the result is stored in the Excel file, to be read by GAMS as input wave force. Here, four examples with wave heights and periods that are realistic for the location where the Symphony will be placed will be presented:

-Wave height $H = 2 \text{ m}$, wave period $T_m = 10 \text{ s}$: The resulting value of the objective function (final energy extracted, which has been maximized) is $energy = 215340 \text{ J}$. This number has not so much significance by itself, but can be used for comparison with the following examples. The position, velocity, wave force and generator torque are plotted in Figure 4.6. In all the following figures, a scaling is performed on the position, velocity and electromagnetic torque, for visibility. Also, only a piece of the diagram is presented for readability and good incorporation in the page. All variables show a periodic pattern, which is as expected, because the wave is monochromatic.

The most important observation is that the velocity is perfectly in phase with the wave excitation force, which is the basic principle for optimal energy absorption, as mentioned in the literature. As there is restriction on the amplitude of oscillation, a form of latching control is applied, which can be seen by the fact that the position is locked for some time at the highest and lowest level at each cycle. At these moments, of course, the velocity is almost zero. This means that the optimal amplitude of oscillation, for this wave and under the assumption of a linear spring, is higher than 1.3 m. The generator torque mostly has an opposite sign than the velocity, which means that the product $-T_e(t) \cdot \omega_t(t)$ is mostly positive, thus the energy flows mostly from the Symphony to the grid. The generator torque in each half cycle has a peak, a dip and then again a longer peak. The most logical explanation for this is that the first peak corresponds with the top position, where the floater stays a short amount of time. The generator torque, and consequently the PTO force, needs to counteract the spring force, to keep the floater in that position. Then, the generator torque decreases, so that the floater can gain some speed. The second peak almost corresponds with the maximum velocity, so GAMS is probably doing this to maximize the product $-T_e(t) \cdot \omega_t(t)$, as this increases the value of the objective function.

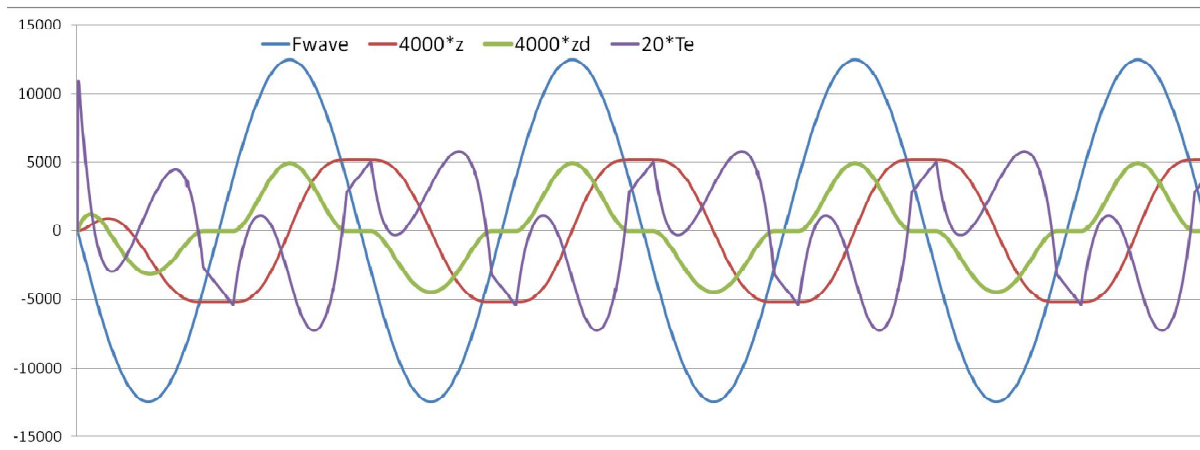


Figure 4.6: GAMS result for monochromatic wave of 2 m height and 10 s period

-Wave height $H = 4$ m, wave period $T_m = 10$ s: The resulting value of the objective function is $energy = 476984$ J, much higher than previously, as expected, because the wave force is higher. The position, velocity, wave force and electromagnetic torque are plotted in Figure 4.7. The observations are similar as previously, with the difference that the generator torque is higher, which is because of the higher wave force that has to be handled. The torque limits are even reached during each cycle. Also, the floater stays at its furthest position from the equilibrium point for a longer time, thus there is more latching. This is because the unconstrained amplitude of oscillation is now higher than in the previous case (because of the higher wave), thus there is a larger ‘cutting-off’.

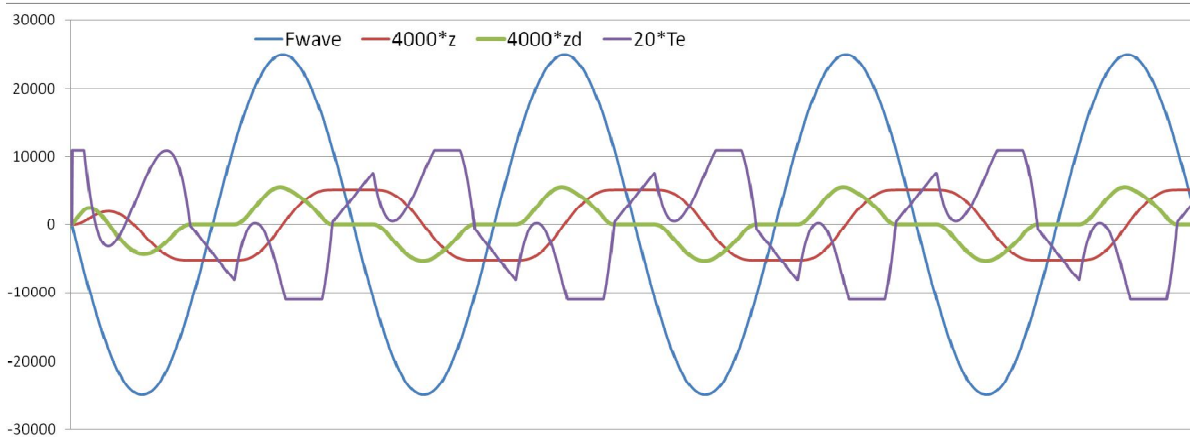


Figure 4.7: GAMS result for monochromatic wave of 4 m height and 10 s period

-Wave height $H = 2\text{ m}$, wave period $T_m = 6\text{ s}$: The resulting value of the objective function is $energy = 251223\text{ J}$, which is quite similar to the first case. The position, velocity, wave force and electromagnetic torque are plotted in Figure 4.8. Again, the velocity is perfectly in phase with the wave force. The interesting thing to note is that now there is almost a perfect sinusoidal oscillation, without latching. This also makes the electromagnetic torque follow a somehow smoother pattern. The fact that the velocity is almost continuously non-zero and gets a bit higher values than in the first case of a 10 s wave possibly explains why the obtained energy is a bit higher now, as the product $-T_e(t) \cdot \omega_t(t)$ increases in this way.

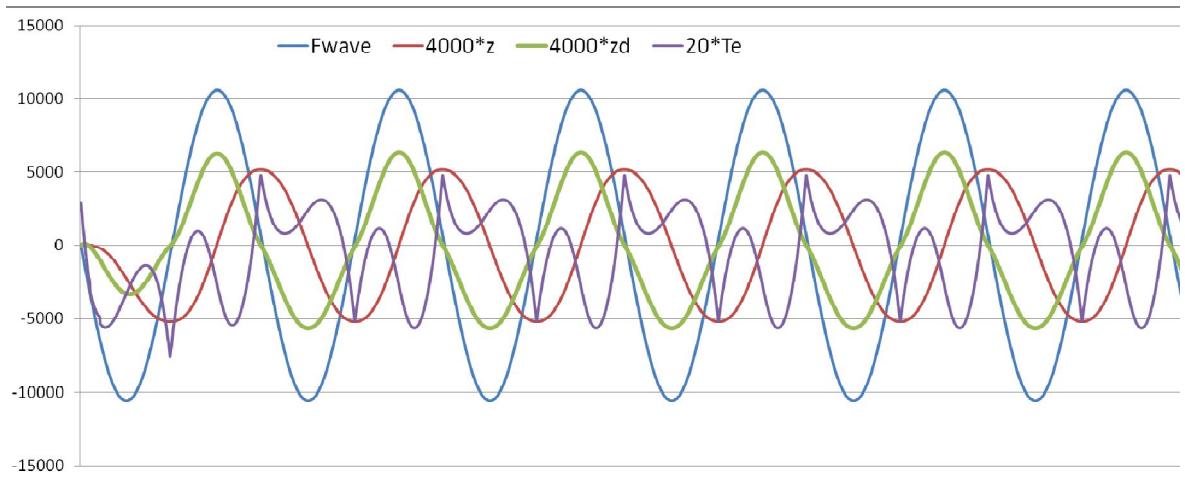


Figure 4.8: GAMS result for monochromatic wave of 2 m height and 6 s period

-Wave height $H = 2\text{ m}$, wave period $T_m = 14\text{ s}$: The resulting value of the objective function is $energy = 162807\text{ J}$, which is lower than in the first case. The position, velocity, wave force and generator torque are plotted in Figure 4.9. The locking in the outmost positions takes longer now because of the slower wave and this, among other things, possibly explains the less amount of energy that is extracted. The generator torque follows a similar pattern like in the 10 s waves.

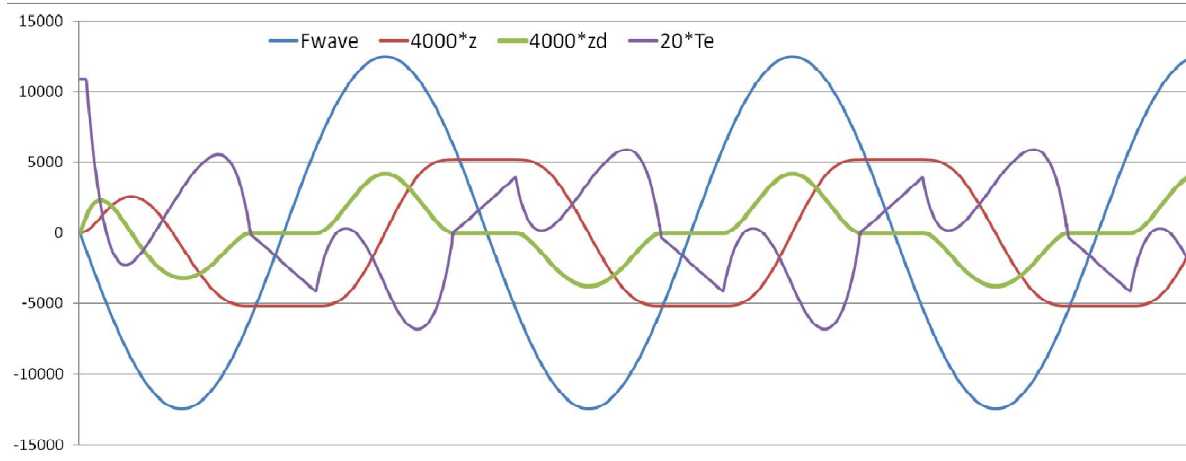


Figure 4.9: GAMS result for monochromatic wave of 2 m height and 14 s period

It can generally be said that the GAMS result is very sensitive to the wave height and a bit sensitive to the wave period, for regular waves.

4.5.2 Irregular waves

The waves in reality do not have a fixed height or period. An example is given in Figure 4.10 [40], where the surface elevation is plotted as a function of time for a regular wave (top) and an irregular wave (bottom). An important statistical parameter is the significant wave height H_s , which is defined as the average height of the highest 1/3rd of all the waves during a certain period. By applying Fourier Transform on irregular waves, the spectrum $S(f)$ is obtained, which is related to the energy contained in each frequency f [40]. An example of a wave spectrum is shown in Figure 4.11 [41]. Another important parameter is the energy period T_{en} , which is defined as [41]:

$$T_{en} = \frac{\int_0^{\infty} f^{-1} \cdot S(f) \cdot df}{\int_0^{\infty} S(f) \cdot df} \quad (4.13)$$

The Matlab model generates irregular waves that follow the so-called Bretschneider spectrum. The formula of such a spectrum is [42]:

$$S(f) = \frac{5}{16} \cdot H_s^2 \cdot \frac{f_0^4}{f^5} \cdot e^{-\frac{5}{4} \left(\frac{f}{f_0}\right)^{-4}} \quad (4.14)$$

where f_0 is the peak frequency, thus the frequency at which $S(f)$ has its maximum value [41].

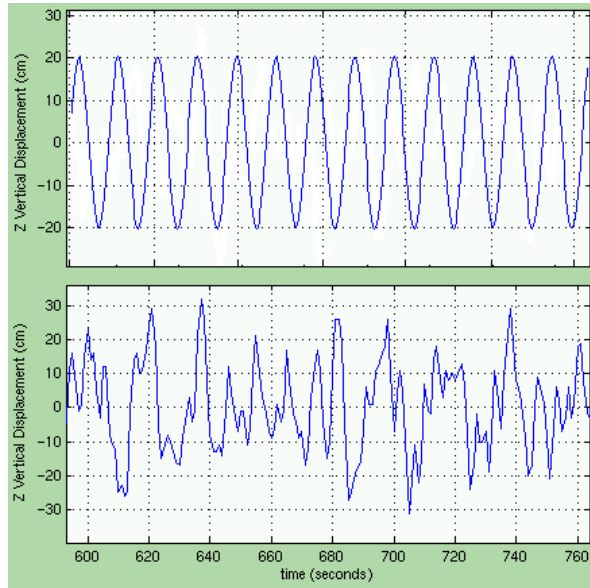


Figure 4.10: Comparison between regular and irregular waves

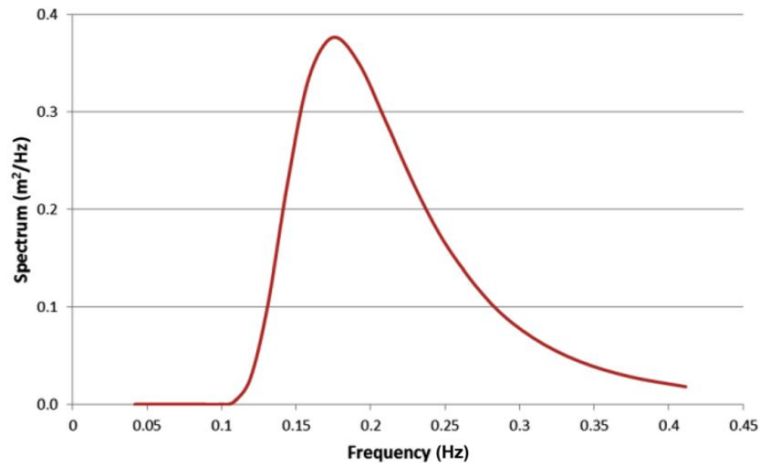


Figure 4.11: Typical wave spectrum, frequency domain

The only parameters that are varied by the user are H_s and T_{en} . A sampling is made and the result is stored in the Excel file, to be read by GAMS as input wave force. Here, four examples with significant wave heights and energy periods that are realistic for the location where the Symphony will be placed will be presented:

-Significant wave height $H_s = 1\text{ m}$, wave energy period $T_{en} = 10\text{ s}$: The resulting value of the objective function (final energy extracted, which has been maximized) is *energy = 24349 J*. This number is quite insignificant by itself, but can be used for comparison with the other examples. The position, velocity, wave force and electromagnetic torque are plotted in Figure 4.12. In all the following figures, a scaling is performed on the position, velocity and electromagnetic torque, for visibility. Also, only a piece of the diagram is presented for readability and good incorporation in the page. It can be seen that also in this case of an irregular wave, the velocity is perfectly in phase with the wave excitation force. The oscillation of the floater is of course not sinusoidal anymore and there is practically no latching in this case. This is due to the small height of the wave, thus the optimal amplitude of oscillation does not exceed the limit of 1.3 m . The floater has no tendency to go further

than the limit (which would be the case in a higher wave), thus no latching is needed. The sign of the electromagnetic torque is mostly opposite to the sign of the velocity, thus the energy flows mostly from the Symphony to the grid.

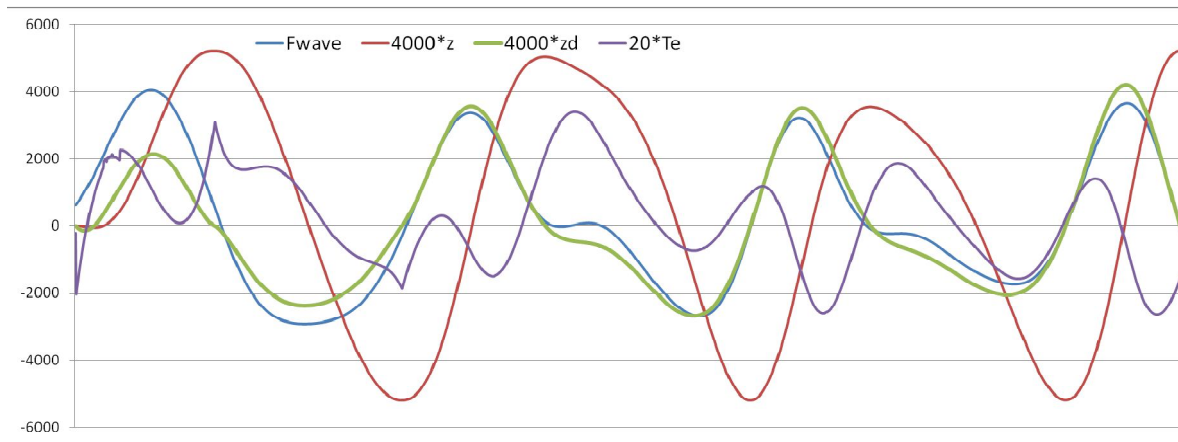


Figure 4.12: GAMS result for Bretschneider wave of 1 m height and 10 s period

-Significant wave height $H_s = 3$ m, wave energy period $T_{en} = 10$ s: The resulting value of the objective function is now $energy = 260329$ J, much higher than previously, as expected, because the wave is much higher, so it contains more energy. The position, velocity, wave force and electromagnetic torque are plotted in Figure 4.13. The results are similar as in the previous case concerning the fact that the velocity is in phase with the wave force, only now there is clearly latching. This is logical, because with this higher wave, the floater would normally oscillate with a higher amplitude, but it remains at the outmost positions due to the constraint. The electromagnetic torque shows a similar pattern as in the monochromatic waves: at every cycle, there is a peak, to keep the floater almost in the outmost position, counteracting the spring force, a dip, to let the floater gain some velocity and again a peak approximately at the point of maximum velocity, to maximize the product $-T_e(t) \cdot \omega_t(t)$, as this increases the value of the objective function. The torque is higher than in the previous case and at some points the limits are even reached. The cycles are of course different, because this realistic wave does not have a fixed height or period, as in the ideal case.

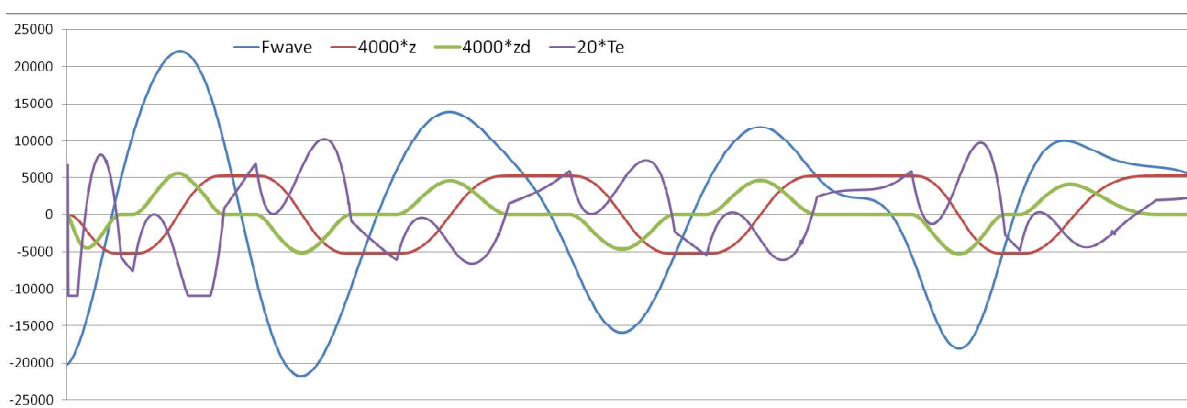


Figure 4.13: GAMS result for Bretschneider wave of 3 m height and 10 s period

-Significant wave height $H_s = 2\text{ m}$, wave energy period $T_{en} = 6\text{ s}$: The resulting value of the objective function is $energy = 121932\text{ J}$. This is in between the two previous values (for $H_s = 1\text{ m}$ and $H_s = 3\text{ m}$, as expected). The position, velocity, wave force and electromagnetic torque are plotted in Figure 4.14. As in the fast monochromatic wave, the oscillation is smoother and there is no latching. The electromagnetic torque also follows a quite smoother pattern. The change in wave period does not affect the fact that the velocity is in phase with the wave force.

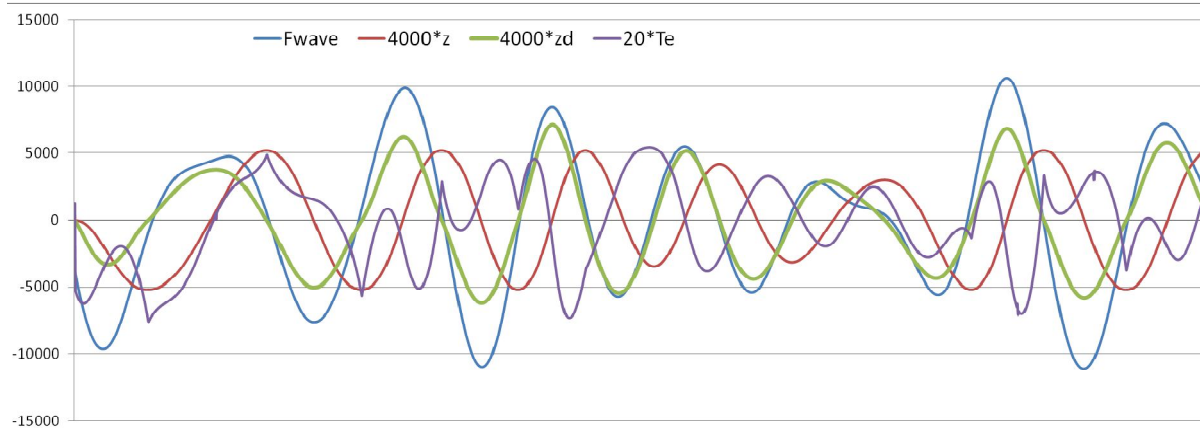


Figure 4.14: GAMS result for Bretschneider wave of 2 m height and 6 s period

-Significant wave height $H_s = 2\text{ m}$, wave energy period $T_{en} = 14\text{ s}$: The resulting value of the objective function is $energy = 118787\text{ J}$. This exact value, like the value of the previous case, has no particular meaning, because of the random character of this wave. In another wave with the same H_s and T_{en} , there will be some difference. The only remark is that these two values (for the two $H_s = 2\text{ m}$ waves) are in-between the values for a $H_s = 1\text{ m}$ wave and a $H_s = 3\text{ m}$ wave, as expected. The position, velocity, wave force and electromagnetic torque are plotted in Figure 4.15. Again, the velocity is in phase with the wave force. As in the monochromatic slow wave, the latching is longer compared to the case of a 10 s wave. This probably means that the optimal oscillation amplitude increases as the wave period increases.

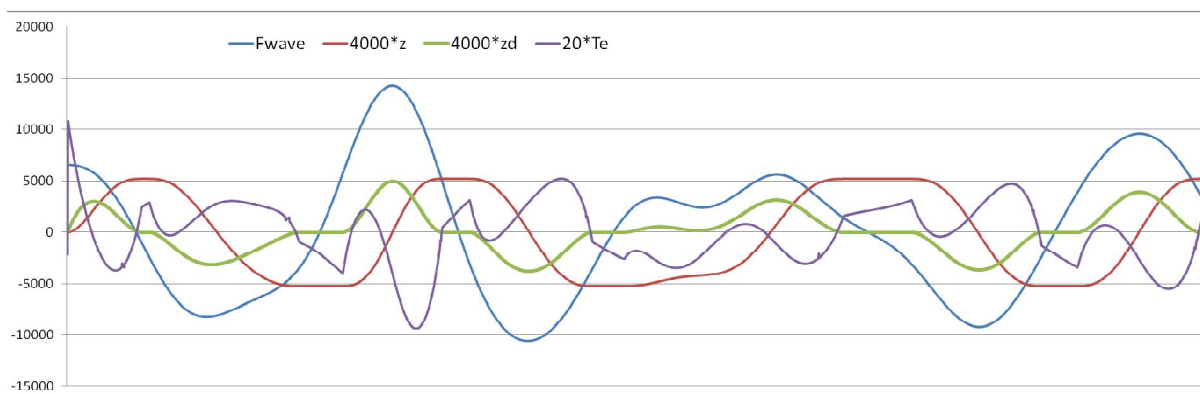


Figure 4.15: GAMS result for Bretschneider wave of 2 m height and 14 s period

Generally, it can be said that GAMS performs very well with irregular waves, as the velocity is kept perfectly in phase with the wave force, regardless of the height or period of the wave.

4.5.3 Special case

It is interesting to see what would happen if there were no restrictions at all on the amplitude of oscillation. For this case, the input wave in GAMS is the previously used wave with significant wave height $H_s = 3\text{ m}$ and energy period $T_{en} = 10\text{ s}$. All equations are used, but there are no limits on z . The resulting value of the objective function is now $energy = 1322880\text{ J}$. This is much higher than the value with restriction, as expected, because the floater can now oscillate with a very high amplitude. The position, velocity, wave force and electromagnetic torque are plotted in Figure 4.16. The fact that the phase of the velocity and the phase of the wave force are the same does not change. It is clear that the oscillation is completely smooth now concerning the position, as there is no latching. By looking at the GAMS results, it can be seen that the position can reach up to more than $\pm 9\text{ m}$ approximately, which is really high compared to the normal situation. In reality this is impossible for the Symphony, but this indicates what the optimal amplitude of oscillation theoretically is, at this certain wave and for the assumption of a linear spring. Another interesting observation is the very high generator torque, which even reaches its limits almost at every cycle. This happens mostly when the floater is at its outmost position, so the generator torque counteracts the quite high spring force there, so that the high amplitude of oscillation can be maintained.

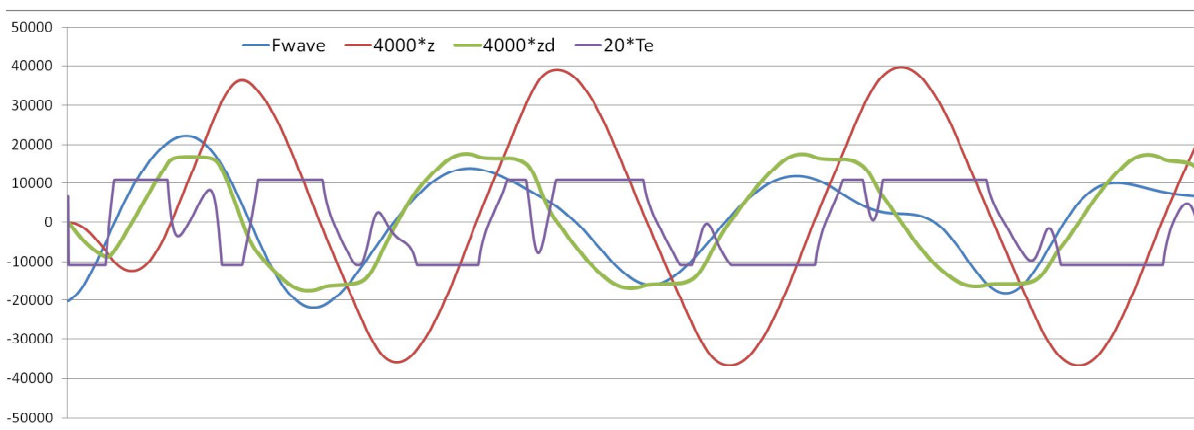


Figure 4.16: GAMS result for no amplitude restriction

4.6 Sensitivity analysis

4.6.1 Sensitivity to parameters

Now, an investigation is done on how certain parameters affect the GAMS result. In all cases here, the same wave will be used. A choice is made for a Bretschneider wave with significant wave height $H_s = 3\text{ m}$ and energy period $T_{en} = 10\text{ s}$. The resulting value of the objective function $energy$ for all these cases is presented in Table 4.1. Note that in each case, all other parameters are kept constant at their reference values. The 'Realistic Limit' is used, which implies a spring force according to Equation 4.3.

Table 4.1: Sensitivity to parameters

Case	Original situation	Lower mass, $m_{tot} = 3000 \text{ kg}$	Higher mass, $m_{tot} = 10000 \text{ kg}$	Weaker spring, $k = 500 \text{ N/m}$
<i>energy (J)</i>	260329	263241	257425	264067
Case	Stiffer spring, $k = 13000 \text{ N/m}$	Lower inertia, $I_t = 1 \text{ kg} \cdot \text{m}^2$	Higher inertia, $I_t = 10 \text{ kg} \cdot \text{m}^2$	Lower amplitude, $z_{max} = 0.7 \text{ m}$
<i>energy (J)</i>	256263	271656	244782	151500
Case	Higher amplitude, $z_{max} = 2 \text{ m}$	Lower torque, $T_{e,max} = 400 \text{ Nm}$	Higher torque, $T_{e,max} = 800 \text{ Nm}$	No drag force
<i>energy (J)</i>	369216	259058	260661	269396

It is obvious that most of the parameters have very little to almost no effect on the GAMS result, concerning the extracted energy. This is because the electromagnetic torque is in GAMS a ‘free’ variable, in the sense that it can be given any value within the bounds, without depending on any other variable. Thus, GAMS can ‘compensate’ for the changes in the other forces that result from the parameter changes. Anyway, this is a positive conclusion, because it means that possible small mistakes and assumptions that have been made for the real parameters of the Symphony do not play any significant role in the calculation of the upper boundary for the energy that the Symphony can extract from a certain wave.

The only parameter that has a serious impact on the result is the limit on the amplitude of oscillation. The possible energy yield increases a lot when the boundary becomes less strict, because then the amplitude of oscillation increases, getting closer to the optimal value. This is thus dominant and needs to be taken into account when the Symphony model will be up-scaled.

4.6.2 Sensitivity to spring modelling

For the sake of experimenting, the GAMS code is left to run with the functions of F_{spring} that were shown in Figure 4.2 and the resulting value of the objective function is shown in Table 4.2. The previous Bretschneider wave with significant wave height $H_s = 3 \text{ m}$ and energy period $T_{en} = 10 \text{ s}$ is used. All other constraints, parameters and equations remain the same. It can be seen that the difference between the cases is insignificant concerning the extracted energy. Experiments have shown that the electromagnetic torque has an unstable pattern with these spring force functions, so it is not a good option to use them. See Figure 4.17, where the $-9491 \cdot z - 600 \cdot z^{15}$ function has been used for the spring force. The position and velocity are fine, though.

However, the good thing is that the resulting value of the objective function in all these cases is lower than the value with the assumption of a linear spring, which is as expected. Thus, the linear spring method can safely be used to calculate an upper energy boundary that cannot be reached with any control system, but can also not be surpassed for sure.

Table 4.2: Sensitivity to spring modelling

Spring force function	energy (J)
Linear, $F_{spring} = -9491 \cdot z$	260329
$F_{spring} = -9491 \cdot z - 1800 \cdot z^{11}$	233058
$F_{spring} = -9491 \cdot z - 600 \cdot z^{15}$	236812
$F_{spring} = -9491 \cdot z - 200 \cdot z^{19}$	239944

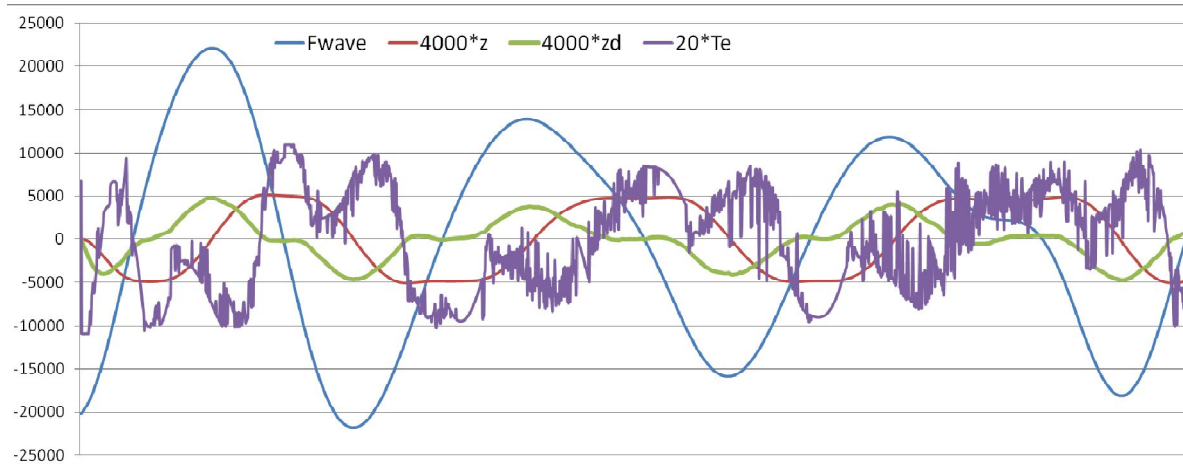


Figure 4.17: Unstable torque pattern when using a nonlinear spring force in GAMS

4.6.3 Sensitivity to sampling rate

Finally, an analysis is made, to observe the sensitivity of the GAMS result to the number of samples that are taken from a wave. For a feasible problem with an acceptable running time in the case of the highest sampling (per 0.01 s, which is the same as the Matlab time domain model time step), waves of total duration of 25 s are taken. Two monochromatic waves are chosen here: a wave with height $H = 2 \text{ m}$ and period $T_m = 10 \text{ s}$ and a wave with height $H = 2 \text{ m}$ and period $T_m = 6 \text{ s}$.

From table 4.3, it can be seen that the more samples of the wave force that are taken, the higher the resulting value of the objective function in GAMS becomes. This is especially obvious for the fast wave with a period of 6 s. For waves with a much longer total duration than 25 s, the differences in extracted energy for different sampling rates are expected to be very high. It is thus important to keep the sampling rate close to the Matlab time step, in order to obtain realistic and accurate results for the upper energy boundary. As there is only an insignificant difference between the results for the 'real' wave, which has points every 0.01 s, and the results for the 'half' wave, sampled every 0.02 s, the previously used sampling rate per 0.02 s can safely be continued to be used in the next experiments. This sampling rate makes it possible to consider waves of total duration of 50 s, otherwise, if the 0.01 s rate were used, the total duration of the waves would have needed to be reduced to 25 s.

Table 4.3: Sensitivity to sampling rate

Sampling per / segments in GAMS	<i>energy (J) for $H = 2 m$, $T_m = 10 s$</i>	<i>energy (J) for $H = 2 m$, $T_m = 6 s$</i>
0.1 s / 251 segments	90594	74503
0.05 s / 501 segments	95602	99370
0.02 s / 1251 segments	99342	115938
0.01 s / 2501 segments	100797	122043

5. Simulation Results

5.1 Introduction

In the previous chapter, the theoretical potential of the Symphony was calculated. However, GAMS only performs an optimization process, many assumptions were made and knowledge in advance of the whole wave is required. It is important to see what happens in reality and this is done by performing simulations in the realistic Matlab time domain model. By running this model, the results represent the realistic behaviour of the Symphony. More specifically, information is obtained about the exact oscillation response to a certain wave. The values of the position, velocity, acceleration, electromagnetic torque, as well as of all the forces acting on the floater, can be calculated at every instant and plots can be made. Other quantities, such as the energy extracted from the waves or the energy losses, can also be calculated. Thus, experiments can be done in Matlab, to evaluate or regulate certain things.

This chapter starts with an investigation about two important parameters of the controller for the Symphony. It is theoretically explained that only a proportional part of the PI controller should be used, thus no integrating part, due to an unwanted 'memory' effect. Also, it is experimentally proven that the energy should always flow only from the Symphony to the grid and not vice versa. Next, the most important part of this thesis is presented. The Matlab time domain model is run both for monochromatic and irregular waves as inputs. The realistic extracted energy, as well as the movement of the floater and the electromagnetic torque, are calculated and presented in tables and graphs. In this way, a comparison can be made with the optimal GAMS result. It is shown that the control system of the Symphony performs very well in all realistic sea states, because, when the proportional part of the controller is well tuned, the extracted energy is close to the theoretical maximum and the velocity of the floater is almost in phase with the wave force. Finally, a sensitivity analysis is made, to find out how important the impact of changes in some parameters is for the final result. It is shown that there is not much sensitivity to the proportional constant of the controller, but that the spring needs to be tuned correctly, for good results. Moreover, the Symphony can only keep operating without electrical components under low sea waves.

From now on, for everything that concerns purely the Matlab model, waves with a total duration of 100 s or 200 s will be used, so as to obtain a better image. There is no restriction to the duration in Matlab. However, when a comparison between Matlab and GAMS is made, only a duration of 50 s will be used.

5.2 Controller components investigation

First of all, an investigation needs to be performed about the necessity of the integrating part of the PI controller, as well as about the direction in which the energy may flow. In Figure 5.1, which comes from the Simulink model and is a close-up view of the PI controller, the block that determines the direction in which the energy may flow is put at 3 different positions. Note that in reality it is put only in 1 of the 3 positions, but all of them are shown in the figure just to have a clear image. The

block has a function $f(u)$ which can be translated as ‘let the signal pass if the signal is bigger or equal than the value a , otherwise make the output zero’. It is $a \leq 0$. This means that the value of a , which is set by the user, determines whether the electrical machine can act only as a brake on the turbine (always a positive output of the PI controller, the energy can only flow from the Symphony to the grid) or can act both as a brake and an accelerator on the turbine (positive/negative output of the PI controller, the energy can flow from/to the Symphony). The signal that comes from the left of this figure is the energy error, which has been presented in Chapter 3, and the signal that leaves the figure on the right is the output of the PI controller, which will afterwards be multiplied with the velocity of the floater etc. To sum up, a is the highest possible energy error that is allowed to pass. For example, if $a = 0$, action is taken by the controller only when the energy error is positive and if $a = -1000 J$, action is taken by the controller only when the energy error is more than $-1000 J$. For lower values of the energy error, the output of the $f(u)$ block is zero.

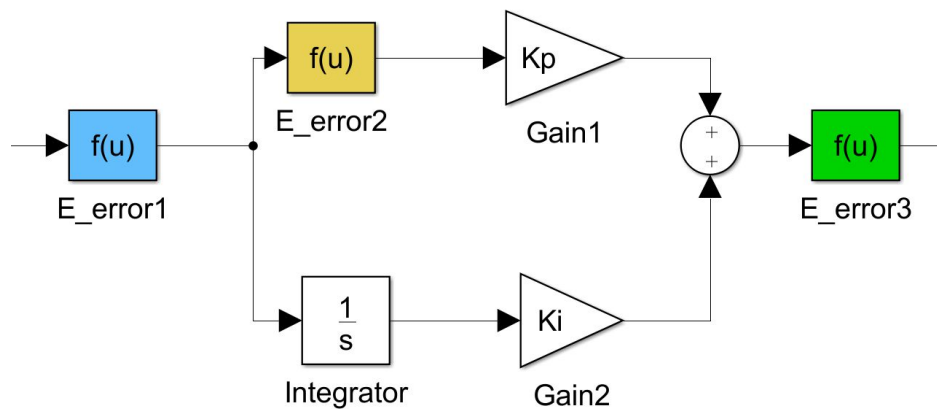


Figure 5.1: Close-up view of the PI controller, with various positions for energy flow direction determination block

5.2.1 Integrating part

To examine the impact of an integrating part, thus $K_i > 0$, each of the 3 possible positions of the $f(u)$ block is analyzed:

Blue position, before the PI controller: In this case, if $a = 0$, it means that only positive error signals are allowed to pass to the PI controller. The output of the P-part will be sometimes zero and sometimes positive, but the output of the I-part will be continuously positive, with a constantly increasing value, due to the integrating action of a positive signal. Thus, after a certain amount of time, this output will be so big that it will be dominant and ‘overshadow’ the P-part. Negative error signals, which would normally result in no action to be taken (due to $a = 0$), will now result in a strongly positive output of the PI controller, which means the generator will act as brake on the turbine. Thus, the amplitude of oscillation of the floater will be kept too low and the controller loses its function. Similar problems can occur if $a < 0$, as negative error signals can result in a positive output of the PI controller or vice versa. So, it is not a good option to put the block in this position.

Yellow position, only on the P-part: An advantage of this position compared to the blue position is that the error signal passes completely to the I-part, regardless of the value of the parameter a .

However, again the controller carries a strong ‘memory’ of the past due to the integral. For example, let’s imagine that the energy error is negative most of the time. Suddenly a very high waves comes, thus the error will quickly become positive. Normally a braking action should be taken, but because of the strongly negative integral, an accelerating action is taken, which pushes the floater too far from the equilibrium position. The purpose of the control system is to act optimally on the instant situation, without being too much affected by past situations, especially in a stochastic, unpredictable environment. Thus, this position for the block is also not really desired.

Green position, after the PI controller: In this case, parameter a is not well-linked to the energy error anymore. The decision to brake or accelerate the turbine is taken on the basis of the output of the PI controller and not on the basis of the energy error. These two things can have a different sign, according to whether the P-action or I-action is dominant. This means that this position for the block is not at all a good option.

It is thus shown that in all cases, a positive value of K_i causes a ‘memory’ effect, which disrupts the desired behaviour of the control system and may cause an unwanted response in the oscillation of the floater. Thus, for the rest of this thesis, $K_i = 0$ will be used. Another argument for this decision is that in regular PI control cases, a variable needs to reach a certain desired value as soon as possible, without too much overshoot. An integrating part is then used to make the error (the difference between the actual value of the variable and the desired value) zero in steady state. In the case of the Symphony, there is no parameter that needs to reach a fixed value and there is no steady state, especially in realistic irregular waves, as the oscillation needs to adapt constantly.

5.2.2 Energy flow direction

It was argued previously that there should be no integrating part ($K_i = 0$), thus there is no difference whether the $f(u)$ block is placed in the blue or yellow position. If the green position is to be used, an appropriate scaling needs to be made on the parameter a , but the logic is the same. For ease, from now on, the block will stay on the yellow position, as can also be seen in Figure 3.2. Now, an investigation will be performed about the optimal value of the parameter a . For this, two randomly chosen Bretschneider waves and one monochromatic wave, all with a duration of 100 s, will be used.

i) Bretschneider wave with significant wave height $H_s = 2$ m, wave energy period $T_{en} = 10$ s: By temporarily setting $a = 0$, the optimal value of K_p , in other words the value for which the energy extraction is maximum, is found to be $K_p = 0.2$. This will be kept constant from now on in this example. Matlab is run for different values of a and the values of $E_{initial}$ (energy output of the Symphony, without copper and cable losses), $E_{copperloss}$, $E_{cableloss}$ and E_{final} (final energy output that goes to the grid) are calculated by the software. The results are shown in Table 5.1 (the same wave is used every time of course). Note that the more negative a is, the more it is allowed for energy to flow from the grid to the Symphony.

Table 5.1: Energy output for different values of the parameter a

a (J)	$E_{initial}$ (J)	$E_{copperloss}$ (J)	$E_{cableloss}$ (J)	E_{final} (J)
0	182237	2851	2127	177258
-20	182237	2851	2127	177258
-150	181683	2852	2128	176702
-800	172800	2851	2090	167858
-1200	153082	3026	2186	147868
-20000	141067	3310	2257	135500

It can be seen that the lower a is, the lower the energy output of the Symphony is. For small absolute values of a , there is none to very small difference. At higher absolute values of a , a significant impact on the energy output is observed. This is clearly an undesirable situation.

The copper losses seem to increase for lower values of a . This is logical, because energy flows in two directions, in both of which there are losses on the internal resistance of the machine. The cable losses seem to be quite stable over the whole range. This indicates that the average of the absolute power at the converter is approximately the same. However, it is not the losses that are responsible for the less final energy obtained by decreasing the value of the parameter a , because, firstly, they are very small compared to the extracted energy and, secondly, the initial energy also decreases as a decreases. This means that, regardless of the machine and cable, letting the energy flow in both directions is not a good option for the Symphony.

To understand why this happens, it is necessary to focus on the oscillation of the floater. In Figure 5.2, the position of the floater is plotted for different values of a .

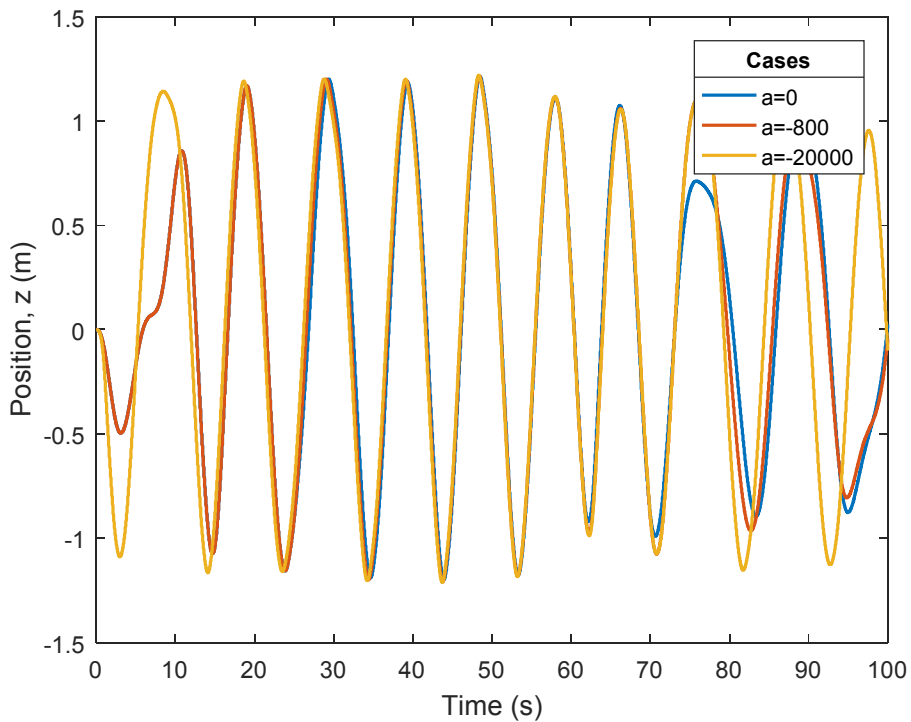


Figure 5.2: Position of the floater as a function of time, for different values of the parameter a

It can be seen that, the more negative a is, the more the oscillation becomes purely sinusoidal with a fixed amplitude of approximately $1.1 m$, which is equal to the value of $z_{control}$, as stated in the Matlab script. This means that the absolute priority of the controller is to keep the energy error zero, by making the floater oscillate in a fixed pattern. In this way, less priority is given to the extracted energy, because this flows more and more in both directions. This can be seen more clearly in Figure 5.3, where the power at the turbine $P_{initial} = -T_e \cdot \omega_t$ is plotted as a function of time, for the same values of a as in the previous figure. Positive power means flow from the Symphony to the grid and negative power means the opposite. It is clear that, as a becomes more negative, the power flows more frequently from the grid to the Symphony and it is this that causes the lower energy yield.

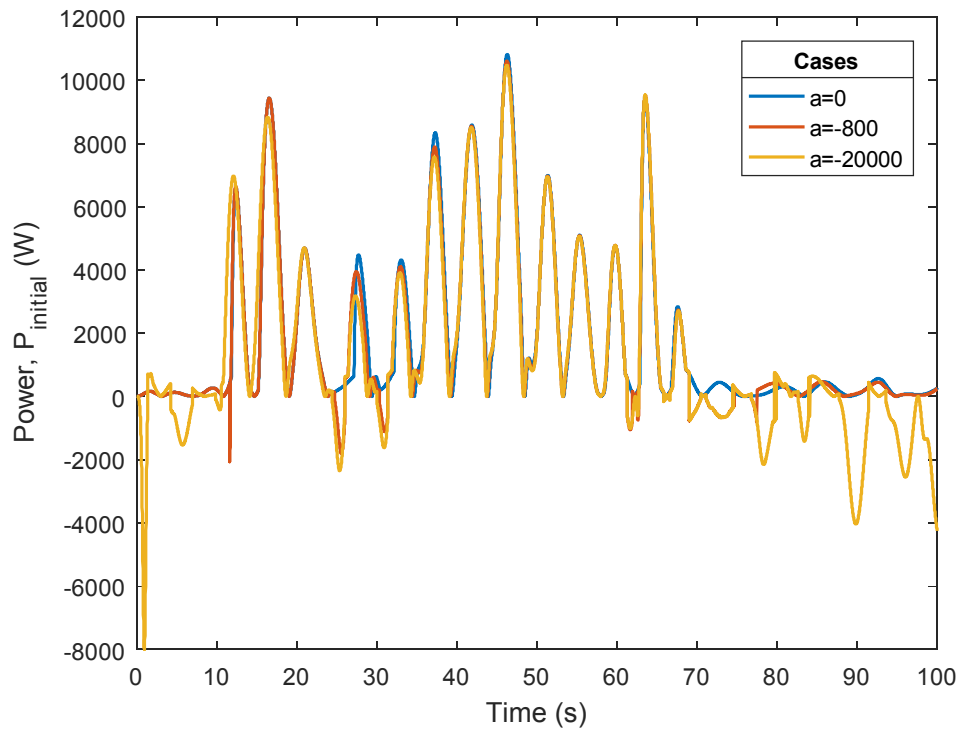


Figure 5.3: Power as a function of time, for different values of the parameter a

ii) *Bretschneider wave with significant wave height $H_s = 4 m$, wave energy period $T_{en} = 10 s$:* By choosing a higher wave, the same experiment is done. By temporarily setting $a = 0$, the optimal value of K_p is found to be $K_p = 0.2$. This will be kept constant from now on in this example. The results of running the software are shown in Table 5.2.

Table 5.2: Energy output for different values of the parameter a

a (J)	$E_{initial}$ (J)	$E_{copperloss}$ (J)	$E_{cableloss}$ (J)	E_{final} (J)
0	266035	5926	4161	255947
-20	266035	5926	4161	255947
-150	265979	5926	4166	255886
-800	253815	6014	4285	243515
-1200	247690	6080	4314	237295
-20000	211574	6637	4390	200545

The results are quite similar as previously: the lower a is, the lower the energy output of the Symphony is. The extracted energy is of course higher than in the previous case, because the wave force is higher.

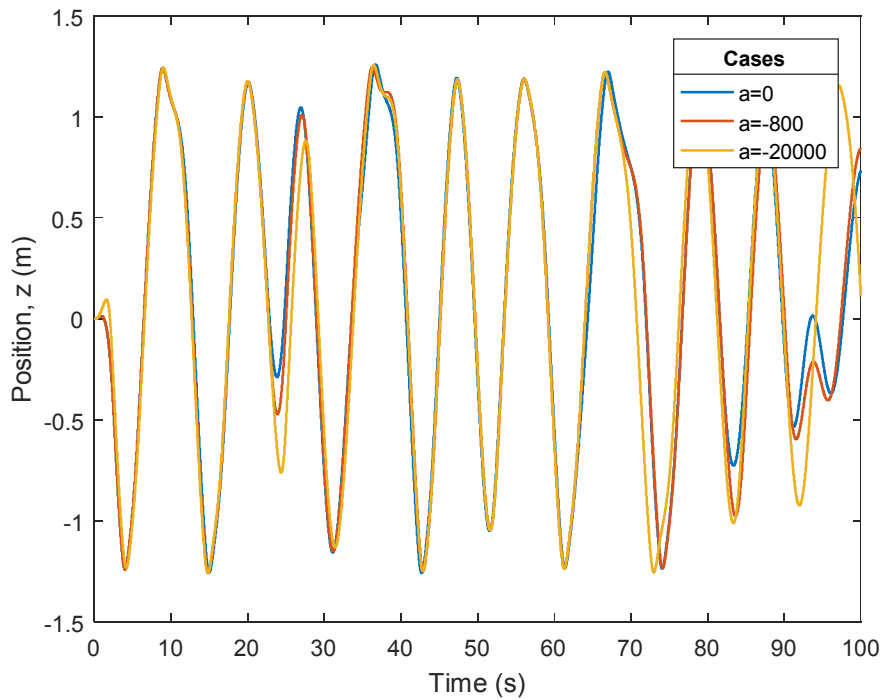


Figure 5.4: Position of the floater as a function of time, for different values of the parameter a

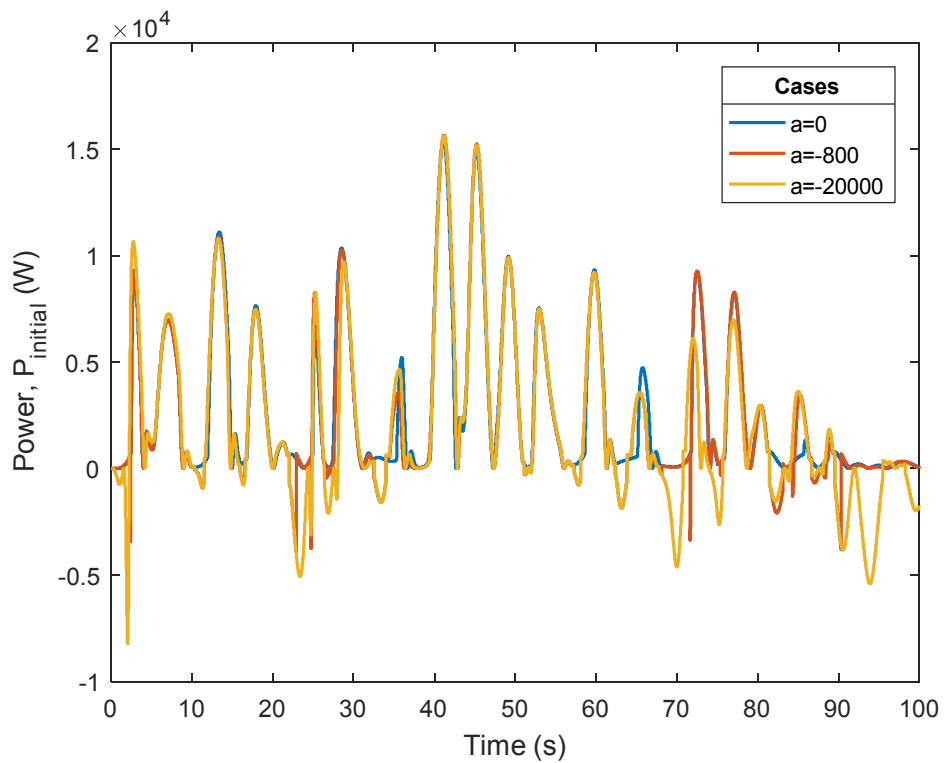


Figure 5.5: Power as a function of time, for different values of the parameter a

In Figure 5.4, the position of the floater is plotted for different values of a . Similar observations as previously can be made. In Figure 5.5, the power at the turbine $P_{initial} = -T_e \cdot \omega_t$ is plotted as a function of time, for the same values of a as in the previous figure. Positive power means flow from the Symphony to the grid and negative power means the opposite. It is clear that, as a becomes more negative, the power flows more frequently from the grid to the Symphony and it is this that causes the lower energy yield.

In any case, both wave examples show that it is not a good option to allow the energy to flow in both directions, because the energy yield decreases significantly.

iii) Monochromatic wave with wave height $H = 1$ m, wave period $T_m = 7$ s: This monochromatic wave is used to further prove the previous remark that a low value of a implies that more focus is given to a fixed pattern oscillation than to the energy yield. The wave period is 7 s, but the spring constant is not adapted, so the natural period of the Symphony remains at the standard value of 10 s. The value of K_p for this example will be arbitrarily chosen as $K_p = 2$. This is not important anyway. Only two cases are considered: for $a = 0$, it is $E_{final} = 23317$ J and for $a = -20000$, it is $E_{final} = -41349$ J. Clearly, a low value for a is not acceptable, because more energy has flown from the grid to the Symphony than the other way, which can be seen by the negative sign of the energy. The reason why this happens can be understood from Figure 5.6, where the wave force and the position of the floater are plotted for these two values of a . The wave force is downscaled for visibility.

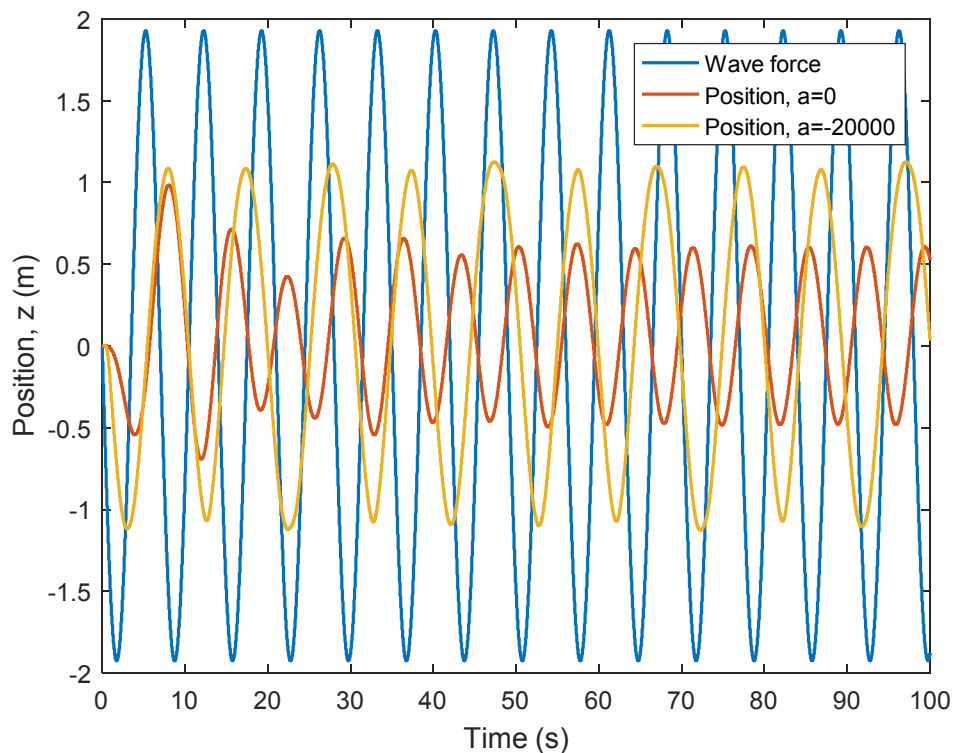


Figure 5.6: Scaled wave force and position of the floater as a function of time, for different values of the parameter a

Apart from the previous remark that a low value of a causes the floater to oscillate with the desired amplitude of $z_{control}$, as given by the control system, there is another even more important remark.

At $\alpha = 0$, the floater oscillates with the period of the wave. This is observed by the fact that there is a constant phase shift between the position of the floater and the wave force. However, when α is very negative, the period of oscillation is approximately 10 s, thus not equal to the wave period anymore. This is observed by the constantly changing phase shift between the position of the floater and the wave force.

This means that in a realistic irregular wave, the oscillation is adapted to the period of the wave only for $\alpha = 0$. This happens at the moments when the power is zero during each cycle, because then there is a short time interval, during which the floater gets no damping from the generator, thus the oscillation period becomes equal to the wave period. For lower values of α , the controller has a tendency to keep the period of oscillation fixed at the natural period of the Symphony, regardless of the actual waves that are coming and have varying periods. Thus, the velocity of the floater cannot be kept in phase with the wave force, as would the ideal control system do, as shown by GAMS. In this way, the controller loses its correct function in some way, because the actual waves are not taken into account anymore.

5.2.3 Conclusion

It was shown that the best option is to not use an integrating part in the controller and to only let positive energy errors pass. If the energy error is negative, no action should be taken by the PI controller. Thus, for the rest of this thesis, $K_i = 0$ and $\alpha = 0$. The only tuning that needs to happen is on the proportional part of the controller, K_p .

5.3 Evaluation/optimization results for monochromatic waves

Now that decisions have been made about the crucial components of the controller, an investigation can be made to find out how good this control system performs in the presence of monochromatic waves. For this, Matlab is left to run with various monochromatic waves that have heights and periods likely to occur at the location where the Symphony will be placed. These waves have a total duration of 100 s, which is more than enough for the monochromatic case, as the sequence repeats itself constantly. For each of these waves, K_p is tuned to the value that maximizes the final energy output during these 100 s. For the same waves, GAMS is also left to run for the first 50 s of the wave and the upper boundary of the energy output is calculated by the software. Only the 'Realistic Limit' will be used in this chapter. Thus, a comparison can be made between the extracted energy in Matlab and GAMS, on the basis of the first 50 s. Note again that GAMS does not take into account the idea of a controller, as it just freely assigns values to the electromagnetic torque T_e at every instant, within boundaries of course. Apart from the energy, the average power can also be calculated by the following equation:

$P_{mean} = \frac{E_{final}}{T}$	(5.1)
----------------------------------	-------

where $T = 50$ s in this case.

The results are presented in Table 5.3. Some very important conclusions can be drawn from this. Firstly, the controller performs outstandingly, as in most cases the real energy output is very close to the energy output of the ideal controller, as calculated by GAMS. The numerical results of GAMS

should not be taken too strictly, due to all the assumptions and approximations, but a general idea is obtained as to where the optimal solution lies. Secondly, the Matlab realistic energy output increases at higher waves, as expected. It should be noted that, for the same wave period, the Matlab/GAMS ratio decreases a little bit at higher waves, but, again, this is not something that needs too much focus. Finally, the optimal value of K_p seems to be quite independent of the wave height, but slightly dependent on the wave period. As the wave period increases, the optimal value of K_p increases. However, experiments have shown that, for a certain wave, the change in energy obtained is insignificant, when K_p varies between 0.5 and 3 approximately. This means that the optimal value of K_p that is presented in the table must also not be taken too strictly.

Table 5.3: Matlab/GAMS comparison for monochromatic waves

Wave parameters	Optimal K_p for 100 s	Matlab energy E_{final} (J) for 50 s	Matlab average power P_{mean} (W) for 50 s	GAMS energy (J) for 50 s	Matlab/GAMS ratio for 50 s
$H = 1\text{ m}$ $T_m = 7\text{ s}$	0.2	80619	1612	94124	86%
$H = 1\text{ m}$ $T_m = 10\text{ s}$	0.5	76301	1526	89731	85%
$H = 1\text{ m}$ $T_m = 13\text{ s}$	1.2	64037	1280	77962	82%
$H = 2\text{ m}$ $T_m = 6\text{ s}$	0.1	220123	4402	251223	88%
$H = 2\text{ m}$ $T_m = 10\text{ s}$	0.7	177294	3545	215340	82%
$H = 2\text{ m}$ $T_m = 14\text{ s}$	2.1	123845	2476	162807	76%
$H = 3\text{ m}$ $T_m = 10\text{ s}$	0.8	274553	5491	346328	79%
$H = 4\text{ m}$ $T_m = 10\text{ s}$	0.8	371286	7425	476984	78%

The previous observations can be better explained with the help of some figures made in Matlab. In Figures 5.7, 5.8 and 5.9, the (downscaled) wave force is plotted together with the speed of the floater, both for the GAMS and Matlab simulations, for three different waves. Matlab can easily read the GAMS results, which are stored in an Excel file. From these figures, it can clearly be seen to what extent the velocity of the floater in Matlab is in phase with the wave excitation force. As also seen in Chapter 4, the velocity in GAMS is always perfectly in phase with the wave force. The velocity in Matlab is very close to the GAMS velocity in all cases, concerning the phase. This remark, together with the values of the extracted energy, proves the outstanding performance of the control system in the presence of monochromatic waves.

Another interesting remark is that there is some form of latching in GAMS, especially for higher waves, which can be seen by the fact that the velocity is zero for some time, twice during each cycle, whereas this does not occur in Matlab. This latching is needed to keep the velocity of the floater perfectly in phase with the wave force. GAMS can do this, because the wave is fully known in advance, so the floater is locked at the outmost position and released again at the right moment

concerning the wave. On the other hand, the realistic Matlab model relies only on present measurements, so there is no information as to which would be the right moment to release the floater.

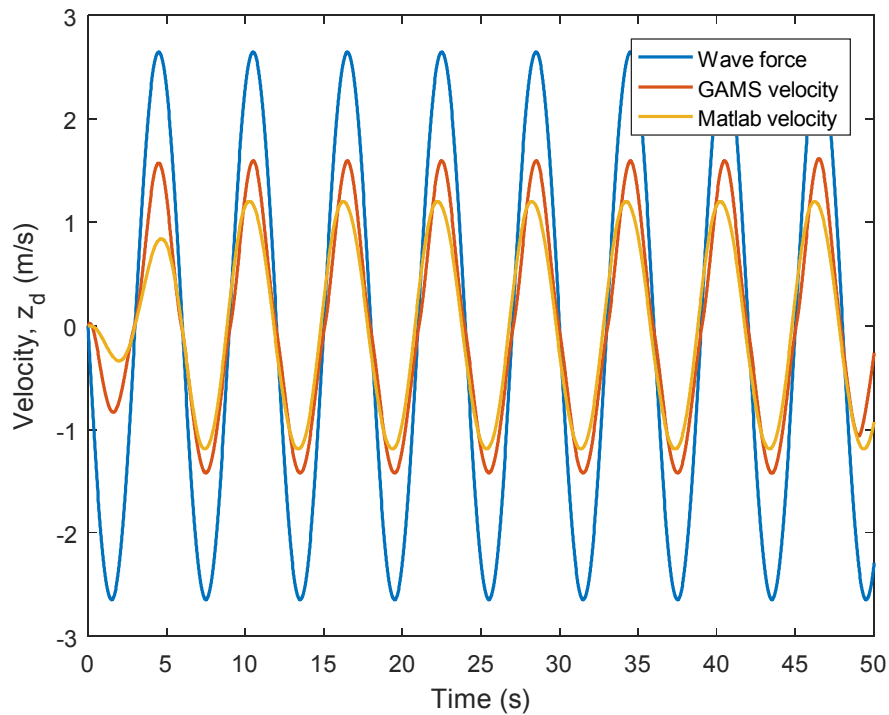


Figure 5.7: Scaled wave force, floater velocity when running GAMS and Matlab (realistic) floater velocity, for a monochromatic wave with $H = 2\text{ m}$ and $T_m = 6\text{ s}$

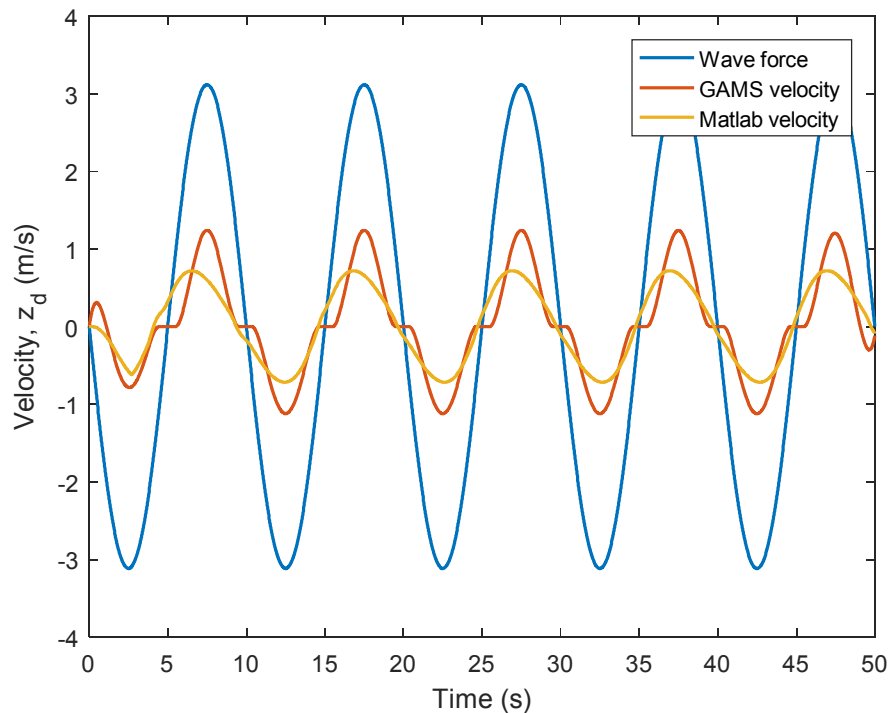


Figure 5.8: Scaled wave force, floater velocity when running GAMS and Matlab (realistic) floater velocity, for a monochromatic wave with $H = 2\text{ m}$ and $T_m = 10\text{ s}$

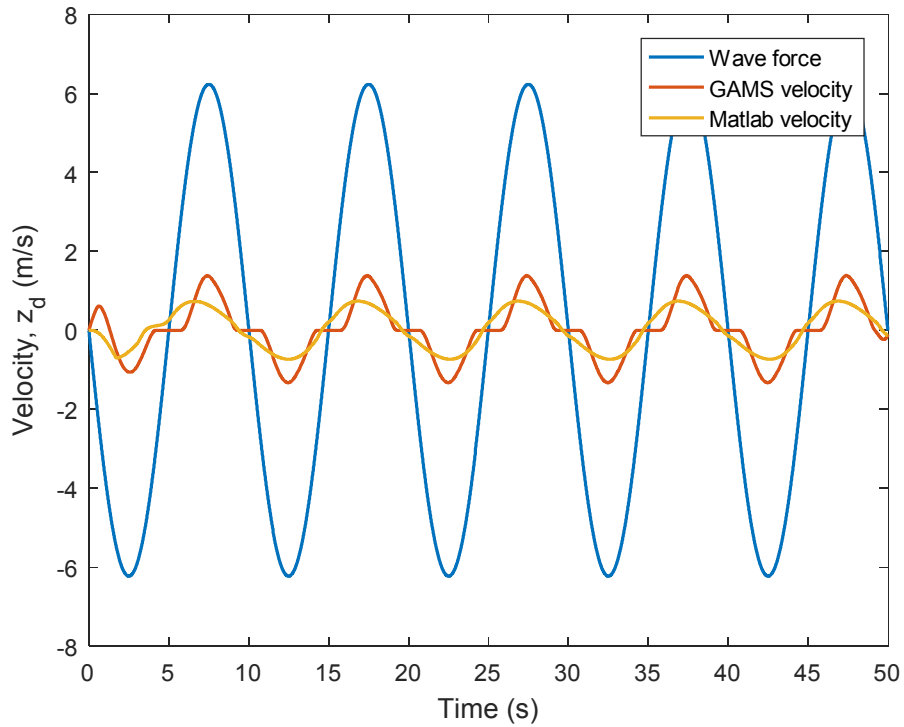


Figure 5.9: Scaled wave force, floater velocity when running GAMS and Matlab (realistic) floater velocity, for a monochromatic wave with $H = 4\text{ m}$ and $T_m = 10\text{ s}$

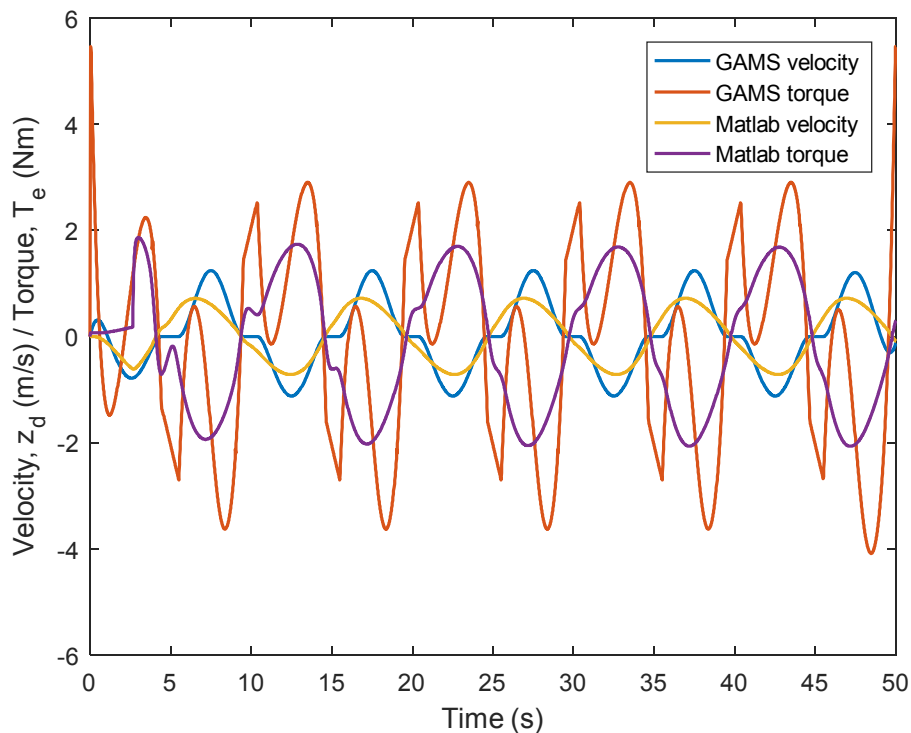


Figure 5.10: Floater velocity and scaled electromagnetic torque, in GAMS and Matlab, for a monochromatic wave with $H = 2\text{ m}$ and $T_m = 10\text{ s}$

Some more interesting observations can be made by plotting the speed of the floater together with the downscaled electromagnetic torque, both for the Matlab and GAMS results. Only one wave

example will be shown here, in Figure 5.10. It can be seen that there is some similarity between the torque that GAMS and Matlab give, as they are both approximately in counter phase with the speed. Both the velocity and torque are higher in GAMS and this partly explains the higher energy output. The most important difference is that the real torque, as calculated from Matlab, follows a smoother pattern than in GAMS, and this is because in Matlab the electromagnetic torque depends on the speed (it is equal to the controller constant, multiplied with the energy error, multiplied with the speed, so it follows approximately the speed pattern), whereas in GAMS the electromagnetic torque is just a variable, to which values are assigned, quite independently from the other variables.

To sum up, the controller functions very well in monochromatic waves, something which was proven both by the energy output and by the movement of the floater.

5.4 Evaluation/optimization results for irregular waves

The previous section was made to gain a better understanding of the behaviour of the control system in the theoretical case of monochromatic waves. It is necessary to see what happens under realistic conditions. In Appendix B, the scatter diagram for Leixões, Portugal is presented [6]. This shows the probability of occurrence Pr of a wave with a certain significant wave height H_s and a certain energy period T_{en} . For the next experiments, waves are chosen that follow the Bretschneider spectrum and have a set (H_s, T_{en}) that has a high probability to occur. In other words, the most important blocks of the scatter diagram are chosen and the corresponding waves are generated by the Matlab model, to be used as input both in the Matlab and GAMS model. The waves that will be used here have a total duration of 200 s, in order to draw better conclusions. For each of the chosen blocks in the scatter diagram, 3 wave examples will be generated, in order to have a good statistical sample. The parameter that needs to be tuned to its optimal value (for maximum energy) in the Matlab model is only K_p . This is done on the basis of the full 200 s wave. The results are presented in Table 5.4. In each example, the maximum energy that can be obtained in Matlab (at optimal K_p), both at the total 200 s and at the first 50 s, the energy in GAMS at the first 50 s and the ratio between the Matlab and GAMS energy are calculated and shown in the table. Then, for each of the selected blocks in the scatter diagram, thus for each set (H_s, T_{en}) , the mean value of K_p , as well as the mean value of the Matlab/GAMS extracted energy ratio, are calculated, so as to have a more reliable overview. Note that at very low waves, K_p does not need to be tuned, because the Matlab result is the same for any value of K_p . This is due to the switch in the controller, which was presented in Chapter 3. When the waves are so low, the energy error is always negative, so the electromagnetic torque is continuously calculated on the basis of the internal damping, not on the basis of the PI controller.

Table 5.4: Matlab/GAMS comparison for irregular Bretschneider waves

Wave parameters	Example #	Optimal K_p for 200 s	Matlab energy E_{final} (J) for 200 s	Matlab energy E_{final} (J) for 50 s	GAMS energy (J) for 50 s	Matlab/GAMS ratio for 50 s
$H_S = 0.75\ m$ $T_{en} = 5.5\ s$ $Pr = 2.41\%$	1	—	24843	8866	17220	51%
	2	—	21764	6374	12909	49%
	3	—	17079	2081	11196	19%
	Mean values	—	—	—	—	40%
$H_S = 1.25\ m$ $T_{en} = 6.5\ s$ $Pr = 10.14\%$	1	0.2	123132	48926	88666	55%
	2	0.5	81452	11169	64356	17%
	3	0.4	97799	24402	81755	30%
	Mean values	0.4	—	—	—	34%
$H_S = 1.25\ m$ $T_{en} = 7.5\ s$ $Pr = 5.80\%$	1	0.2	113158	9102	26346	35%
	2	0.03	140323	64763	90440	72%
	3	0.4	130102	25424	84355	30%
	Mean values	0.2	—	—	—	46%
$H_S = 1.75\ m$ $T_{en} = 6.5\ s$ $Pr = 7.04\%$	1	0.06	198688	72587	138030	53%
	2	0.2	159972	20081	112191	18%
	3	0.2	170771	22714	81705	28%
	Mean values	0.2	—	—	—	33%
$H_S = 1.75\ m$ $T_{en} = 7.5\ s$ $Pr = 7.22\%$	1	0.4	241320	44277	111656	40%
	2	0.3	216135	33427	95246	35%
	3	0.4	203395	33301	122744	27%
	Mean values	0.4	—	—	—	34%
$H_S = 1.75\ m$ $T_{en} = 8.5\ s$ $Pr = 5.39\%$	1	0.6	259273	88134	145032	61%
	2	1.3	249611	58114	105801	55%
	3	0.5	273131	64366	120293	54%
	Mean values	0.8	—	—	—	57%
$H_S = 2.25\ m$ $T_{en} = 8.5\ s$ $Pr = 4.28\%$	1	0.5	356815	66802	122918	54%
	2	0.9	363279	45056	84042	54%
	3	0.7	316938	35616	99383	36%
	Mean values	0.7	—	—	—	48%
$H_S = 2.25\ m$ $T_{en} = 9.5\ s$ $Pr = 3.78\%$	1	2.2	425160	131193	179272	73%
	2	0.9	375907	49140	84555	58%
	3	2	338918	146354	216104	68%
	Mean values	1.7	—	—	—	66%
$H_S = 2.75\ m$ $T_{en} = 8.5\ s$ $Pr = 2.82\%$	1	0.6	500404	110497	192406	57%
	2	0.5	429456	220134	310119	71%
	3	0.9	481828	116931	189014	62%
	Mean values	0.7	—	—	—	63%
$H_S = 2.75\ m$ $T_{en} = 10.5\ s$ $Pr = 1.88\%$	1	0.5	441404	111255	163128	68%
	2	0.5	503274	84466	155820	54%
	3	1.7	441797	101195	178616	57%
	Mean values	0.9	—	—	—	60%
$H_S = 3.25\ m$ $T_{en} = 9.5\ s$ $Pr = 1.77\%$	1	1.3	514146	145222	244123	59%
	2	1.2	536354	126817	206465	61%
	3	0.3	553000	118488	178596	66%
	Mean values	0.9	—	—	—	62%

$H_s = 3.75\text{ m}$ $T_{en} = 9.5\text{ s}$ $Pr = 1.43\%$	1	1.2	767762	228996	355598	64%
	2	2.5	670000	174748	263234	66%
	3	1.2	760434	189112	320375	59%
	Mean values	1.6	–	–	–	63%
$H_s = 3.75\text{ m}$ $T_{en} = 11.5\text{ s}$ $Pr = 0.70\%$	1	0.2	541038	152449	241193	63%
	2	0.7	691852	137785	227218	61%
	3	0.4	677631	232683	334866	69%
	Mean values	0.4	–	–	–	64%
$H_s = 4.25\text{ m}$ $T_{en} = 9.5\text{ s}$ $Pr = 0.83\%$	1	0.5	885637	200706	301123	67%
	2	0.2	891570	285717	425227	67%
	3	0.4	794385	180875	342435	53%
	Mean values	0.4	–	–	–	62%

From these results, some significant observations can be made. The most important thing is that the control system of the Symphony shows a very good performance in realistic conditions. This can be seen from the fact that in most cases, the final extracted energy is between 50% – 70% of the theoretical limit, as calculated by GAMS. Of course, due to all the assumptions and approximations in GAMS, this percentage can be a bit lower or higher in reality. The Matlab/GAMS percentage can take lower values and has a lot of fluctuation at lower waves, though. At higher waves, there is more stability in the percentage. So, the question rises about how reliable and representative these percentages are. It can be seen that in many cases, especially in the cases that the percentage is low, the energy extracted during the total 200 s is much more than four times the energy extracted during the first 50 s. This means that the energy that can be extracted from these waves is unequally distributed over the whole duration, which is as expected, due to the irregularity. Also, 50 s is a really short time to draw strong conclusions, especially when it is the beginning of the wave, because then the floater needs to be set in motion from standstill. If a method is found to make it possible for longer duration waves to be used in GAMS, the percentages are expected to rise and be more stable. Nevertheless, the table gives a general idea about how good the control system is, as the energy in Matlab and GAMS are of the same order of magnitude. Another observation is that the real extracted energy increases as the wave height increases, as expected, and does not really depend on the wave period. Finally, the optimal value of K_p seems to follow a random pattern, however it is always between 0.2 – 2.5 approximately. The sensitivity analysis in the next section will show whether these fluctuations have a large impact or not.

To gain an even better image of the performance of the controller, some graphs are made. From all the previous waves, three are randomly chosen, namely example # 1 with $H_s = 1.25$, $T_{en} = 6.5\text{ s}$, example # 1 with $H_s = 2.75$, $T_{en} = 8.5\text{ s}$ and example # 1 with $H_s = 3.75$, $T_{en} = 11.5\text{ s}$. These examples provide a variety of wave heights and periods. For each wave, three plots are made: one plot that shows the downscaled wave force, the floater position in Matlab and the floater position in GAMS, one plot that shows the downscaled wave force, the floater velocity in Matlab and the floater velocity in GAMS and one plot that shows the velocity and electromagnetic torque in Matlab and the velocity and electromagnetic torque in GAMS. All this is shown in Figures 5.11 to 5.19.

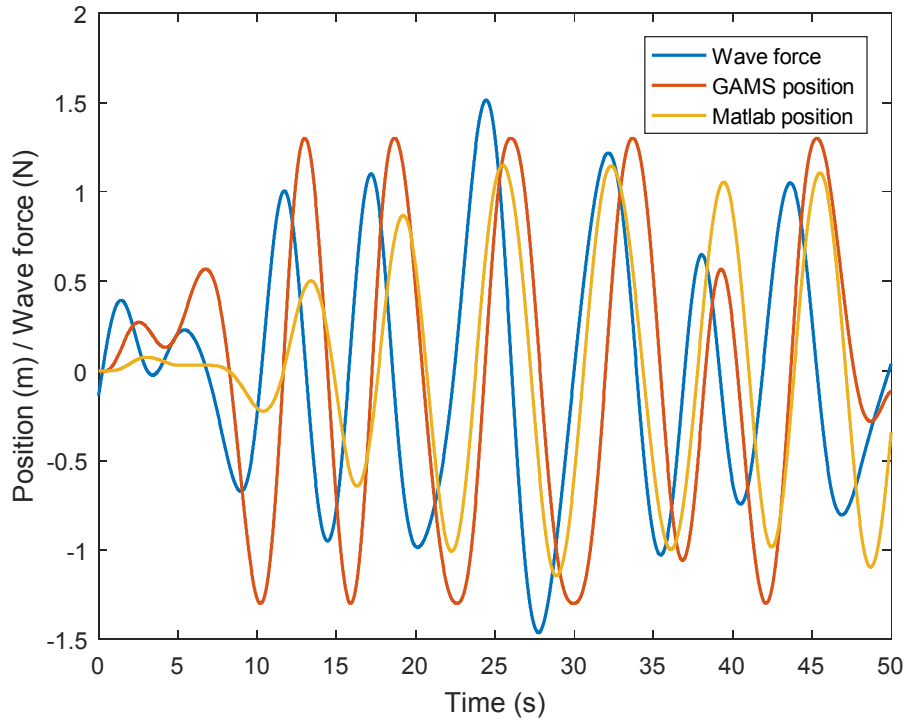


Figure 5.11: Scaled wave force, floater position when running GAMS and Matlab (realistic) floater position, for a Bretschneider wave with $H_s = 1.25\text{ m}$ and $T_{en} = 6.5\text{ s}$

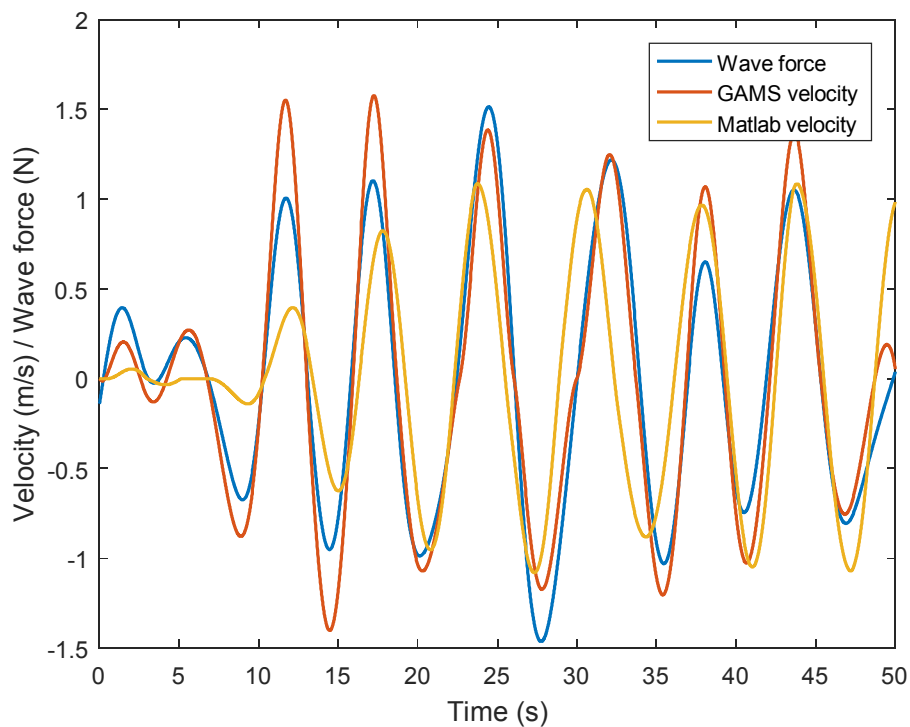


Figure 5.12: Scaled wave force, floater velocity when running GAMS and Matlab (realistic) floater velocity, for a Bretschneider wave with $H_s = 1.25\text{ m}$ and $T_{en} = 6.5\text{ s}$

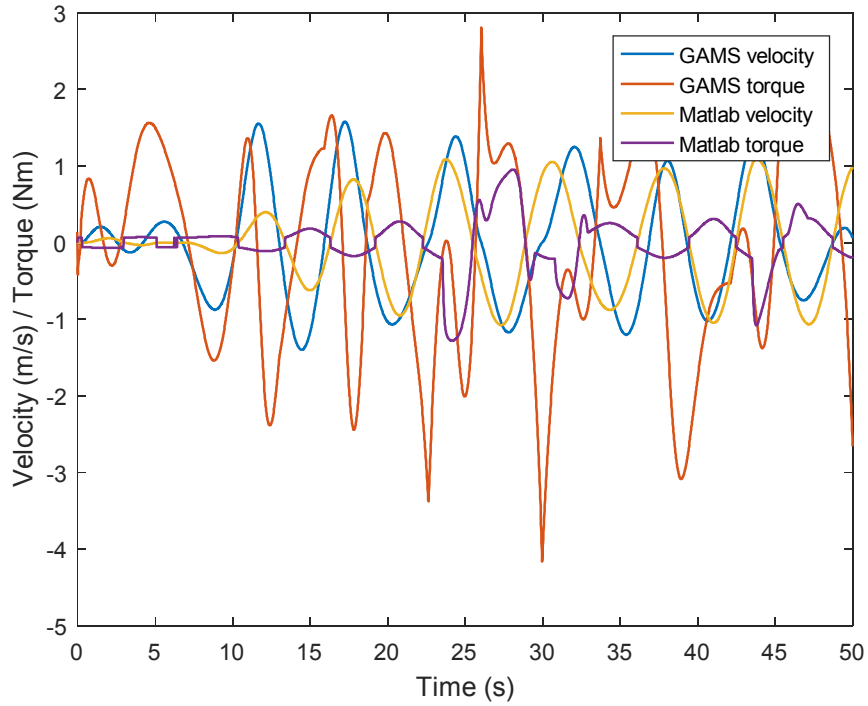


Figure 5.13: Floater velocity and scaled electromagnetic torque, in GAMS and Matlab, for a Bretschneider wave with $H_s = 1.25\text{ m}$ and $T_{en} = 6.5\text{ s}$

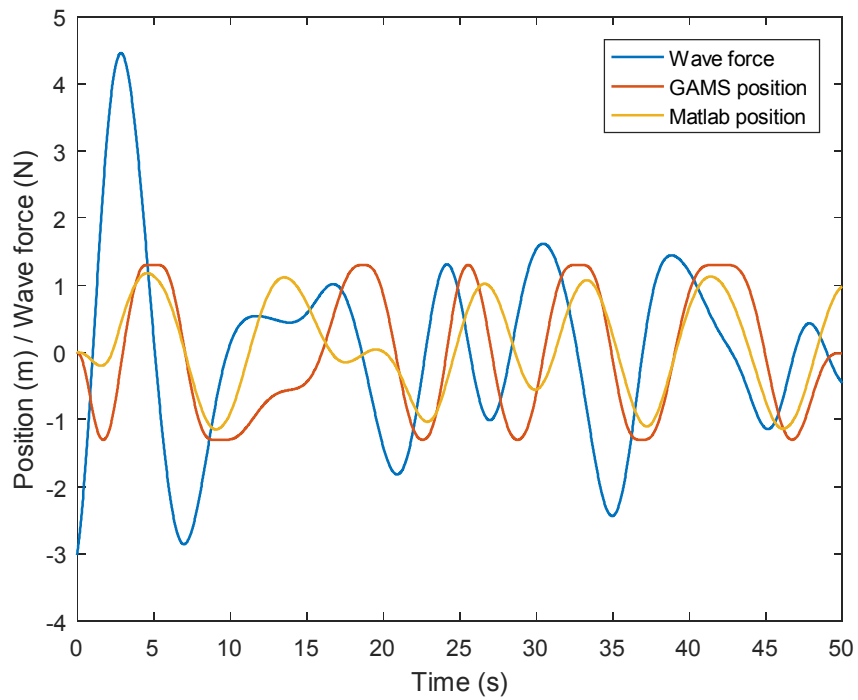


Figure 5.14: Scaled wave force, floater position when running GAMS and Matlab (realistic) floater position, for a Bretschneider wave with $H_s = 2.75\text{ m}$ and $T_{en} = 8.5\text{ s}$

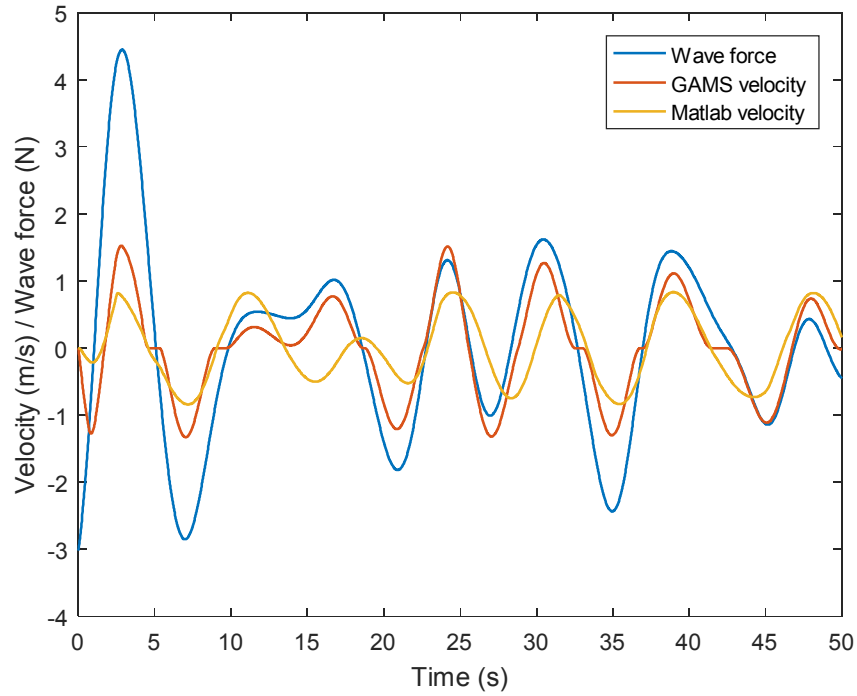


Figure 5.15: Scaled wave force, floater velocity when running GAMS and Matlab (realistic) floater velocity, for a Bretschneider wave with $H_s = 2.75\text{ m}$ and $T_{en} = 8.5\text{ s}$

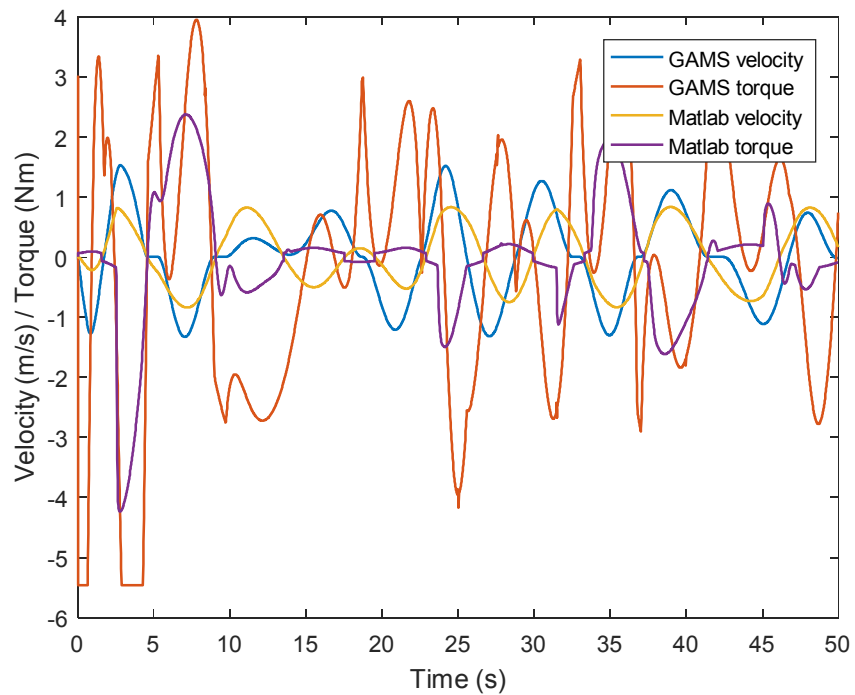


Figure 5.16: Floater velocity and scaled electromagnetic torque, in GAMS and Matlab, for a Bretschneider wave with $H_s = 2.75\text{ m}$ and $T_{en} = 8.5\text{ s}$

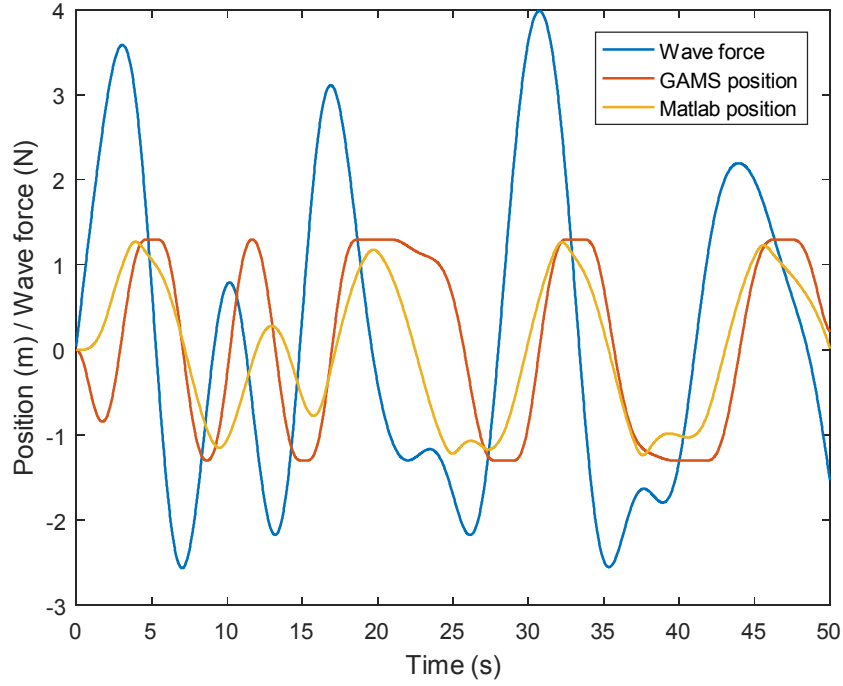


Figure 5.17: Scaled wave force, floater position when running GAMS and Matlab (realistic) floater position, for a Bretschneider wave with $H_s = 3.75 \text{ m}$ and $T_{en} = 11.5 \text{ s}$

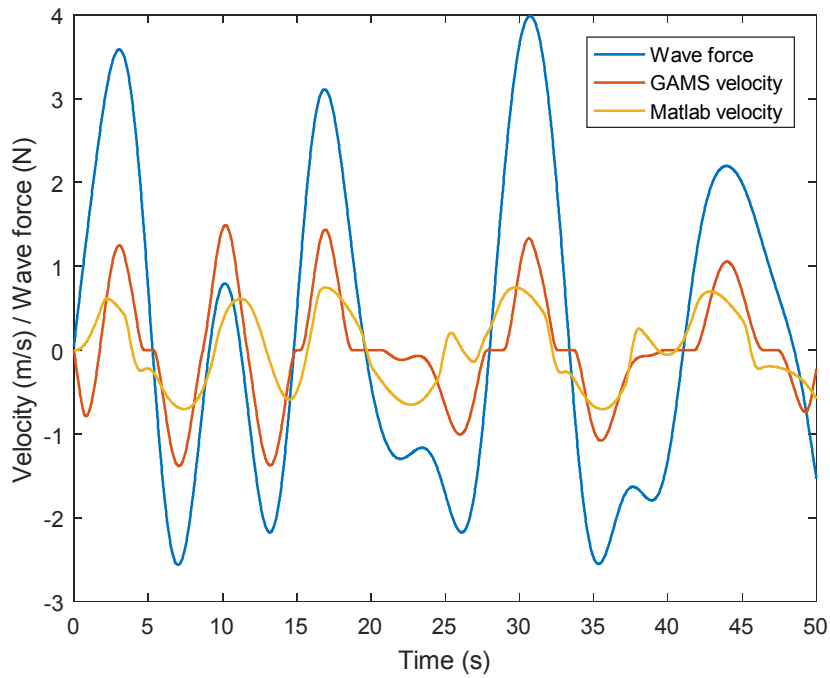


Figure 5.18: Scaled wave force, floater velocity when running GAMS and Matlab (realistic) floater velocity, for a Bretschneider wave with $H_s = 3.75 \text{ m}$ and $T_{en} = 11.5 \text{ s}$

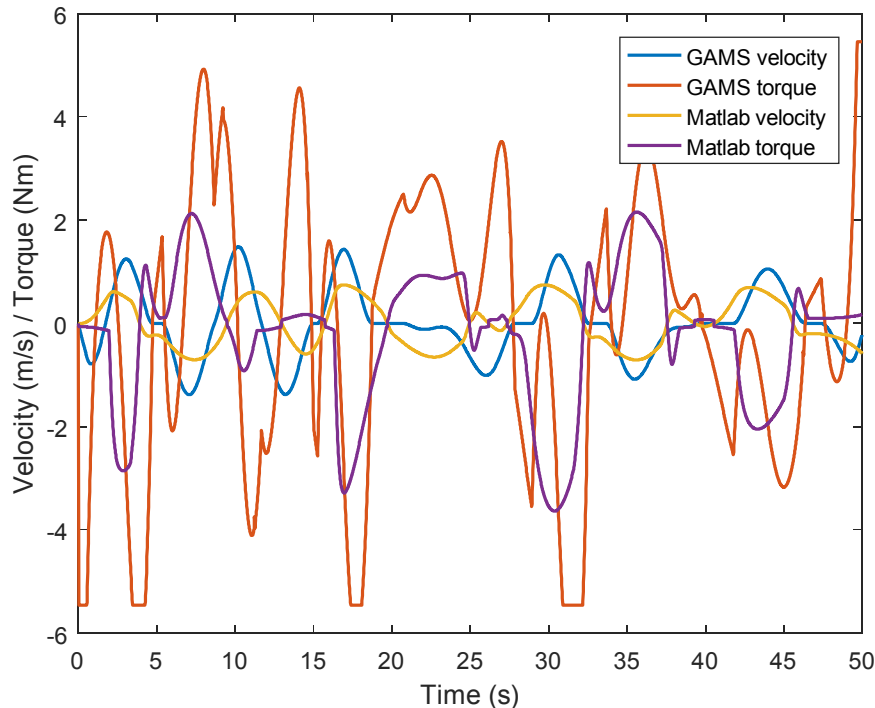


Figure 5.19: Floater velocity and scaled electromagnetic torque, in GAMS and Matlab, for a Bretschneider wave with $H_s = 3.75 \text{ m}$ and $T_{en} = 11.5 \text{ s}$

It can be seen that the position and velocity of the floater are quite similar in Matlab and GAMS at some points and differ both in phase and magnitude at other points. The most important difference is that there is no latching in Matlab, whereas there is some latching in GAMS. This can be explained by the fact that the Matlab controller only uses present inputs, whereas in GAMS the whole wave is known in advance, as mentioned previously too. In any case, the velocity in Matlab is mostly almost in phase with the wave force, which explains the good results concerning the energy output. Another interesting remark is that the position in Matlab is continuously within 1.2 m approximately from the equilibrium point, thus not too far in the stiff spring region. This means that the controller fulfils its role well, because the point is to keep the mechanical energy of the floater equal to the mechanical energy that it would have in an ideal sinusoidal oscillation with an amplitude of 1.1 m , with a linear spring. This ideal situation is not achievable of course, due to the continuously changing irregular waves, but the controller works very well in this direction.

Concerning the electromagnetic torque, it is clear from the figures that the torque in Matlab is quite lower than the torque in GAMS at many instants. This possibly partly explains the less amount of energy extracted by Matlab, as the instant power, $-T_e \cdot \omega_t$, is lower (the Matlab floater velocity, thus also the angular speed of the turbine, is also a bit lower than in GAMS mostly). On the other hand, the electromagnetic torque in Matlab is perfectly in counter phase with the velocity of the floater, because these two quantities are proportional to each other, with a proportionality constant that depends on the energy error, of course. This is not always the case in GAMS, where arbitrary values can be given to the torque at each instant. Finally, another good characteristic of the controller is that the Matlab torque does not have a too 'rough' pattern, as it 'follows' the floater in some way.

To sum up, it can again be said that the controller functions very well in realistic irregular waves, something which was shown both by the energy output and by the movement of the floater.

5.5 Sensitivity analysis

It is important to see to what extent the changes in some parameters affect the behaviour of the Symphony. For this reason, a sensitivity analysis is performed. There are three parameters that will be examined: the linear spring constant, the value of K_p and the limits on the electromagnetic torque. In each of the three parameter sensitivity experiments, three randomly chosen Bretschneider waves from the previous section will be used, namely a wave with $H_s = 1.25, T_{en} = 6.5 s$, a wave with $H_s = 2.75, T_{en} = 8.5 s$ and a wave with $H_s = 4.25, T_{en} = 9.5 s$. These waves provide a sample that covers sufficiently the range of wave heights and periods. From now on, only the Matlab time domain model will be used, not GAMS, so everything will be on the basis of the full duration of 200 s.

5.5.1 Sensitivity to the linear spring constant

The thing that is examined here is how big the impact is on the final energy output, if the Symphony is not perfectly tuned to the energy period of the wave. For each of the three mentioned waves, K_p is put and kept at the optimal value and the spring constant of the linear region is varied. All other parameters remain the same. By varying the linear spring constant k_{lin} , the corresponding natural period of the mass-spring system T_0 is calculated as follows:

$$T_0 = 2\pi \cdot \sqrt{\frac{m_{tot} + m_{eq}}{k_{lin}}} \quad (5.2)$$

The results of the sensitivity analysis are presented in Table 5.5. The green coloured boxes refer to the standard case for the wave under consideration. Only small variations are made in the natural period, because, in reality, a too bad tuning is not likely.

Table 5.5: Sensitivity of the Symphony to the linear spring constant, for three different waves

Spring constant k_{lin} / natural period T_0	$77475 \frac{N}{m}$ 3.5 s	$37963 \frac{N}{m}$ 5 s	$22463 \frac{N}{m}$ 6.5 s	$14829 \frac{N}{m}$ 8 s	$10516 \frac{N}{m}$ 9.5 s	$7843 \frac{N}{m}$ 11 s
Energy E_{final} (J) for $H_s = 1.25, T_{en} = 6.5 s$	5286	33361	123132	139234	89810	55644
Spring constant k_{lin} / natural period T_0	$31374 \frac{N}{m}$ 5.5 s	$19368 \frac{N}{m}$ 7 s	$13136 \frac{N}{m}$ 8.5 s	$9491 \frac{N}{m}$ 10 s	$7176 \frac{N}{m}$ 11.5 s	$5615 \frac{N}{m}$ 13 s
Energy E_{final} (J) for $H_s = 2.75, T_{en} = 8.5 s$	135115	393934	429456	455356	432423	380591

Spring constant k_{lin} / natural period T_0	$37963 \frac{N}{m}$ 5 s	$22463 \frac{N}{m}$ 6.5 s	$14829 \frac{N}{m}$ 8 s	$10516 \frac{N}{m}$ 9.5 s	$7843 \frac{N}{m}$ 11 s	$6074 \frac{N}{m}$ 12.5 s
Energy E_{final} (J) for $H_s = 4.25$, $T_{en} = 9.5$ s	156799	552551	810061	891570	899816	898259

It is clear that there is a significant impact on the energy output, when the spring is not well tuned to the energy period of the incoming wave, especially at low and fast waves. For a good performance of the Symphony, the natural period of the device should not differ more than 2 s approximately from the energy period of the wave. Resonance is thus an important feature of the Symphony that needs to be taken into account as much as possible in real operating conditions. Another special remark from the table is that the energy output is less affected when the Symphony is tuned to a higher natural period than the energy period of the wave, compared to when the Symphony is tuned to a lower natural period than the energy period of the wave. In all examples, there is even a small increase in the energy output at a bit higher natural periods, compared to the energy output at the standard case. This can be explained by the fact that the power that can be extracted from a certain wave increases when the wave period increases [9]. Thus, by tuning the Symphony to a higher natural period, more significance is given to the slower components of the whole Bretschneider wave, which contain more energy. Thus, it is better to be tuned to a too high natural period than to a too low one. Of course, the optimal tuning is to the energy period of the incoming wave.

5.5.2 Sensitivity to K_p

Here, an examination is performed as to how much the energy output of the Symphony is affected by variations in the value of the proportional constant of the controller, K_p . All other parameters remain at their standard values. The results of the sensitivity analysis are presented in Table 5.6. The green coloured boxes refer to the standard case for the wave under consideration. A range of K_p between 0.01 – 3 is used, because, as seen from the results in Section 5.4, this is the normal range for optimal values of K_p .

Table 5.6: Sensitivity of the Symphony to K_p , for three different waves

K_p	0.01	0.05	0.1	0.2	0.6	1.1	1.5	2
Energy E_{final} (J) for $H_s = 1.25$, $T_{en} = 6.5$ s	105578	120621	122848	123132	121963	121201	120811	120438
K_p	0.03	0.08	0.4	0.9	1.5	2	2.5	3
Energy E_{final} (J) for $H_s = 2.75$, $T_{en} = 8.5$ s	408871	441716	479976	481828	481136	480436	479785	479197
K_p	0.05	0.07	0.2	0.5	0.9	1.3	1.9	2.3

Energy E_{final} (J) for $H_s = 4.25$, $T_{en} = 9.5$ s	863811	864165	874204	885637	880209	875052	869999	867707
--	--------	--------	--------	--------	--------	--------	--------	--------

It can be seen that the energy output remains quite stable in most of the range of K_p under consideration, for all three wave examples. The differences are insignificant. This shows once more that the control system for the Symphony is very good, as it makes the device operate well, regardless of the variations in K_p , the optimal value of which, as shown previously, follows a random pattern. Thus, a value for K_p somewhere between 0.2 – 2.5 can be chosen without problems, as any of the exact numbers in between this range will give, for a certain wave, an energy output that does not differ significantly from the maximum possible energy output (at optimal K_p). The exact numerical choice is a subject of further research and can be made when the necessary hardware for the controller will be designed.

5.5.3 Sensitivity to the electromagnetic torque

Finally, an analysis is performed to see how much the energy output of the Symphony is affected by the lower and upper limits of the electromagnetic torque $|T_{e,max}|$. The electrical machine that has been chosen now can give a torque T_e between -546 Nm and 546 Nm. It is interesting to examine how the Symphony would perform with a less powerful machine or what would happen in case of failure of the electrical parts, thus when there is no torque at all. All other parameters remain at their standard values. The results of the sensitivity analysis are presented in Table 5.7. The green coloured boxes refer to the standard case for the wave under consideration. Only lower values of $|T_{e,max}|$ will be examined, because experiments have shown that the current limits of ± 546 Nm are almost never reached, thus there would be no difference with a more powerful machine. Apart from the extracted energy, also the maximum distance from the equilibrium point that the floater reaches is presented, to see if the floater does not go too far, with this less electromagnetic torque, thus less PTO force, to stop it.

Table 5.7: Sensitivity of the Symphony to $|T_{e,max}|$, for three different waves

$ T_{e,max} $ (Nm)	546	450	300	150	100	50	0
Energy E_{final} (J) for $H_s = 1.25$, $T_{en} = 6.5$ s	81452	81452	81452	81452	81256	78694	0
Maximum position $ z_{max} $ (m)	1.12	1.12	1.12	1.12	1.12	1.23	1.47
$ T_{e,max} $ (Nm)	546	450	300	150	100	50	0

Energy E_{final} (J) for $H_s = 2.75$, $T_{en} = 8.5$ s	481828	481828	486884	514708	0	0	0
Maximum position $ z_{max} $ (m)	1.17	1.17	1.24	1.88	STOP	STOP	STOP
$ T_{e,max} $ (Nm)	546	450	300	150	100	50	0
Energy E_{final} (J) for $H_s = 4.25$, $T_{en} = 9.5$ s	885637	889990	0	0	0	0	0
Maximum position $ z_{max} $ (m)	1.24	1.29	STOP	STOP	STOP	STOP	STOP

It can be seen that at all waves, lowering the torque limit only a bit has no significant impact or no impact at all on the behaviour of the Symphony. This is more clear at low waves, because there the maximum electromagnetic torque that is reached during operation is far below the limit in any case, so only when the limit becomes very low, an impact is observed. Then, by lowering the limit a bit more, there is a difference in the extracted energy, as well as an increase in the maximum position that the floater reaches. As the machine cannot provide enough torque anymore to keep the floater in the linear spring region, the floater reaches well into the stiff spring region due to the wave force that is responsible for its motion. This increase in the outermost position causes higher speeds, so this explains the increase in energy extraction that is observed, especially in the second example. After some point in lowering the limits, the electromagnetic torque that the machine can provide is too low to keep the floater within the acceptable bounds of ± 2 m, so the simulation stops. This is the meaning of the 'STOP' result. This effect is larger for higher waves of course, because they tend to push the floater further from the equilibrium point, due to the higher wave force. Only at low waves can the Symphony keep functioning without electromagnetic torque to act as a brake.

6. Conclusions & Recommendations

6.1 Introduction

This chapter sums up the basic results and observations from this thesis. Firstly, the major conclusions are drawn. These concern the spring tuning, the method and results concerning the theoretical optimal case, the parameters of the controller, the realistic simulation results and the sensitivity analysis. Then, suggestions are given for future work, concerning the hardware to be developed, possible improvements in the controller and in the GAMS code and the usage of the correct form of the radiation force.

6.2 Conclusions

In this thesis, an important analysis was made about the control system of the Symphony Wave Power Device. The target was to extract as much energy as possible from the incoming waves and convert it into electrical energy. From the whole report, there are six major conclusions that can be drawn. They will be presented here in the same order as in the report.

6.2.1 Spring tuning

First of all, an important observation is that the turbine, because of its high inertia, which can be translated to an equivalent mass, increases significantly the total mass of the moving parts of the Symphony, which are in fact a mass-spring-damper system. This needs to be taken into account in the design of the membrane and in the determination of the air pressure in the chamber, as these affect the spring constant. In this way, the device can keep its natural frequency equal to a desired value.

6.2.2 GAMS modelling

Secondly, it is possible to determine the behaviour of a practically perfect controller for the Symphony, in terms of energy extraction from the waves, with the help of the GAMS optimization software. However, as there are significant nonlinearities in the forces that act on the floater, many assumptions and approximations are needed to model these forces in GAMS. More specifically, the spring force, drag force and iron loss torque are approximated by linear or polynomial functions. Also, mean values are taken for the relation between the velocity or acceleration of the floater and the angular velocity or angular acceleration of the turbine, respectively. Moreover, a sampling is needed and only short duration waves can be used, in order to have a feasible problem and acceptable running time. All these assumptions have as a result that an exact calculation of the maximum energy that can be extracted from a certain wave is not possible, however upper boundaries can be put and a satisfying idea is obtained as to where the optimal solution lies.

6.2.3 GAMS results

Thirdly, the results of the optimization procedures with GAMS show that, in the ideal case, the velocity of the floater is kept constantly in phase with the wave excitation force, something which has also been discussed in the literature. This is thus a goal towards which a good control system should strive. The reason why this is easily possible in GAMS is because this software 'knows' the whole wave in advance, which is not the case in most realistic conditions, unless a prediction method is being used. Also, the GAMS results show that the only factor to which the theoretical boundary is really sensitive, is the allowed amplitude of oscillation. This should thus be taken into account in a larger model of the Symphony. Finally, if sampling is performed on the wave, it is necessary to have a high enough sampling rate.

6.2.4 Controller parts

Concerning the actual controller, based on the concept of an energy error, that is being used for the Symphony, an important conclusion is that only a proportional part should be used, as an integrating part would make it quite unreliable. Also, the energy must flow only from the Symphony to the grid and not the other way, otherwise the extracted energy decreases significantly. Moreover, the copper losses of the electrical machine, as well as the losses on the cable that goes to shore, are insignificant for the whole performance, but should be taken into account in the calculations.

6.2.5 Matlab results

By conducting simulations in the Matlab time domain model, the most important conclusion for this thesis can be drawn. This is that the actual controller performs very well in all sea states that are likely to occur at the location where the Symphony will be placed. The extracted energy from realistic irregular waves reaches up to 70% of the upper boundary, as calculated by GAMS. The controller manages to keep the oscillation of the floater close to the desired pattern, in the linear spring region. Additionally, the velocity of the floater is kept almost in phase with the wave excitation force. Moreover, the electrical generator provides a quite smooth electromagnetic torque pattern and the limits are not reached most of the time. Thus, it is a very good idea to keep this control system for the Symphony.

6.2.6 Sensitivity

Finally, a sensitivity analysis, which has also been performed with the help of the Matlab time domain model, provided an important insight for some parameters. The spring needs to be properly tuned to the energy period of the incoming waves, for optimal energy extraction. On the other hand, the proportional constant of the controller can be tuned in a wide range without problems. Also, the Symphony can keep operating in case of electrical failure only if the waves are sufficiently low.

6.3 Recommendations

From this thesis, it can be seen that a considerable amount of work has been done on the Symphony, mainly in the area of the control system. However, there are still a variety of things that need to or can be done, before the device is actually placed in the sea and starts providing renewable energy. Here, some suggestions for further work are given, which can be put into certain categories.

6.3.1 Hardware

All the experiments and results so far have only been based on computer simulations with the appropriate software. Thus, the most important recommendation is to develop the necessary electronic hardware for the controller and the converter. The controller takes as inputs the position and velocity of the floater and the angular velocity of the turbine, so the appropriate sensors need to be chosen, too. It would be better to develop this hardware when the Symphony will be fully built, so that realistic tests can be made. Then, other parameters, such as the energy losses or imperfections of the converter, can also be taken into account, in order to obtain a better image of the performance of the controller.

6.3.2 Other control systems

This thesis has shown that the particular control system, which makes use of an energy error, performs very well. This does not mean that there is not an even better solution. It is theoretically possible to develop a control system that will extract even more than 70% of the theoretical energy limit, as calculated by GAMS. Various methods can be used for this, with the help of the available literature. Latching control, thus keeping the floater in its outmost positions for some time during each cycle, is a good option to test. In any case, it is most likely that some kind of prediction of future values of the wave elevation/force will be needed to achieve these higher percentages of the theoretical maximum. This can be done either by a measurement device at some distance from the Symphony, such as a floating buoy, or by mathematical methods, such as model predictive control.

6.3.3 GAMS improvements

Another useful recommendation is to improve the GAMS code, so as to obtain even more realistic results concerning the calculation of the upper limit of energy that can be extracted from a certain wave. This includes finding better functions to represent the spring force, drag force and iron loss torque, not just polynomial approximations, implementing the dependence of the $\frac{\omega_t}{z_d}$ ratio on the position of the floater and using the real equation for the calculation of the cable losses, not just assuming 2% in all cases. Also, waves of longer duration than 50 s should be used, to make a better comparison with the realistic Matlab model. For this, it will be necessary to find a way to make GAMS able to run with far more than 2501 time segments, as has been done now. This could include either making some more assumptions about the forces or using other available GAMS tools, which have not been explored in this thesis. In this way, the Matlab/GAMS ratios of extracted energy will be closer to reality and can possibly rise. Additionally, if other parameters or factors of the Symphony are to be taken into account in future work, they can also be added to the GAMS model easily. Finally, this GAMS model can even be used for optimization problems of other wave energy devices than the Symphony, if the necessary modifications are made in the code, of course.

6.3.4 Radiation force

Last but not least, the radiation force plays an important role in wave energy devices, as seen in the literature. It is difficult to be modelled and taken into account in the control system, because it contains an integral that carries a 'memory' effect. Now, this force was approximated only by an added mass and a hydrodynamic damping, because of the relatively small size of the Symphony. When, however, the Symphony will be scaled up, the full form of this force will need to be used and

implemented in the time domain model. This could bring up new challenges that will have to be tackled.

References

- [1] F. M. Mulder, “Renewable Energy”, TU Delft lecture notes, available online at https://blackboard.tudelft.nl/bbcswebdav/pid-2586249-dt-content-rid-8716030_2/courses/37322-151601/RE1a-2015-08-31.pdf
- [2] D. Wikkerink, “Generator Design for the Symphony Wave Power Device”, TU Delft, 2017
- [3] A. Jarquin Laguna, “Introduction to Ocean Energy Technologies”, TU Delft lecture notes, available online at https://blackboard.tudelft.nl/bbcswebdav/pid-2900264-dt-content-rid-9959262_2/courses/41455-161702/01_OE44075_Intro_ocean_energy_2016%281%29.pdf
- [4] ACRRES, “Aquatic Biomass”, available online at <http://acrres.nl/aquatic-biomass/>
- [5] D. A. Vermaas, “Salinity gradient energy”, TU Delft lecture notes, available online at https://blackboard.tudelft.nl/bbcswebdav/pid-2902353-dt-content-rid-9970646_2/courses/41455-161702/03_OE44075_Blue%20Energy_2016.pdf
- [6] N. Leijtens, “Optimal Buffer Design for the Symphony Wave Power System”, University of Twente, 2016
- [7] NEU, “A new way for wave and tidal energy”, 2015, available online at <http://www.newstettereuropean.eu/new-way-wave-tidal-energy/>
- [8] J. Kolken, “Testopstelling turbine Symphony”, Inholland, 2017
- [9] J. Falnes and J. Hals, “Heaving buoys, point absorbers and arrays”, Philosophical Transactions of the Royal Society A, 2002, vol. 370, pp. 246-277
- [10] EMEC, “Wave devices”, available online at <http://www.emec.org.uk/marine-energy/wave-devices/>
- [11] J. de Jong, “Design of Power Take Off Turbine for the Symphony Wave Energy Converter”, Inholland, 2015
- [12] E. Friis-Madsen, H. C. Soerensen and S. Parmeggiani, “Wave Dragon”, available online at <https://www.slideshare.net/ErikFriisMadsen/icoe-2012-wave-dragon-b>
- [13] C. Heuberger, A. Janse, H. Pot and I. Sfikas, “Tidal Energy in the English Channel”, TU Delft, 2017
- [14] A. Kooiman, “Adjustments of the gas spring in the Symphony Wave Power device”, University of Twente, 2016
- [15] “Symphony Wave Power”, available online at <https://symphonywavepower.com/>
- [16] J. A. M. Cretel, G. Lightbody, G. P. Thomas and A. W. Lewis, “Maximisation of Energy Capture by a Wave-Energy Point Absorber using Model Predictive Control”, IFAC, 2011, pp. 3714-3721

- [17] ALXION, "Technical Characteristics 800 STK Alternators"
- [18] ThyssenKrupp Stahl, "Our products. Non grain oriented electrical steel PowerCore®."
- [19] Brown University, "Introduction to Dynamics and Vibrations", available online at http://www.brown.edu/Departments/Engineering/Courses/En4/Notes/vibrations_free_undamped/vibrations_free_undamped.htm
- [20] D. Valério, P. Beirão and J. S. da Costa, "Reactive control and phase and amplitude control applied to the Archimedes Wave Swing", Conference paper, 2007
- [21] N. Mohan, T. M. Undeland and W. P. Robbins, "Power Electronics, Converters, Applications and Design", Third Edition, John Wiley & Sons, Inc., 2003
- [22] "Temperature Coefficient of Resistance", available online at <https://www.electrical4u.com/temperature-coefficient-of-resistance/>
- [23] The Engineering ToolBox, "Resistance and Resistivity", available online at https://www.engineeringtoolbox.com/resistance-resistivity-d_1382.html
- [24] J. Falnes, "Principles for capture of energy from ocean waves, phase control and optimum oscillation", NTNU
- [25] D. V. Evans, "A theory for wave-power absorption by oscillating bodies", Journal of Fluid Mechanics, 1976, vol. 77, pp. 1-25
- [26] J. Falnes, "Optimum Control of Oscillation of Wave-Energy Converters", International Journal of Offshore and Polar Engineering, 2002, vol. 12, no. 2, pp. 147-155
- [27] U. A. Korde, "On the control of wave energy devices in multi-frequency waves", Applied Ocean Research, 1991, vol. 13, no. 3, pp. 132-144
- [28] A. S. Zurkinden, F. Ferri, S. Beatty, J. P. Kofoed and M. M. Kramer, "Non-linear numerical modeling and experimental testing of a point absorber wave energy converter", Elsevier Ocean Engineering, 2014, vol. 78, pp. 11-21
- [29] P. Ricci, J. Lopez, M. Santos, J. L. Villate, P. Ruiz-Minguela, F. Salcedo and A. F. de O. Falcão, "Control Strategies for a simple Point-Absorber Connected to a Hydraulic Power Take-off", Proceedings of the 8th European Wave and Tidal Energy Conference, 2009, pp. 746-755
- [30] J. S. da Costa, P. Beirão and D. Valério, "Internal model control applied to the Archimedes Wave Swing", Portugal, 2007
- [31] D. Valério, P. Beirão, M. J. G. C. Mendes and J. S. da Costa, "Comparison of control strategies performance for a Wave Energy Converter", Portugal
- [32] F. Fusco and J. V. Ringwood, "Short-Term Wave Forecasting for Real-Time Control of Wave Energy Converters", IEEE transactions on sustainable energy, 2010, vol. 1, no. 2, pp. 99-106

- [33] T. K. A. Brekken, "On Model Predictive Control for a Point Absorber Wave Energy Converter", IEEE Trondheim PowerTech, 2011
- [34] M. Richter, M. E. Magaña, O. Sawodny and T. K. A. Brekken, "Nonlinear Model Predictive Control of a Point Absorber Wave Energy Converter", IEEE transactions on sustainable energy, 2013, vol. 4, no. 1, pp. 118-126
- [35] J. Cretel, A. W. Lewis, G. Lightbody, G. P. Thomas, "An Application of Model Predictive Control to a Wave Energy Point Absorber", Ireland
- [36] I. E. Sfikas, "Βέλτιστη ταυτόχρονη τοποθέτηση μονάδων διεσπαρμένης παραγωγής και αποθηκευτικών μονάδων σε δίκτυα ηλεκτρικής ενέργειας (Optimal simultaneous placement of dispersed production units and storage units in electrical energy networks)", NTUA, 2013
- [37] GAMS, available online at <https://www.gams.com/>
- [38] MIT, "Design of Ocean Systems", 2011, available online at https://ocw.mit.edu/courses/mechanical-engineering/2-019-design-of-ocean-systems-spring-2011/lecture-notes/MIT2_019S11_OWE.pdf
- [39] "Water wave diagram", available online at https://commons.wikimedia.org/wiki/File:Water_wave_diagram.jpg
- [40] CDIP, "Wave Measurement", available online at <http://cdip.ucsd.edu/?nav=documents&sub=index&stn=106&xitem=waves>
- [41] J. Pastor and Y. Liu, "Wave Energy Resource Analysis for Use in Wave Energy Conversion", Journal of Offshore Mechanics and Arctic Engineering, 2015, vol. 137
- [42] "Random Wave Spectra", available online at <https://github.com/petebachant/MakeWaves/wiki/Random-wave-spectra>

Appendix

A. The GAMS code

Here, the developed GAMS code for this thesis is presented. Everything after a * symbol is viewed as a comment. The way it is presented here, the Bretschneider wave with significant wave height $H_s = 3 \text{ m}$ and wave energy period $T_{en} = 10 \text{ s}$ is read from the first Excel file (beginning) and only the wave force is written on the second Excel file (ending).

```
$title wave
sets
t time segments /t1*t2501/

$CALL GDXXRW Monochromatic_GAMS.xlsx Set=t rng=AG2:AG2502 Rdim=1 Set=a
rng=AH1:AH1 Cdim=1 Par=x rng=AG1:AH2502 Rdim=1 Cdim=1
*Monochromatic H=3 T=10
*Necessary commands to read from the Excel file

$GDXIN Monochromatic_GAMS.gdx
Set a(*);
$LOAD a
Parameter x(t,a);
$LOAD x
$GDXIN

scalar
m "total mass" /6520/
c "hydrodynamic damping" /25/
k "linear spring constant" /9491/
It "turbine inertia" /4.8715/

variables
energy total energy extracted
z(t) position
zd(t) velocity
zdd(t) acceleration
fpto(t) pto force
Te(t) electromagnetic torque
y(t) wave force just for calculation;

z.lo(t)=-1.3;
z.up(t)=1.3;
*Position limits

z.fx('t1')=0;
zd.fx('t1')=0;
zdd.fx('t1')=0;
*Fixed values for t=0
```

```

Te.lo(t)=-546;
Te.up(t)=546;
*Torque limits

```

equations

```

cost objective function
vel(t) velocity calculation
acc(t) acceleration calculation
force(t) force balance
pto(t) pto force calculation
calculation(t) check equation;

```

```

cost.. energy=e=0.02*0.98*sum(t,-Te(t)*59.971*zd(t)-
0.004531283*power(Te(t),2));
vel(t)$ (ord(t) gt 1).. zd(t)=e=(z(t)-z(t-1))/0.02;
acc(t)$ (ord(t) gt 1).. zdd(t)=e=(zd(t)-zd(t-1))/0.02;
force(t).. m*zdd(t)=e=-k*z(t)-
0.9961589168568*power(zd(t),7)+20.9262987445565*power(zd(t),5)-
217.3838722964995*power(zd(t),3)+257.013694990181*power(zd(t),2)-
177.9187064039331*zd(t)-c*zd(t)+x(t,'a1')+fpto(t);
pto(t).. fpto(t)=e=-59.971*(59.971*zdd(t)*It-Te(t)-
4.170293771684*power(zd(t),3)+23.613697449688*zd(t));
calculation(t).. y(t)=e=x(t,'a1');

```

```

model owf /all/;

```

```

option minlp=sbb;
option nlp=snopt;

```

```

option iterlim=1e9;
option reslim=1e9;

```

```

owf.optfile=1;
owf.workspace=1000;
*Necessary options for good code running

```

```

solve owf using minlp maximizing energy;

```

```

display energy.l,z.l,zdd.l,zd.l,y.l,Te.l;

```

```

execute_unload "Results_GAMS.gdx" y.l z.l zd.l Te.l

```

```

execute 'gdxrw.exe Results_GAMS.gdx o=Results_GAMS.xlsx var=y.l
rng=Bretschneider_3m_10s!B3:CRF4'
*Necessary commands to write on another Excel file

```

B. Scatter diagram

Here, the scatter diagram for the location where the Symphony will be placed, namely Leixões, Portugal, is presented. This diagram gives the probability of occurrence of a wave with a certain significant wave height H_s and a certain energy period T_{en} .

P[H_s T_e](%)	vs	=< 0.5m	0.5- 1m	1- 1.5m	1.5- 2m	2- 2.5m	2.5- 3m	3- 3.5m	3.5- 4m	4- 4.5m	4.5- 5m	5-6m	6-7m	7-8m	8-9m	9-10m	10- 12m	P[T_e]
=< 4 s																		0,0
4 - 5 s			0,07	0,03														0,1
5 - 6 s			2,41	4,53	1,73	0,23												8,9
6 - 7 s			2,21	10,14	7,04	2,57	0,59	0,03										22,6
7 - 8 s			0,33	5,8	7,22	3,77	2,01	0,99	0,18	0,01								20,3
8 - 9 s			0,01	2,03	5,39	4,28	2,82	1,74	1,05	0,53	0,11							18,0
9 - 10 s				0,38	2,29	3,78	2,52	1,77	1,43	0,83	0,6	0,36						14,0
10 - 11 s				0,05	0,34	1,77	1,88	1,35	1,12	0,75	0,7	0,83	0,17	0,03				9,0
11 - 12 s				0,01	0,12	0,41	0,71	0,52	0,7	0,51	0,55	0,61	0,34	0,07	0,01			4,6
12 - 13 s						0,05	0,13	0,23	0,16	0,22	0,29	0,33	0,18	0,13	0,05	0,03		1,8
13 - 14 s							0,01	0,05	0,06	0,08	0,1	0,07	0,06	0,05	0,09	0,05	0,01	0,6
14 - 15 s										0,01	0,01	0,03	0,05	0,02	0,03			0,2
15 - 16 s																0,01		0,0
16 - 17 s																0,01		0,0
17 - 18 s																		0,0
18 - 19 s																		0,0
19 - 20 s																		0,0
20 - 21 s																		0,0
21 - 22 s																		0,0
> 22 s																		0,0
P[H_s] (%)		0,0	5,0	23,0	24,1	16,9	10,7	6,7	4,7	2,9	2,4	2,2	0,8	0,3	0,2	0,1	0,0	100